NOAA Technical Report NESDIS 42

Simulation Studies of Improved Sounding Systems

Washington, DC
February 1989

U.S. DEPARTMENT OF COMMERCE
National Oceanic and Atmospheric Administration
National Environmental Satellite, Data, and Information Service

NOAA TECHNICAL REPORTS
National Environmental Satellite, Data, and Information Service

ronmental Satellite, Data, and Information Service (NESDIS) manages the Nation's civil
lite systems, as well as global national data bases for meteorology, oceanography,
geophysics, and solar-terrestrial sciences. From these sources, it develops and disseminates environmental data and information products critical to the protection of life and property, national defense, the national economy, energy development and distribution, global food supplies, and the development of natural resources.

Publication in the NOAA Technical Report series does not preclude later publication in scientific journals in expanded or modified form. The NESDIS series of NOAA Technical Reports is a continuation of the former NESS and EDIS series of NOAA Technical Reports and the NESC and EDS series of Environmental Science Services Administration (ESSA) Technical Reports.

These reports are available from the National Technical Information Service (NTIS), U.S. Department of Commerce, Sills Bldg., 5285 Port Royal Road, Springfield, VA 22161 (prices on request for paper copies or microfiche, please refer to PB number when ordering) or by contacting Nancy Everson, NOAA/NESDIS, 5200 Auth Road, Washington, DC 20233 (when extra copies are available). A partial listing of more recent reports appear below:

NESDIS SERIES

NESDIS 1 Satellite Observations on Variations in Southern Hemisphere Snow Cover. Kenneth F. Dewey and Richard Heim, Jr., June 1983. (PB83 252908)

NESDIS 2 NODC 1 An Environmental Guide to Ocean Thermal Energy Conversion (OTEC) Operations in the Gulf of Mexico. National Oceanographic Data Center, June 1983. (PB84 115146)

NESDIS 3 Determination of the Planetary Radiation Budget from TIROS-N Satellites. Arnold Gruber, Irwin Ruff and Charles Earnest, August 1983. (PB84 100916)

NESDIS 4 Some Applications of Satellite Radiation Observations to Climate Studies. T.S. Chen, George Ohring and Haim Ganot, September 1983. (PB84 108109)

NESDIS 5 A Statistical Technique for Forecasting Severe Weather from Vertical Soundings by Satellite and Radiosonde. David L. Keller and William L. Smith, June 1983. (PB84 114099)

NESDIS 6 Spatial and Temporal Distribution of Northern Hemisphere Snow Cover. Burt J. Morse and Chester F. Ropelewski (NWS), October 1983. (PB84 118348)

NESDIS 7 Fire Detection Using the NOAA--Series Satellites. Michael Matson, Stanley R. Schneider, Billie Aldridge and Barry Satchwell (NWS), January 1984. (PB84 176890)

NESDIS 8 Monitoring of Long Waves in the Eastern Equatorial Pacific 1981-83 Using Satellite Multi-Channel Sea Surface Temperature Charts. Richard Legeckis and William Pichel, April 1984. (PB84 190487)

NESDIS 9 The NESDIS-SEL Lear Aircraft Instruments and Data Recording System. Gilbert R. Smith, Kenneth O. Hayes, John S. Knoll and Robert S. Koyanagi, June 1984. (PB84 219674)

NESDIS 10 Atlas of Reflectance Patterns for Uniform Earth and Cloud Surfaces (NIMBUS-7 ERB--61 Days). V.R. Taylor and L.L. Stowe, July 1984. (PB85 12440)

NESDIS 11 Tropical Cyclone Intensity Analysis Using Satellite Data. Vernon F. Dvorak, September 1984. PB85 112951)

NESDIS 12 Utilization of the Polar Platform of NASA's Space Station Program for Operational Earth Observations. John H. McElroy and Stanley R. Schneider, September 1984. (PB85 1525027AS)

NESDIS 13 Summary and Analyses of the NOAA N-ROSS/ERS-1 Environmental Data Development Activity. John W. Sherman III, February 1984. (PB85 222743/43)

NESDIS 14 NOAA N-ROSS/ERS-1 Environmental Data Development (NNEEDD) Activity. John W. Sherman III, February 1985. (PB86 139284 A/S)

NESDIS 15 NOAA N-ROSS/ERS-1 Environmental Data Development (NNEEDD) Products and Services. Franklin E. Kniskern, February 1985, (PB86 213527/AS)

NOAA Technical Report NESDIS 42

Simulation Studies of Improved Sounding Systems

H. Yates[1]
D. Wark[1]
H. Aumann[2]
N. Evans[2]
N. Phillips[3]
J. Susskind[4]
L. McMillin[1]
A. Goldman[5]
M. Chahine[2]
L. Crone[1]

[1]National Environmental Satellite, Data, and Information Service
[2]Jet Propulsion Laboratory
[3]National Meteorological Center, National Weather Service
[4]Goddard Space Flight Center, NASA
[5]University of Denver

Washington, DC
February 1989

U.S. DEPARTMENT OF COMMERCE
Robert A. Mosbacher, Secretary

National Oceanic and Atmospheric Administration
William E. Evans, Under Secretary

National Environmental Satellite, Data, and Information Service
Thomas N. Pyke, Jr., Assistant Administrator

TABLE OF CONTENTS

SIMULATION STUDIES OF IMPROVED SOUNDING SYSTEMS

ABSTRACT. Two instrument designs for indirect satellite sounding of the atmosphere in the infrared are represented by the High-resolution Infra-Red Sounder, Model 2 (HIRS-2) and by the Advanced Meteorological Temperature Sounder (AMTS). The former is one of a complement of three sounding instruments used operationally by the NOAA satellites; and the latter is conceptual and has not been carried on a satellite, but has design features which should, in principle, improve indirect soundings in the troposphere.

This study was conceived to test the relative capabilities of the two instruments by simulating satellite measurements from a group of temperature soundings, allowing the two participants to retrieve the temperature profiles from the simulated data, and comparing the results with the original temperature profiles.

Four data sets were produced from radiosonde data extrapolated to a suitable altitude, representing continents and oceans, between 30S and 30N. Two sets were for simulated clear conditions, and two were for simulated partly cloudy states. Optical transmittances, computed by a procedure of one of the participants, were distorted in ways designed to give no advantage of prior knowledge to either participant. For the cloudy portion of the study, clouds were modeled by their height, size, abundance, multiplicity of layers, and emissivity.

From the information available to each participant, temperature profiles were retrieved by the two different methods in use, statistical regression and inversion of the radiative transfer equation, to forestall the obscuration of significant results by the retrieval methods employed (that is, the test is one of instruments, not methods of retrieval). Statistical representations for comparison of the retrieved temperature profiles with the original profiles form the only results of the test, the original profiles being withheld in anticipation of future use of those data.

For one of the clear sets, containing 1600 soundings, the temperature soundings were made available to the participants, for private exploration of procedures and a statistical base. The other set, containing 384 soundings, formed the test set proper. The temperature soundings for this set were kept secret from both participants. A similar procedure with respect to availability of temperature and cloud information was followed for the cloudy portion of the study, with six examples for exploration, and 40 soundings for the test set in which the temperature and cloud information was unknown to the participants.

Results show the essential consequence of greater spectral purity, concomitant increase in the number of spectral intervals, and the better spatial resolution in partly clouded areas. At the same time, the limitation of the HIRS-2 without its companion instruments leads to some results, particularly in the stratosphere, which should be ignored in comparing the two instruments. Nevertheless, there is a clear superiority of AMTS results in the troposphere, amounting to several tenths of a degree, in both the clear and partly cloudy areas. This would indicate that some of the design features of the AMTS should be considered when future infrared sounding instruments are designed.

1. INTRODUCTION (H. Yates)

Temperature and humidity soundings of the earth's atmosphere from space evolved from a proposal made by Dr. L. D. Kaplan in 1959 [1]. The first research instruments designed to test the concept were flown on Nimbus-3 and -4 in 1969 and 1970. The first operational deployment of sounding instruments aboard NOAA spacecraft was on the ITOS series beginning in 1972. Continued refinement and improvement of the operational instruments followed, and continues today. It is anticipated that refinement and improvement will continue into the foreseeable future since viable suggestions for providing more accurate soundings and more complete coverage remain to be tested.

The first experimental instruments were called SIRS-A and SIRS-B (Satellite Infrared Spectrometer). These instruments were Fastie-Ebert spectrometers with an individual detector in the focal plane for each spectral channel used. They were followed by the experimental Infrared Temperature Profile Radiometer (ITPR) on Nimbus-5, a filter instrument rather than a spectrometer. In the experimental line of instruments are also two microwave radiometers, Nimbus-E Microwave Spectrometer (NEMS) and Scanning Microwave Spectrometer (SCAMS) on Nimbus-5 and -6, respectively. Based upon these experimental instruments, the Vertical Temperature Profile Radiometer (VTPR) provided the first operational soundings from the ITOS series starting in October 1972. This was supplanted by the TIROS Operational Vertical Sounder (TOVS) aboard the improved operational satellite, TIROS-N. TOVS, which became operational on December 1, 1978, which has been maintained since that date, consists of three separate instruments: the High Resolution Infrared Sounder, the Microwave Sounding Unit (MSU), and the Stratospheric Sounding Unit (SSU) provided by the British Meteorological Office. Today, we are considering improvements to the TOVS system, primarily through greater reliance on microwave channels using an Advanced Microwave Sounding Unit (AMSU) and possibly more advanced infrared instruments such as the Advanced Meteorological Temperature Sounder (AMTS) or the High Resolution Interferometer Sounder (HIS).

In every instance in the above sequence of instruments, simulation studies were performed prior to launch which indicated a level of performance that was never achieved in actual operations. Simulation studies are important in order to provide a good indication of the accuracy and coverage one can expect with some confidence. They are, in fact, more important managers of operational satellites today than they have been in the past. While NASA operated the experimental Nimbus satellites, it was possible to test new instruments and concepts in space before committing to an operational deployment. Today, with Nimbus canceled and no available alternative space platform on which to test, the decision to change or augment the operational instruments must be based on limited aircraft or balloon measurements and simulation tests. The weaknesses and shortcomings of the simulation tests in the past have led the management of NESDIS to seek more valid tests which will provide a more accurate prediction of performance in space of any proposed new instrumental configuration. Toward this end, NESDIS, the National Meteorological Center (NMC) of the National Weather

Service (NWS), and the NASA/Goddard Space Flight Center (GSFC) have cooperated in the design of a simulation test which is currently being used to compare the currently operational TOVS, and the AMTS, a new instrument proposed by the NASA Jet Propulsion Laboratory. The test will also be used to evaluate the HIS when the procedures to do so have been developed and approved by NASA and NOAA.

1.1 Description of the Test

Past simulations appear to have several weaknesses: (1) simulation of all aspects of the real environment in which the space instrument will work is either not possible or very difficult and expensive leading to short-cuts; (2) in the simulation process, the true temperature or humidity profile is known at the start, whereas in real operation the only "truth" to which the derived profiles can be compared is the set of radiosonde soundings, which are themselves imperfect; (3) they have been carried out by the proponents of a new instrument system and hence may not be as objective as desired. The objectives of the current test are to simulate as closely as possible real operational conditions and minimize the effect of the above three factors.

The test starts with the selection of a referee or test manager. In the present case, the manager is Dr. Norman Phillips of the National Weather Service's National Meteorological Center, an expert in temperature structure of the atmosphere and a nonpartisan in the area of instrumentation. The referee selects a large sample of real atmospheric soundings with a representative, global and seasonal distribution, and divides it into two sets: a collocation data set, and a test data set. Both sets are required because some of the concepts being tested are based upon regression solutions which require a set of soundings (with radiances) from which to generate the coefficients used in the retrieval process. The collocation data set of temperatures is therefore available to all participants.

Both sets of temperatures are supplied to a laboratory capable of calculating radiances from temperature profiles. This laboratory, independent of those conducting the actual test, utilizes procedures for calculating radiances that are acceptable to the test participants but does not disclose to those participants the temperature profiles from which they have calculated the radiances. Each test participant, using the coefficients generated from the collocation data set (provided their method is based upon a regression solution), retrieves the temperature profile from the radiances calculated from the test data set. They then send their derived profiles back to the test referee who compiles a statistical evaluation such as that which is normally available in operational procedures. He does not, at any time, disclose a one to one comparison between an original sounding and a derived sounding, and he does not release to any outside party test results other than the statistical result. In this fashion, the test remains pure and available to be used for testing later ideas, which can then be compared with the earlier results on a common ground.

The actual conditions are made as close to reality as possible. For example, in the real world, one does not have the boundary term, the actual temperature of the surface of the earth or the sea, and the test provides only what would be available operationally such as the NMC shelter temperature analysis. Clouds are simulated in a manner as close to reality as possible, employing partly cloudy and totally cloudy scenes, clouds of varying opacity and multi-layer cloud situations. Some parameters, such as instrument noise, are introduced in varying amounts so that the tests will also provide some measure of the cost-benefits relationship between performance and those engineering parameters where there is a design choice.

This test will certainly not be perfect. It cannot account, for example, for the differences between satellite soundings and radiosondes that are due to the inaccuracies inherent in the radiosondes themselves, both the random difference between the individual members of one type of sonde and the biases that are known to exist between different types of sondes. However, it will provide a useful means of comparing competing concepts on a common basis and will come far closer than ever before to predicting performance from space. As such it will be a key tool in the process of defining the satellite sounding system of the future.

2. INSTRUMENT DESCRIPTIONS

2.1 High-resolution Infrared Radiation Sounder-2 (HIRS-2) (D. Wark)

Requirements for the HIRS-2 evolved during several years when experimental and operational instruments were carried on the NIMBUS and NOAA satellites. The history of the instruments indicates a progression designed to provide the most suitable and practical set of measurements to satisfy the needs for temperature, humidity, and ozone retrievals. Objectives were accomplished by expanding the number of spectral intervals and the spatial coverage, while increasing the spatial resolution. Table 2.1.1 lists some of the instruments and their characteristics [2-6].

Table 2.1.1 Infrared sounding instruments anteceding HIRS-2

ACRONYN	SATELLITE	SPECTRAL RANGE (μm)	NO. OF SPECTRAL INTERVALS	SPECTRAL RESOLUTION (cm^{-1})	SPATIAL RESOLUTION (km)	SCAN
SIRS	NIMBUS-3	11-15	8	5	226	NO
IRIS	NIMBUS-3	5-20	1051	5	307	NO
SIRS-B	NIMBUS-4	11-36	14	5	226	3 STEPS
IRIS-D	NIMBUS-4	5-25	1051	2.8	94	NO
SCR	NIMBUS-4	10.5-15	9	3-12	130-185	NO
ITPR	NIMBUS-5	3.45-15	7	5.3-430	28	14 STEPS 10 LINES
SCR	NIMBUS-5	2.35-15	16	3.4-100	29-42	3 BOXES
VTPR	NOAA-2 TO 5	12-19	8	3.5-18	55	23 STEPS
HIRS	NIMBUS-6	0.7-15	17	2.8-892	24	42 STEPS

2.1.1 Spatial resolution and coverage

For instruments anteceding ITPR, soundings were made from a single set of simultaneous measurements of radiance. To account for clouds interfering with radiation from the atmospheric gases, it was necessary to devote one or two largely-independent measurements to the determination of cloud heights and amounts. As a result, those measurements could not be used for soundings, causing degradation in the quality of results for the lower troposphere.

To correct for this deficiency in partly cloudy areas, instruments were designed to sample with enhanced resolution the areas from which individual soundings were to be obtained. By a technique in which adjacent measurements were compared [7], the radiances for cloudless portions could be deduced even in the absence of a completely cloud-free observation.

A single pair of adjacent observations is likely to introduce serious errors into the deduced values of clear radiances unless certain conditions prevail: there is a single cloud layer at the same height in the fields-of-view of the pair; there are no significant horizontal gradients of air tem-

perature, humidity or surface temperature; and there is a large difference in cloud cover between the two fields-of-view. The alternative is to have enough adjacent measurements to permit a judgment of the unclouded radiances from statistical analysis. The lower limit on the number of measurements required is nine (3x3), but a better result is obtained if the number is almost 50.

To establish the resolutions, the spacing between soundings must be specified. Requirements for the First GARP Global Experiment (FGGE) were for soundings to be spaced 500 km apart. Considering needs for numerical prediction models of the near future, this dimension was reduced to 250 km. Therefore, the mean spacing of the HIRS-2 measurements was specified to be about 1/7 of 250 km, or 35 km.

Global coverage is desirable each 12 hours if possible. But an upper limit of 60 degrees was planned upon the local zenith angle (the zenith angle of the satellite as viewed from the earth) of the observations; beyond that limit, observations would not be useful for numerous reasons. For the TIROS-N/NOAA series of satellites at nominal altitudes of 833 km, this restriction results in an unavoidable data gap between 35S and 35N. The deficiency is not judged to be serious.

The final consideration in resolution is the effect of the clouds' dimensions. At very low resolution, the probability of observing either clear or overcast conditions within the field-of-view is small. As resolution is increased, there will be increasing numbers of observation at or approaching clear or overcast conditions. Very cloudy conditions will be rejected in the analyses of the data, but higher yields of acceptable data result from improved resolution. Unpublished results from studies of this problem indicate that resolutions should be a few kilometers and not more than a few tens of kilometers.

From these considerations, and from technological constraints, the resolution and scan pattern for HIRS-2 were established. Figure 2.1.1 depicts the fields-of-view projected on the earth. There are 56 spots per scan line, with resolutions varying between about 12 x 18 km^2 and 30 x 58 km^2. It may be noted that there is a large gap between observations in the nadir on successive scan lines to that there will be no overlap at the extreme positions at the left and right. The 2240 km scan width leaves a gap of about 500 km at the equator.

2.1.2 Spectral intervals and spectral resolution

From Table 2.1.1 we see that there has been an evolutionary increase in the number of spectral intervals sampled. In the SIRS-A there were seven intervals in the 15 μm CO_2 band and one in the window at 11 m, all with resolutions of 5 cm^{-1}. As shown by Weinreb and Crosby [8], an increase in the number of intervals there would have little benefit other than a statistical suppression of noise. On the other hand, the absence of measurements in H_2O bands was a handicap because of the inability to account for the influence of water vapor absorption in the more transparent portions of the carbon dioxide band. This led to the inclusion of six

intervals in the H_2O rotational band between 18 μm and 36 μm in the SIRS-B.

Another expansion of the number of intervals was to languish as new spectral intervals and greater sampling capabilities were exploited. The ITPR made use of the 3.7 μm window, better spatial resolution and increased sampling rates. The VTPR, on the other hand, was confined to the spectral region 12-18.8 μm, with better geographical coverage and moderate spatial resolution. The designs of these instruments were guided mainly by the condition of technology and by spacecraft limitations. Each had a single water vapor channel to aid in temperature retrievals and to provide an estimate of total water vapor.

The prototype for the HIRS-2 was the HIRS, which incorporated as well as spectral intervals equivalent to those in SIRS-A, several channels in the N_2O and CO_2 bands at 4.8 μm and 4.3 μm; the greater dependence of the Planck function at those wavelengths was deemed to provide significantly greater information than from the 15 μm measurements alone. Two channels in the 6.3 μm water vapor band were designed to give water vapor profiles (not just total water vapor), the short wavelength window at 3.7 μm was retained for specifying cloud effects, and a channel at 0.69 μm was added to

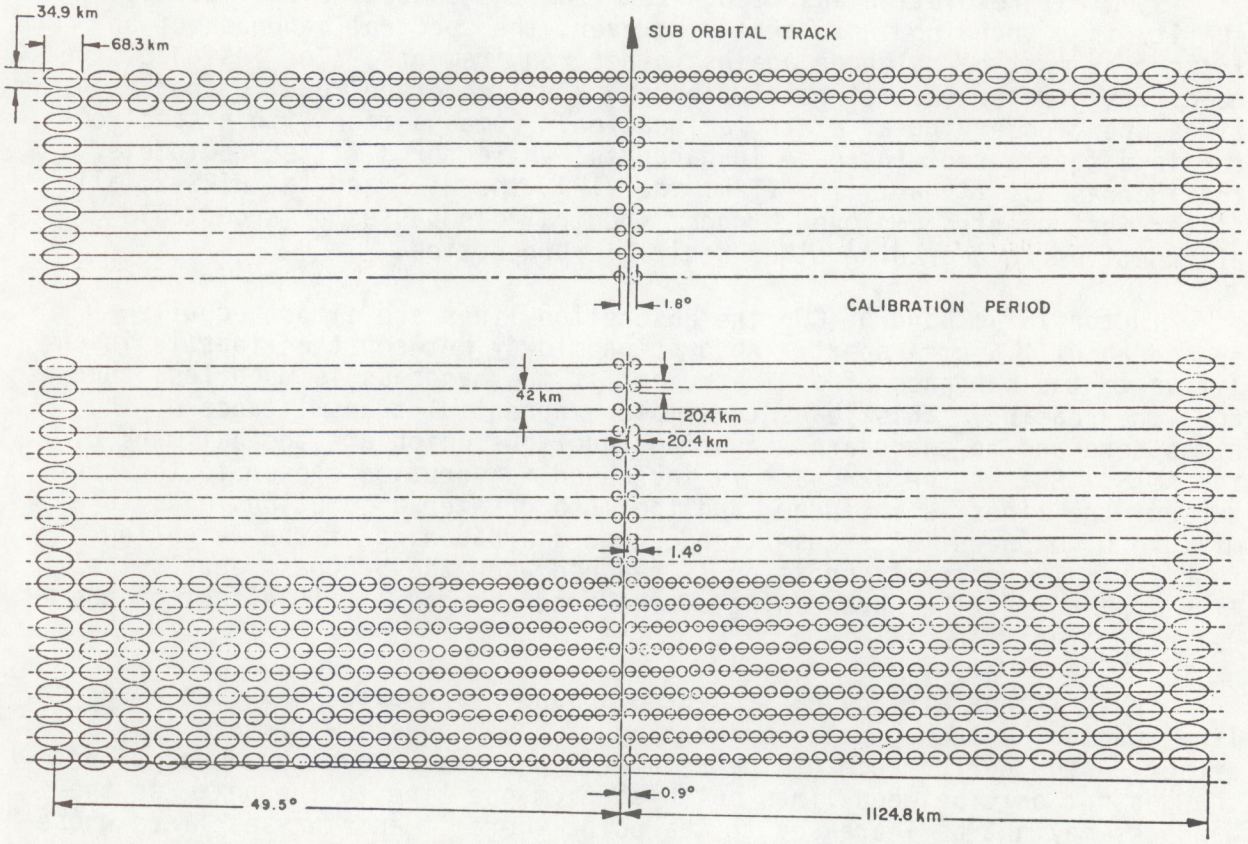

Figure 2.1.1 Scan pattern of the HIRS-2 projected on the earth from a satellite at 833 km altitude. Left to right motion is achieved by a step-scanning mirror which remains fixed during the 60 ms observation; successive scan lines result from the satellite motion, with a repetition rate of 6.4 seconds. Circular and oval outlines show the observed areas.

assist in the cloud estimates during daytime (the short wavelength window is significantly affected by reflected solar radiation).

The HIRS-2 modifications to HIRS included: the addition of one channel in the 6.3 μm water vapor band to increase the capability for determining water vapor profiles; a channel in the 9.6 μm ozone band, which was to provide a means of correcting for the influence of the weak 14.3 μm band on the nearby CO_2 channels, as well as meeting a secondary objective of estimating total ozone; and a second short wavelength channel at 4 μm to provide further aid in evaluating the reflected solar radiation.

It is seen that the transition over the years was to expand the scope of the instruments from that of obtaining temperature retrievals to the inclusion of water vapor profiles and some estimate of total ozone as well. In addition, new tools were added in the form of short wavelength channels, both for determining the effects of clouds and for exploiting the variable nature of Planck radiation with wavelength. However, the additions introduced the unwanted influence of reflected solar radiation in some channels, which demanded further spectral information.

Spectral resolution was recognized from the outset as an important quality in a sounding instrument. However, the spectral bandpass of an instrument must be balanced against other requirements. For instance, the needs for greater spatial resolution and areal coverage require shorter times spent observing at a single location. Compensation with a spectrometer is a square-root increase in bandpass, while for a filter radiometer the increase is linear. The ITPR, the VTPR, the HIRS and the HIRS-2, all filter instruments, employed broader spectral bandpasses as acceptable alternatives to degrading other desirable properties.

In the 15 μm band of CO_2 the absorption lines are almost equally spaced about 1.6 cm^{-1} apart. Absorption midway between the lines is insensitive to the bandpass of an instrument if the bandpass is much less than the line spacing. This leads to simple exponential transmittance of the atmosphere and to the sharp weighting functions which are the hallmark of the AMTS. But as the bandpass is increased, absorption closer to the centers of the lines is included, and the much greater absorption leads to a mixture of exponential transmittances and a broadening of the weighting function. The poorest condition is reached when the bandpass equals the line spacing; further broadening of the bandpass has little effect on the weighting function.

Thus, if one already has accepted a bandpass greater than the absorber line spacing, a much greater broadening of the bandpass will have little effect on the performance of the retrieval process. However, absorption changes not only between lines but also from one line to the next, so the bandpass may not be increased to the point where it encompasses lines whose strengths are greatly different. This imposes upper limits to bandpasses. In several unpublished studies, it has been shown that a useful compromise can be achieved with multi-layer film filters having half-widths of about 15 cm^{-1} in the 15 μm band.

Bandpasses in the other spectral regions are subject to similar arguments, but the reasoning may differ where line spacings are not equal. The HIRS-2 bandpasses have all been compromises, since detector noise imposes the ultimate limitation. Given the dwell time of 60 ms, the optical design and loss factors, and the detector's detectivity, what bandpass is required in each spectral interval? If that specification is unacceptable, what other factor in the design is to be sacrificed? Table 2.1.2 summarizes some of the resulting characteristics of the HIRS-2.

Table 2.1.2 Some characteristics of the HIRS-2 channels.

Channel	Frequency (cm^{-1})	Bandpass (cm^{-1})	Absorber	Level (mb)	Purpose
1	668	3.5	CO_2	30	Atmos. Temp.
2	679	10	CO_2	60	Atmos. Temp.
3	691	12	CO_2	100	Atmos. Temp.
4	704	16	CO_2	400	Atmos. Temp.
5	716	16	CO_2	600	Atmos. Temp.
6	732	16	CO_2	800	Atmos. Temp.
7	748	16	CO_2	900	Atmos. Temp.
8	898	35	Window	Sfc.	Sfc.Temp./Clds.
9	1028	25	O_3	25	Ozone Inf./Amt.
10	1217	60	H_2O	900	Water Vapor
11	1364	40	H_2O	700	Water Vapor
12	1484	80	H_2O	500	Water Vapor
13	2190	23	N_2O	1000	Atmos. Temp.
14	2213	23	N_2O	950	Atmos. Temp.
15	2240	23	N_2O/CO_2	700	Atmos. Temp.
16	2270	23	N_2O/CO_2	400	Atmos. Temp.
17	2361	23	CO_2	5	Atmos. Temp.
18	2512	35	Window	Sfc.	Sun Reflect.
19	2617	100	Window	Sfc.	Sfc.Temp./Clds.
20	14367	1000	Window	Cld.	Sun Reflect.

2.2 Advanced Meteorological Temperature Sounder (AMTS) (H. Aumann and N. Evans)

2.2.1 AMTS System Rational and Description

During the past 20 years considerable progress has been made in remote sensing of vertical temperature profiles; different techniques have been developed to recover profiles globally with an accuracy of 2 to 2.5K. This accuracy, however, falls short of the requirements for numerical prediction models. The need for improved sounding is accentuated by the fact that during the past decade, models have evolved far more rapidly than the capabilities of satellite-borne temperature sounders to supply accurate data. For example, the various numerical circulation models developed at NASA-GSFC, NOAA, GFDL, and NCAR have eight layers or more below the 100 mb pressure level. The current generation of sounders is capable of sounding the troposphere at only three or four levels. The limitation in vertical resolution is caused mainly by the broadness of weighting functions of current instruments. When the weighting functions are broad, emitted energy reaching the satellite in each channel will have components originating from a thick layer of the atmosphere, thereby making reconstruction of fine-scale vertical details practically impossible. Because of this, as well as cloud contamination, contamination by O_3, H_2O and other minor constituents, and surface effects, the rms errors in the retrieved temperature profiles remain high.

The proposed AMTS is a high spectral resolution ($\nu/\Delta\nu$ = 1200) infrared sounder capable of doubling the vertical resolution of atmospheric temperature profiles and improving their accuracy by 0.5K to 1.0K. In addition the proposed sounder permits improved determination of a wide variety of meteorological parameters on cloudiness, surface temperatures and air-surface interactions. These improvements are accomplished in part through multispectral observations with a set of narrow band-pass channels properly selected from the high J-lines in the R-branch of the 4.3 μm CO_2 band. This set is complemented by a set of window, humidity and temperature channels in the 3.7, 6.3, 9 and 15 μm regions positioned away from absorption lines due to minor atmospheric constituents [9]. A representative AMTS channel set, used for the HIRS/AMTS comparison tests, is shown in Table 2.2.1. Table 2.2.2 illustrates the effects of absorption by O_3 and H_2O on the HIRS and AMTS temperature sounding channels. Weighting functions for the AMTS temperature sounding channels are shown in Figure 2.2.1, and for some of the water vapor channels in Figure 2.2.2.

The R-branch of the 4.3 μm CO_2 band between 2383 cm^{-1} and 2390 cm^{-1} is the best spectral region for temperature sounding channel selection. It takes advantage of the temperature dependence of the high-J lines, which acts to enhance the pressure effect in the troposphere where the temperature decreases with height. It also makes use of the strong dependence of the Planck function on changes in temperature. Consequently a set of 4.3 μm CO_2 band channels was selected to determine the temperature profile in the lower troposphere and a corresponding set from the 15 μm CO_2 band to determine the rest of the temperature profile as shown in Table 2.2.1.

The AMTS was designed to support a method developed by Chahine [10,11]

Table 2.2.1 AMTS channels

Band	Channel Number	Frequency $\nu(cm^{-1})$	Wavelength $\lambda(\mu m)$	Bandwidth $\Delta\nu(cm^{-1})$	Molecular Constituents**	Main Function
	1*	606.95	16.476	0.50		Cloud
	2*	623.20	16.046	0.50	CO_2, N_2O, H_2O, O_3	Filtering
	3*	627.80	15.929	0.50		
	4	634.30	15.765	0.50		
1	5	646.60	15.466	0.50		
	6	654.35	15.282	0.50		Temperature
	7	665.55	15.025	0.50	CO_2, O_3, H_2O, N_2O	Profile
	8	666.85	14.996	0.50		Upper
	9	668.15	14.967	0.50		Atmosphere
	10	669.45	14.938	0.50		
	11	1203.00	8.313	1.00		
2	12	1231.80	8.118	1.00	N_2O, H_2O	H_2O Window
	13	1770.30	5.646	1.50		
	14	1805.50	5.539	1.50		
	15	1839.40	5.437	1.50		
3	16	1844.50	5.422	1.50	H_2O, N_2O, CO_2	H_2O Profile
	17	1850.90	5.403	1.50		
	18	1889.57	5.292	1.50		
	19	1930.10	5.181	1.50		
	20	2384.00	4.195	2.00		
	21	2386.10	4.191	2.00		Temperature
	22	2388.20	4.187	2.00	CO_2, H_2O	Profile
	23	2390.20	4.184	2.00		Lower
4	24	2392.35	4.180	2.00		Atmosphere
	25	2394.50	4.176	2.00		
	26	2424.00	4.125	2.50	N_2O, CO_2, H_2O	Air Surface T
	27	2505.00	3.992	2.50	N_2O, CO_2, H_2O	Surface
	28	2686.00	3.723	2.50		Temp

*60GHz O_2 frequencies can be substituted for Channels 1-3
**In order of decreasing line strengths.

to retrieve vertical temperature profiles from IR radiance measurements, even in the presence of clouds. This method, which has been verified by Susskind [12] using current HIRS sounder data, is based on the assumptions that 1) the cloud distribution is inhomogeneous, and 2) that no field of view is necessarily cloud free. In order to correct for the effects of clouds on the infrared observations, radiance data is required in two spectral regions and over two adjacent fields of view having different amounts of cloud cover. In the case of the AMTS three long-wave channels from the 15 μm CO_2 band were selected to correct for the effects of cloud and haze. (Alternatively it would be possible to use appropriate microwave channels from the 60 GHz O_2 line.)

To account for surface reflectivity and emissivity and to retrieve accurate skin surface temperature of both land and oceans a set of "super window" channels were chosen from the 3.7 μm region. The use of narrow bandpasses is essential for selecting extremely transparent windows.

Table 2.2.2. Effects of contamination by O_3 and H_2O on the observed brightness temperature of Temperature Sounding Channels.

HIRS ($\Delta\nu/\nu$ = 1%)					AMTS ($\Delta\nu/\nu$ = 0.1%)				
Channel ν (cm^{-1})	ΔT (K) O_3	ΔT^* (K) H_2O	ΔT^* (K) O_3+H_2O	Peak sensitivity (mb)	Channel ν (cm^{-1})	ΔT (K) O_3	ΔT^* (K) H_2O	ΔT^* (K) O_3+H_2O	Peak sensitivity (mb)
January, 70th parallel									
668.4	- .1	0	- .1	30	668.2	0	0	0	3
679.05	- .03	0	- .03	60	669.4	.02	0	.02	20
690.2				100	666.8	.04	0	0	30
703.7	- .83	- .09	- .92	280	665.6	0	0	0	70
716.4	-2.01	- .08	-2.09	475	654.4	- .02	0	- .02	90
732.4	-1.59	- .64	-2.23	725	646.6	- .06	0	- .06	180
749.5	-1.20	- .41	-1.61	surface	634.3	- .07	0	- .07	270
2190.4	0	- .04	- .04	surface	2384.0	0	0	0	350
2212.6	0	0	0	650	2386.1	0	0	0	570
2240.1	0	0	0	340	2388.2	0	0	0	700
2276.3	0	0	0	170	2390.2	0	0	0	850
					2392.4	0	0	0	surface
					2394.5	0	0	0	surface
July, 20th parallel									
668.4	.1	.02	.12	30	668.2	.01	0	.01	3
679.05	.42	0	.42	60	669.4	.10	0	.10	20
690.2				100	666.8	.37	0	.37	30
703.7	- .41	- .47	- .88	280	665.6	.19	0	.19	70
716.4	-1.30	- .59	-1.89	475	654.4	.1	0	.1	90
732.4	-1.16	-1.39	-2.55	725	646.6	.1	0	.1	180
749.5	- .89	-3.41	-4.30	surface	634.3	0	- .06	.06	270
2190.4	0	-1.16	-1.16	surface	2384.0	0	0	0	350
2212.6	0	- .74	- .74	650	2386.1	0	- .01	- .01	500
2240.1	0	- .31	- .31	340	2388.2	0	- .01	- .01	650
2276.3	0	- .07	- .07	170	2390.2	0	- .01	- .01	850
					2392.4	0	- .03	- .03	surface
					2394.5	0	- .09	- .09	surface

*Effects of H_2O continuum are not included.

Simulation studies have shown that the AMTS can provide simultaneously many important weather and climate parameters with high accuracy and with the consistency in quality needed to assess climate changes. The retrieved parameters include:

1. Temperature profiles derived in the presence of up to three

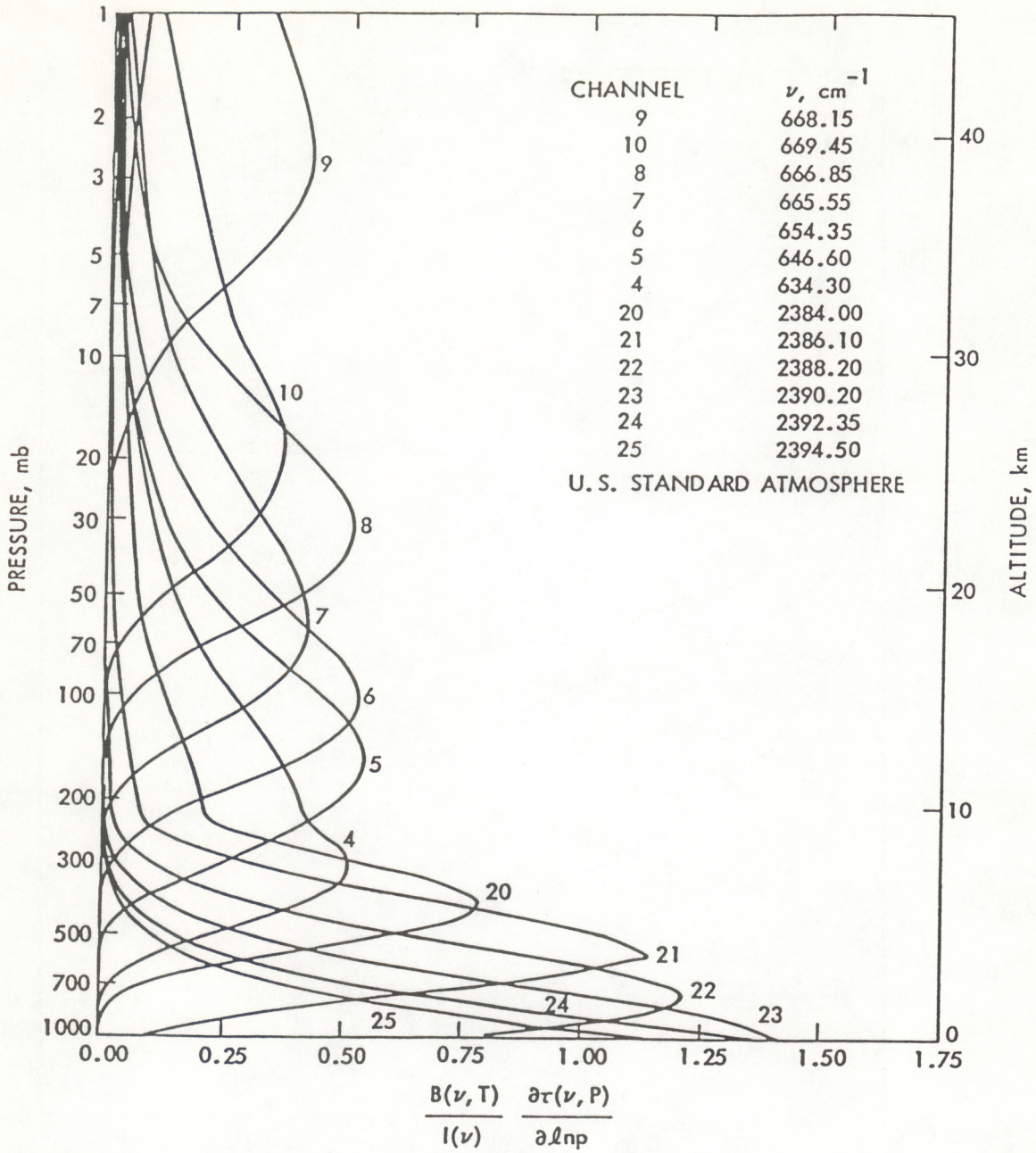

Figure 2.2.1 Weighting functions of AMTS temperature sounding channels.

layers of broken clouds with an absolute accuracy of 1.5K at 8 distinct levels below 100mb.

2. Relative humidity profiles at up to 6 distinct levels between the surface and 200mb, and the total precipitable water vapor.

3. Sea-surface temperature with an absolute accuracy of 1K and a relative accuracy of 0.5K.

4. Air-sea temperature difference with a relative accuracy of

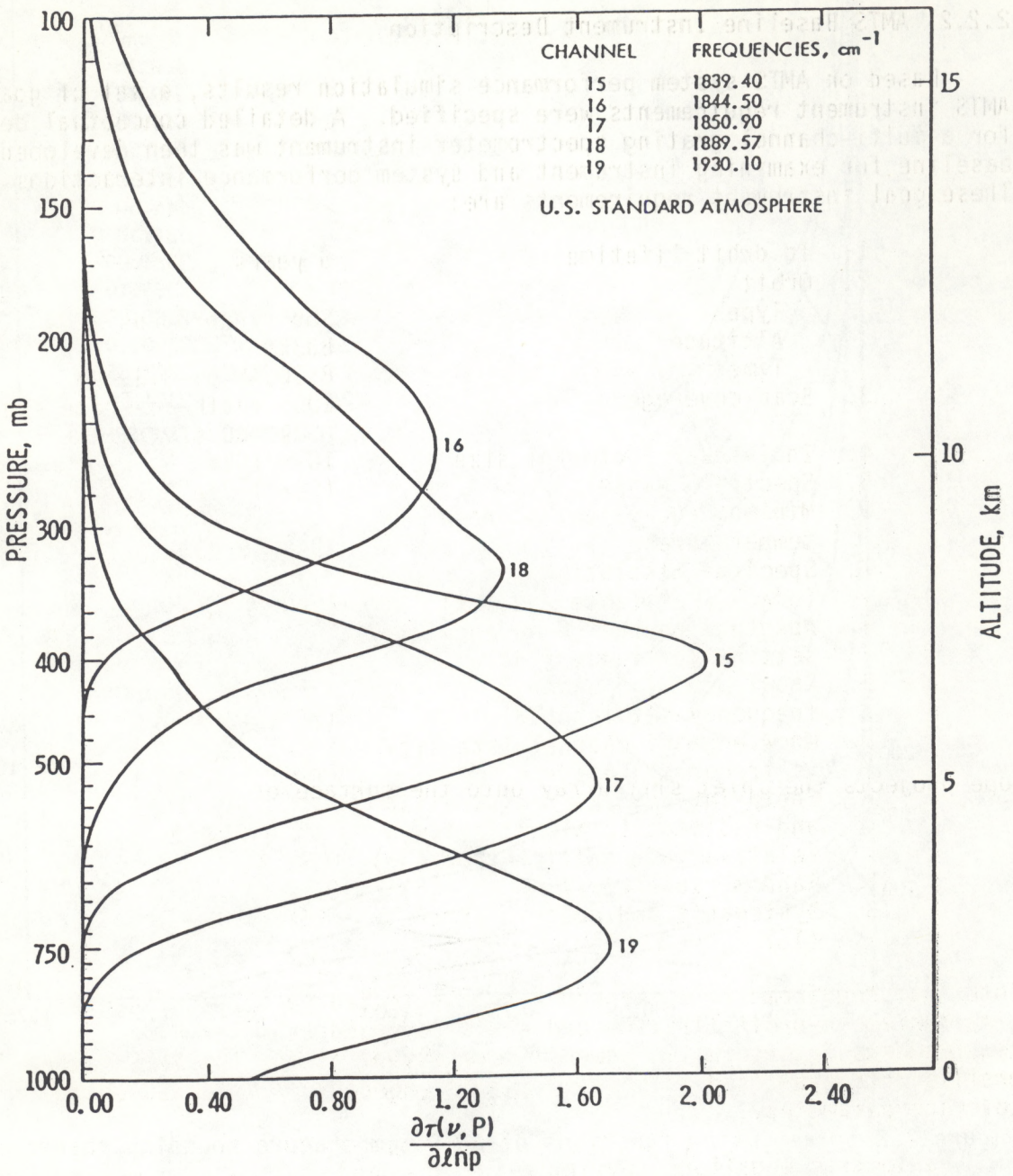

Figure 2.2.2 Weighting functions of AMTS water vapor channels.

± 1K.

5. Surface temperature of land with an absolute accuracy of 1.5K.

6. The fractional cover and height of multiple cloud layers (as seen from above) with an absolute accuracy of 0.05 and 0.25 km respectively.

7. Total ozone burden of the atmosphere.

2.2.2 AMTS Baseline Instrument Description

Based on AMTS system performance simulation results, a set of goal AMTS instrument requirements were specified. A detailed conceptual design for a multi-channel grating spectrometer instrument was then developed as a baseline for examining instrument and system performance interactions. These goal instrument requirements are:

1.	In orbit lifetime	5 years
2.	Orbit	
	Type	Sun synchronous
	Altitude	833km
	Time	8:30 AM or 3:30 PM
3.	Scan coverage	100% earth coverage every 24 hours
4.	Individual footprint size	10 x 10km
5.	Spectral channels	(See Table 2.2.1.1)
6.	Minimum equivalent scene temperatures	194K to 233K
7.	Spectral Resolution - ($\nu/\Delta\nu$) (Ref.Table 2.2.1.1)	1200
8.	Absolute channel frequency setting tolerance (1σ)	7.5×10^{-5}
9.	Knowledge of channel frequency setting (1σ)	1.5×10^{-5}
10.	Knowledge of channel intensity vs frequency response	(TBD)
11.	Footprint spatial registration and radiometric simultaneity relative radiometric error (1σ)	0.1K ΔT
12.	Random radiometric error (1σ)	0.1K ΔT
13.	Systematic radiometric error (1σ)	0.5K ΔT

Note that requirements 1 through 4 were selected to satisfy assumed baseline system in-orbit lifetime and earth coverage requirements. Requirements 5 through 13, however, are essential for the AMTS method of profile retrieval, and are relatively independent of selected earth coverage parameters.

Parametric equations developed for the performance of a generalized grating spectrometer dictated the following optical design criteria for the AMTS instrument:

1. To minimize NEN per IFOV within limitations of a given dwell time, bandwidth, and achievable D*:

   a. Use a high dispersion grating
   b. Operate the grating near Littrow
   c. Use a large rectangular instrument aperture
   d. Use a square IFOV
   e. Where D* is essentially independent of detector area:

- Use a low F/NO detector field lens
- Immerse the detectors.

2. To further minimize NEN per IFOV for a given spatial coverage and spatial resolution, increase dwell time by:

   a. Use of a multi-channel instrument
   b. Use of linear arrays of detectors (and IFOV's) per spectral channel.

3. To control slit function wing response spectral crosstalk, use a wide grating; i.e., one with a large number of grooves.

4. To control scene spatial crosstalk and spatial simultaneity error, use low F/NO optics for the grating inlet collimator and foreoptics telescope.

An optics layout for the AMTS baseline grating spectrometer is shown in Figure 2.2.3. Details of the inlet slit and image plane optics are shown in Figure 2.2.4. This spectrometer design uses an R-2 Echelle grating in the 3rd through 13th orders. The grating is located at the center of curvature of an in-plane, off-axis double passed Bouwers concentric collimator. The inlet slit assembly consists of a linear array of nominally square inlet slits 16 elements long. This inlet slit array serves as the field stop for the instrument. It spatially defines the individual footprint elements, and pre-masks the exit slit assemblies in the spatial dimension to insure footprint spatial simultaneity. An off-axis Schwarzschild telescope projects the inlet slit array onto the surface of the earth from an 833 km altitude as an array of nominal 10 x 10 km individual footprints 160 km long overall at nadir. This array is step scanned +48° crosstrack by a rotating 45° scan mirror. The 10 x 10 km nadir footprints are contiguous, both along track and across track, resulting in 100 percent area coverage (imaging) of a continuous swath 2000 km wide. The focal plane assembly consists of 28 separate, simultaneously illuminated, linear detector arrays--one for each spectral channel. Each array is 16 elements long. Each detector element assembly uses a one percent bandwidth order filter located ahead of the exit slit jaws. An F/1 field lens, located just behind the exit slit jaws, images the instrument pupil--the grating--upon the detector element. Photoconductive HgCdTe detectors are used for Bands 1 and 2. Photovoltaic InSb detectors are used for Bands 3 and 4. Detector immersion lenses are used for the HgCdTe detectors only. The detector dewar is cooled to 75K. The spectrometer optics are cooled to 160K. The optical bundle is mechanically chopped forward of the inlet slit array.

The capability is provided for in-orbit spectral monitoring and alignment, using the 696.94672 nm and 966.54198 nm lines of neon as the spectral reference source. Three separate spectral reference slits, spatially displaced some distance to the sides of the IR signal slit array, are located in a thermally stable entrance slit mask which contains the IR slit array. The relative positions of the entrance slits are accurately known. Three separate pairs of spatial position discriminator detectors, one pair for

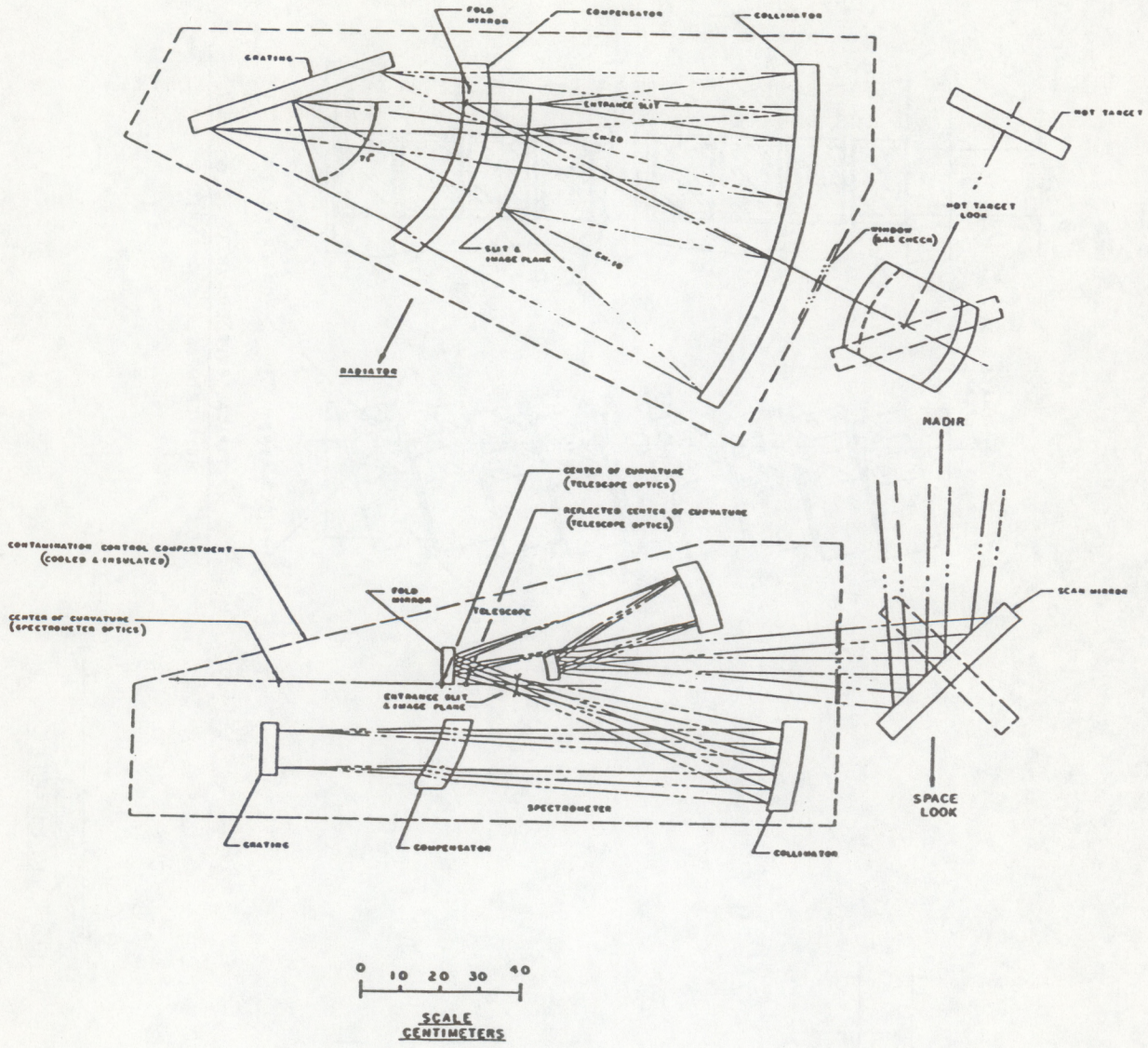

Figure 2.2.3 AMTS baseline grating spectrometer optics layout.

each spectral reference inlet slit, are located on the thermally stable image plane mask. The relative positions of the spectral discriminator detector arrays with respect to each other and to the IR image plane channel slits are also accurately known. Given the knowledge of relative slit positions and of the grating groove spacing, and given the measured spatial displacements of the spectral reference slit images, absolute grating incident and diffracted angles--and channel frequencies--can be determined through the solution of a set of three simultaneous equations. Within limits, channel frequency errors can be corrected by adjusting the grating angle. By rocking the grating angle, monochromatic slit function response

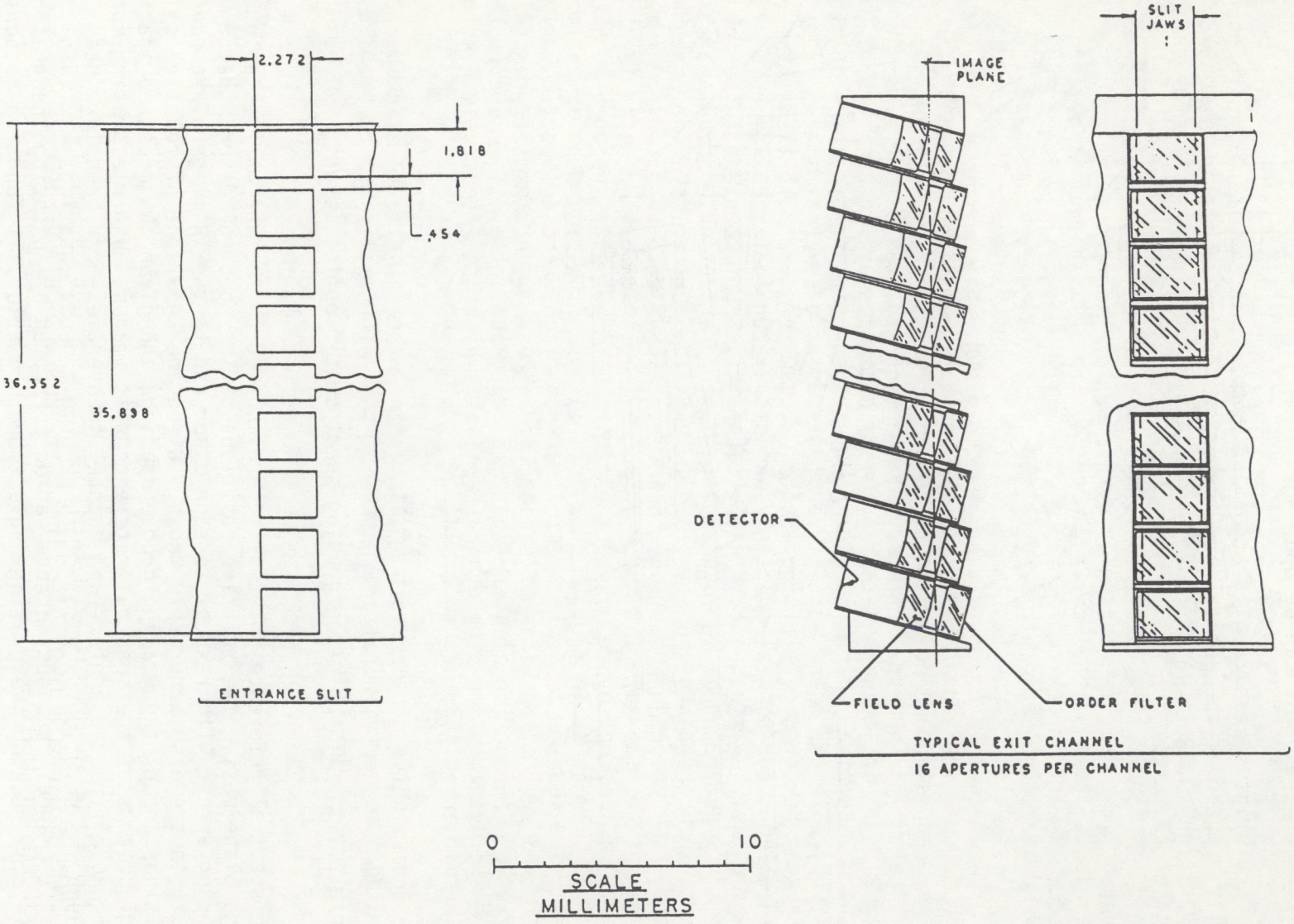

Figure 2.2.4 AMTS baseline grating spectrometer inlet slit and image plane optics detail.

changes of the spectral reference channels due to instrument alignment aberrations can be measured, and the knowledge of IR channel(s) intensity vs frequency response can be updated.

Footprint spatial registration and radiometric simultaneity are essentially assured by the optical and mechanical design of the instrument. The absolute radiometric goal requirement is admittedly pushing the current state of the art. The AMTS profile retrieval algorithm, however, can be "tuned" to reduce the effects of long term systematic radiometric errors, and we believe that substantially larger systematic errors can be tolerated. The most challenging aspect of the AMTS instrument design is the requirement for extremely precise relative radiometry. Identified sources of random radiometric error for the baseline instrument design are listed in Table 2.2.3. (In this context, "random radiometric error" includes all radiometric errors except long term systematic errors.) Error estimates per individual footprint element are summarized for each band. The mean and standard deviation of the one sigma values of the "Noise Effective Delta Temperature (NEΔT) within each spectral band are listed in Table 2.2.3. Buried within these summary estimates are the effects of individual spectral channel performance variations as a function of atmospheric profile and scene spatial contrast variations. Potentially major instrument performance limiting error sources are scene polarization effects and scene spatial crosstalk effects. Scene polarization errors can be effectively eliminated, at the price of instrument complexity, by making the instrument response independent of scene polarization. Scene spatial crosstalk errors cannot be eliminated within the instrument. They can be reduced four orders of magnitude, however, through deconvolution--or image processing--of the apparent measured scene image radiance values. The effects of these error reduction techniques have not been included in NEΔT values listed in Table 2.2.3. It should be noted that scene polarization effects are related to solar scattering from clouds, and are particularly severe over a limited range of scattering angles. Scene spatial crosstalk effects are a function of scene contrast and granularity. They are particularly severe only for high contrast scenes, which are effectively due to solar scattering from broken clouds.

Irrespective of the exact approach for future passive IR atmospheric sounding, the next generation sounding system will require an instrument capable of: 1) multispectral observations of the atmosphere and the surface, 2) relatively high spectral resolution, and 3) very high radiometric precision. A number of error sources identified for the AMTS baseline spectrometer conceptual design and the order of magnitude of the baseline instrument performance errors are predictive of the performance for any next generation IR sounder, whatever the exact system and instrument approach.

2.2.3 AMTS Instrument Noise

Noise equivalent radiance (NEN) values supplied for use in the HIRS/AMTS comparison tests are listed in Table 2.2.4. The NEN values listed are for individual 10 x 10 km (nadir) footprints.

Table 2.2.3. Random radiometric error summary-per footprint element.

ERROR SOURCE	NEΔT (1σ) ~ MEAN/STANDARD DEVIATION (K)				Remarks
	BAND 1	BAND 2	BAND 3	BAND 4	
GROUP 1					NEΔT ~ 1/√N for spatial integration of IFOV's. Error sources are uncorrelated.
a) DETECTOR SIGNAL CHANNEL NOISE	0.104/0.031	0.042/0.035	0.011/0.009	0.035/0.048	
b) SIGNAL CHANNEL DIGITIZATION ERROR	0.004/0.001	0.004/0.003	0.006/0.005	0.017/0.027	
c) DETECTOR CALIBRATION CHANNEL NOISE	0.033/0.001	0.013/0.011	0.004/0.003	0.011/0.015	
d) CALIBRATION CHANNEL DIGITIZATION ERROR	0.001/<.001	0.001/0.001	0.002/0.002	0.005/0.009	
GROUP 2					NEΔT not reduced by spatial integration of IFOV's. Error sources are uncorrelated.
a) GRATING ORDER CROSSTALK	<.001/<.001	<.001/<.001	<.001/<.001	<.001/<.001	
b) GRATING GRASS CROSSTALK	<.001/<.001	<.001/<.001	<.001/<.001	<.001/<.001	
c) SLIT FUNCTION WING RESPONSE CROSSTALK	0.124/0.095			0.026/0.045	
GROUP 3					NEΔT not reduced by spatial integration of IFOV's. Error sources are uncorrelated. Error can be eliminated by increasing instrument complexity.
a) SCENE POLARIZATION	<.001/<.001	<.001/<.001	0.114/0.097	0.309/0.154	
GROUP 4					NEΔT somewhat reduced by spatial integration of IFOV's. Error sources within Group 4 are correlated, but are not correlated with other group errors. Error can be reduced by deconvolution of the radiance image during ground processing.
a) APERTURE DIFFRACTION SPATIAL CROSSTALK	0.562/0.153			7.735/4.155	
b) MIRROR(S) BRDF SPATIAL CROSSTALK	<.001/<.001	<.001/<.001	<.001/<.001	0.017/0.012	
c) CORRECTOR LENS SCATTER CROSSTALK	0.002/<.001	0.002/<.001	0.012/0.006	0.426/0.320	
d) GAS CHECK SCATTER CROSSTALK	0.007/0.001	0.005/<.001	0.018/0.009	0.334/0.201	
e) GRATING DIFFUSE SCATTER CROSSTALK	<.001/<.001	<.001/<.001	<.001/<.001	<.001/<.001	
f) GRATING MASK SCATTER CROSSTALK	<.001/<.001	<.001/<.001	<.001/<.001	<.001/<.001	
g) IMAGE PLANE SCATTER CROSSTALK	<.001/<.001	<.001/<.001	<.001/<.001	<.001/<.001	
GROUP 5					NEΔT not reduced by spatial integration of IFOV's. Error sources are uncorrelated.
a) CHANGES IN SIGNAL CHANNEL AMPLITUDE NON-LINEARITY			(ERRORS BELIEVED SMALL)		
GROUP 6					NEΔT probably not reduced by spatial integration of IFOV's. Error sources are uncorrelated.
a) ELECTRICAL CROSSTALK			(ERRORS BELIEVED SMALL)		
GROUP 7					NEΔT probably not reduced by spatial integration of IFOV's. Error sources are uncorrelated.
a) MICROPHONICS			(ERRORS BELIEVED SMALL)		
GROUP 8					NEΔT not reduced by spatial integration of IFOV's. Error sources are uncorrelated.
a) NON-LINEARITY IN TIME RATE OF CHANGE OF RADIOMETRIC CALIBRATION RESPONSE			(ERRORS BELIEVED SMALL)		
GROUP 9					NEΔT not reduced by spatial integration of IFOV's. Error sources are uncorrelated.
a) VARIATION OF "APPARENT" EMISSIVITY OF HOT CALIBRATION TARGET			(ERRORS BELIEVED SMALL)		

The NEN values in Table 2.2.4 were supplied in the spring of 1980. Since then, the AMTS channel set and the baseline instrument design have been modified to some extent through evolution. The NEN values in Table 2.2.4 are still representative of AMTS performance capability, but are somewhat conservative in the sense that instrument noise values represented are in general somewhat greater than current estimates.

Table 2.2.4 AMTS NEN values for NASA/NOAA HIRS/AMTS comparison test

Channel	Wavenumber (cm^{-1})	Bandwidth (cm^{-1})	NEN (10 x 10km F.P.) ($w/cm^2 Sr\ cm^{-1}$)
1	606.95	0.50	51.2×10^{-9}
2	623.20	0.50	50.4 "
3	627.80	0.50	49.8 "
4	634.30	0.50	49.3 "
5	646.60	0.50	50.1 "
6	654.35	0.50	44.4 "
7	665.55	0.50	44.1 "
8	666.85	0.50	44.0 "
9	668.15	0.50	44.4 "
10	669.45	0.50	44.0 "
11	1203.00	1.00	2009×10^{-12}
12	1231.80	1.00	1834 "
13	1770.30	1.50	462 "
14	1809.50	1.50	291 "
15	1839.40	1.50	219 "
16	1844.50	1.50	201 "
17	1850.90	1.50	194 "
18	1889.57	1.50	147 "
19	1930.10	1.50	135 "
20	2384.00	2.00	56.4 "
21	2386.10	2.00	71.9 "
22	2388.20	2.00	58.6 "
23	2390.20	2.00	67.2 "
24	2392.35	2.00	59.7 "
25	2394.50	2.00	62.4 "
26	2424.00	2.50	38.8 "
27	2505.00	2.50	24.6 "
28	2686.00	2.50	19.7 "

3. SELECTION AND DEFINITION OF ORIGINAL PROFILES (N. Phillips)

3.1 Input profiles

The profiles were constructed from radiosonde reports that were selected, modified, and extended so as to give a meteorologically meaningful test and to eliminate irrelevant distractions that would complicate the interpretation of the results. For example, a completely random selection of radiosondes would not provide a good enough test of maritime conditions, where the greatest benefit of satellite temperatures is presumed to exist. On the other hand, locations over terrain of appreciable elevation were not used because in the real world such locations are typically mountainous, and this is not suitable for standard satellite retrieval methods.

3.2 Sampling considerations

The statistical retrieval technique requires a dependent set of temperature profiles and their associated radiances to establish a set of regression coefficients. Present NESDIS practice requires 400 profiles in such a set, collected over a 2-3 week period. The tests proper must be made on an independent set, however. The test set corresponding to a dependent data set consisted of radiances computed from 96 profiles selected from radiosondes taken in the 2-week period following that of the dependent set.

Four basic groups were prepared (winter and summer refer to Northern Hemisphere).

a. Winter 30N-60N
b. Winter 30S-30N
c. Summer 30N-60N
d. Summer 30S-30N

Each group contained a dependent (400) and test (96) set, for a total of 1984 profiles.[1]

Winter and summer data were taken from the Special Observing Period files of NMC upper air data accumulated for FGGE (IIA data) during the two periods December 24, 1978 - March 10, 1979 and April 29 - July 7, 1979. Five consecutive weeks were used in each period.

Equal representation was given in the dependent and test sets to continental and maritime stations. Equal representation was also given to each 10-degree latitude belt in the 30N-60N zone and to each 20-degree latitude belt in the 30S-30N zone.

---

[1]These sizes were chosen to reflect operational practice. Standard measures of statistical reliability are likely to be overshadowed by questions of meteorological representativeness and independence.

No sounding was considered that

a. Came from a station more than 300 m above sea level
b. Did not reach at least 100 mb
c. Lacked moisture reports (missing) below 700 mb
d. Had not passed the strictest of the NMC data quality checks
e. Had its significant level data missing.

To get the 400 profile dependent data sets, all eligible stations that met these five criteria in one continuous 3-week period were subject to a random final selection, subject only to the constraints of equal continental-maritime representation, equal division between Eurasia and North America in the 30N-60N zone, and equal representation for each of the 10-degree or 20-degree belts in each zone.

The test set of 96 profiles was based on radiosondes in the 2-week period following that of the corresponding dependent data set. Equal representation between land and ocean within each latitude belt was again required.

3.3 Modification and extension of temperature profiles

3.3.1 Temperatures at heights above the radiosonde top pressure

Radiosondes seldom reach pressures less than 10 mb, the typical termination level being more like 30 mb. Radiance computations required a temperature profile to a lower pressure and retrieved temperatures were assessed up to 16 mbs. The radiosondes therefore had to be supplemented above their termination level (for example, p_{top}) with a temperature T_{top}), both for radiance computations and for assessment. This was accomplished by using a reference data set for the years 1966-1968 accumulated by the Analysis and Information Branch at NMC from coincident radiosonde-rocket observations in that period. One-hundred soundings up to 0.1 mb were available in each of four relevant data groups:

Lat Belts	Months	Name
30N-60N	Oct-March	IIIB
30N-60N	Apr-Sept	IIIE
30S-60N	Oct-March	IIIC
30S-30N	Apr-Sept	IIID

These will be referred to as the high level supplement. (The soundings in this supplement set were selected by the availability of rocket data. Almost none of them are maritime. However, at the stratospheric levels in question here, continental observations are presumably reasonably representative of oceanic conditions.) For each radiosonde in the basic set, the five soundings from the appropriate high level supplement were selected that had the closest value of T to the radiosonde value at the smallest pressure value reached by the radiosonde that coincided with one of the pressure levels in the supplement. One of these five was then selected by a random process and joined on to the radiosonde with a small amount

of local vertical smoothing at the juncture. All soundings therefore terminated at 0.1 mb (about 67 km).

3.3.2 Correction to a uniform surface pressure

Following upon this vertical extension to 0.1 mb, the sounding was "stretched" so as to have a surface pressure of 1000 mb and a top pressure of 0.1 mb. Consider a temperature T at pressure p in the complete vertically extended sounding from p_{sfc} to 0.1 mb. T and p were replaced by a temperature T', valid at pressure p'. p' is given by

$$p' \text{ (millibars)} = 0.1 + \frac{(1000-0.1) * (p - 0.1)}{(p_{sfc} - 0.1)}$$

where p_{sfc} is the original surface pressure (which in its turn becomes 1000 mb). The temperature was changed by an adiabatic compression process to T':

$$T' = T (p'/p)^{R/c_p}$$

The largest value of (p'/p) was at the surface where

$$(p'/p)^{R/c_p} = (1000/P_{sfc})^{.28562}$$

This factor ranged between 0.989 to 1.009 for p_{sfc} ranging from 1040 to 975 mb. (Recall the 300 m limit on station elevation.)

This stretching step was desirable to establish complete uniformity in the layers for which retrieved temperatures were to be calculated. For example, if a variable surface pressure were allowed, one retrieval scheme might be willing to report a 1000-880 mb temperature even though the surface pressure was only 975 mb, while another scheme might not. This could confuse comparisons of the two schemes. Furthermore, the means by which the former scheme extended itself to 1000 mb were not relevant to this simulation test.

3.4 Moisture

Observed values (up to at least 700 mb) were required from the radiosonde reports. Their values were not changed in the stretching process used to convert all soundings to a standard surface pressure of 1000 mb; i.e., a value of 0.0055 for specific humidity reported at pressure 850 mb in the original sounding was, in the stretched sounding, reported at the p' value corresponding to 850 mb.

Values of specific humidity that were missing between 700 and 200 mb were supplied from a relative humidity distribution prescribed as a simple function of latitude and pressure, one for winter and one for summer, modified by a random perturbation that was independent of pressure. The latitude selected for this purpose was a function of the 500-mb temperature

of the radiosonde. No specific humidity values were supplied above 200 mb.

3.5 Ozone

Artificial ozone values (number of molecules per cm^3) were defined by referring to two seasonal mean distributions of ozone as a function of latitude and pressure. The 500-mb temperature of the radiosonde was converted into a latitude entry for the mean ozone distribution by a latitude-500 mb temperature transformation. This modeled the strong correlation that exists in the atmosphere between these variables. Randomness was introduced by a random perturbation to the 500-mb radiosonde temperature as it was used in this process.

3.6 Surface Temperature

The temperature of the land or water surface was specified by T(surface) = T' (1000 mb) - ΔT. ΔT over water was set at a mean value plus a random number times a simple function of latitude, the latter (for each season) being patterned after typical values of the air-sea temperature difference reported by synoptic surface ships. Over land the value of ΔT was set by a random number times a specified function of season, latitude, local time, and 1000-mb humidity. Statistics of the ΔT value from the dependent winter and summer sets were as follows:

	$\overline{\Delta T}$	$(\overline{\Delta T^2})^{1/2}$	ΔT_{min}	ΔT_{max}
Winter Land	-1.0	4.3	-18.8	9.2
Winter Ocean	-1.9	2.7	- 7.1	0.9
Summer Land	-2.6	5.2	-18.5	10.5
Summer Ocean	-1.1	1.7	- 4.6	0.9

Statistics for the test sets were similar.[2]

3.7 Cloudy Profile Array

In the cloudy test, retrievals were made from a set of 40 test arrays. Six additional arrays were defined, and full temperature information about these six were provided, so that the retrieval processing groups could verify the reasonableness of the cloud simulation mechanism and array specification procedures. Each of the 46 arrays was based on a single radiosonde, selected and modified as for the clear winter 30N-60N case. Each of these 46 radiosondes was converted into an array of 16 profiles by adding a randomly selected horizontal gradient for each array of the profile properties. This gradient was representative of winter gradients.

---

[2]While these numbers seem reasonable, they are artificially derived and should not be interpreted as having any meaning beyond that.

4. RADIANCE COMPUTATION (J. Susskind, L. McMillin, and A. Goldman)

4.1 General Characteristics

Radiances were simulated for the HIRS, AMTS, and MSU instruments to be used in both the clear and cloudy parts of the test. The MSU was utilized in the cloudy part for the purpose of correcting the IR channels for cloud effects. MSU radiances were also generated for the 1600 colocated soundings in the clear part of the test to generate statistical relationships between the IR and microwave observations to be used in the NOAA/NESDIS cloud correction algorithm.

The radiance computation was designed to accurately reflect the dependence of the HIRS2, AMTS, and MSU observations on atmospheric and surface conditions. In addition to their dependence on atmospheric temperature profile, the dependence of the radiances on atmospheric water vapor and ozone distributions, ground surface-air temperature differences, reflected solar radiation, cloud distribution, and zenith angle of observation is explicitly taken into account. The radiances for a given channel i, with characteristic frequency ν_i, are computed according to

$$R_i = B(\nu_i, T_s)\tau_i(P_s,\theta) + \int_{\tau(P_s,\theta)}^{1} B[\nu_i, T(P_i\tau)]d\tau$$

$$+ \rho_i H_i \tau_i'(P_s), \qquad (4.1.1)$$

where $B[\nu_i,T]$ is the Planck blackbody function evaluated at ν_i and temperature T, $\tau_i(P,\theta)$ is the mean atmospheric transmittance from pressure P to the top of the atmosphere, averaged over channel i, $T(P_i, \tau)$ is the atmospheric temperature at the pressure P_i for which the transmittance is τ, ρ_i is the bi-directional reflectance of incident solar radiation off the ground in the direction of the satellite, H_i is the incoming solar radiation, and $\tau_i'(P_s)$ is the total atmospheric transmittance of incident and reflected solar radiation. The transmittances $\tau_i(P,\theta)$ depend explicitly on the temperature, humidity, and ozone distributions from pressure P to the top of the atmosphere, as well a θ, the satellite zenith angle of observation. For each profile, the temperature, humidity and ozone profiles, the ground temperature, the satellite zenith angle and solar zenith angle are specified by Phillips in tape 1, containing the radiosonde profile information. The bi-directional reflectance is chosen at random to lie between $.05/\pi$ and $.15/\pi$. These values correspond to a Lambertian surface with emissivity between .85 and .95. The surface emissivity was taken as 1, however, to simplify the calculations. This apparent inconsistency is not significant because the effect of non-unit emissivity is small in the infra-red channels. The effect is significant in the MSU however, and for that reason MSU channel 1, which is used to determine surface emissivity, was not simulated in this test.

Radiances for HIRS2 channel 17 are affected a great deal by effects of non-local thermodynamic equilibrium. As a result of this, neither NOAA nor

NASA uses data from this channel in analysis of operational HIRS2 sounding data. This effect is not included in equation (4.1.1.). Therefore, channel 17 data was not simulated in the test.

Table 4.1.1 shows the channel centers and instrumental noise levels used in the test. In the clear test, the 20 x 20 km resolution noise levels were used for AMTS to be consistent with the resolution of HIRS because observations in four 10 x 10 km spots can always be averaged together under clear conditions. In the cloudy test, the 10 x 10 km resolution noise levels were used.

Table 4.1.1 Locations for HIRS and AMTS channels. Noise for the HIRS and AMTS is in $mW/M^2cm^{-1}sr$.

	HIRS			AMTS				MSU	
Ch.	center (cm^{-1})	width (cm^{-1})	noise 20x20 km	center (cm^{-1})	width (cm^{-1})	noise 20x20 km	noise 10x10 km	center GHz	noise (°K)
1	668.4	3.0	0.82	607.0	0.5	0.260	0.512	**50.30	0.25
2	679.2	10.0	0.15	623.2	0.5	0.252	0.504	53.74	0.25
3	691.1	12.0	0.11	637.8	0.5	0.249	0.498	54.96	0.25
4	703.6	16.0	0.08	634.3	0.5	0.246	0.493	57.95	0.25
5	716.0	16.0	0.05	646.6	0.5	0.250	0.501		
6	732.4	16.0	0.06	654.4	0.5	0.222	0.444		
7	748.3	16.0	0.05	665.6	0.5	0.220	0.441		
8	897.7	35.0	0.02	666.8	0.5	0.220	0.440		
9	1027.9	25.0	0.03	668.2	0.5	0.222	0.444		
10	1217.1	60.0	0.03	669.4	0.5	0.220	0.440		
11	1363.7	40.0	0.04	1203.0	1.0	0.0100	0.0201		
12	1484.4	80.0	0.03	1231.8	1.0	0.0092	0.0183		
13	2190.4	23.0	.0011	1770.3	1.5	0.00231	0.00462		
14	2212.7	23.0	.0012	1809.5	1.5	0.00146	0.00291		
15	2240.1	23.0	.0009	1839.4	1.5	0.00110	0.00219		
16	2276.3	23.0	.0007	1844.5	1.5	0.00100	0.00201		
17*	2360.6	23.0	.0008	1850.9	1.5	0.00097	0.00194		
18	2511.9	35.0	.0005	1889.6	1.5	0.00074	0.00147		
19	2617.2	100.0	.0005	1930.1	1.5	0.00068	0.00135		
20				2384.0	2.0	.000282	.000564		
21				2386.1	2.0	.000360	.000719		
22				2388.2	2.0	.000293	.000586		
23				2390.2	2.0	.000336	.000672		
24				2392.4	2.0	.000298	.000597		
25				2394.5	2.0	.000312	.000624		
26				2424.0	2.5	.000194	.000388		
27				2505.0	2.5	.000123	.000246		
28				2686.1	2.5	.000098	.000197		

*Not simulated because of non-local thermodynamic equilibrium effects.
**Not simulated because of surface emissivity effects.

4.2 Uncertainty in knowledge of transmittance function

This test compares a regression retrieval with a direct physical retrieval. The direct physical inversion algorithm for retrieval of temperature profiles involves the computation of radiances expected for the channels given atmospheric and surface conditions. A limiting factor in the accuracy of retrievals obtained by direct physical inversion is the accuracy of the forward problem calculation described above. In reality, one cannot perform the forward calculation perfectly. To simulate the agreement currently achievable between calculated and observed radiances, the radiative transfer calculations performed at the University of Denver were required to differ from those used by NASA in the physical retrieval by 1 to 2% in RMS radiance.

To achieve this goal, Susskind (NASA/GLA) and Goldman (U. of Denver) compared line-by-line transmittance calculations for all AMTS and HIRS2 channels using Susskind, et al. [12] and Goldman and Saunders [28] programs and identical atmospheric profiles and instrument response functions. After small modifications to the assumed CO_2 line shape and temperature dependence of the half-widths, the two programs produced radiances which differed by the appropriate amounts.

The original intent was to have Goldman perform the line-by-line calculations and use them to provide coefficients for the NESDIS [13] fast transmittance model. However, the calculation of transmittances for the HIRS instruments required more computer time than was available so an alternative was required. The two possibilities were the rapid models in use at NESDIS and NASA. Since comparison of two instruments using simulated data requires computational consistency and reasonable, not exact, agreement with nature, either model would have been adequate. However, L. McMillin of NESDIS uses a regression retrieval method which is relative independent of the transmittance algorithm while J. Susskind of NASA uses a physical inversion which is sensitive to the transmittance model. It was decided to use the NASA transmittance model to avoid repeating the lengthy process of matching the NASA model with a second model (NESDIS instead of A. Goldman). Coefficients for the NASA model for both HIRS2 and AMTS had already been computed. In addition, the NASA model contained an explicit dependence of the atmospheric transmittances on the ozone distribution of the atmosphere which is not contained in the NESDIS atmosphere.(1)

The following sections describe the transmittance and radiance calculations used in the test. The method used by Goldman to stimulate the 1 to 2% error between calculated and observed radiance cannot be described

---

(1) At the time this decision was made, NESDIS was not aware that the filter functions utilized in calculating the HIRS2 transmittance functions and NASA model coefficients were those appropriate for TIROS-N, rather than NOAA-C, and furthermore, were truncated at frequencies where the filter functions fell to 3% of their maximum values.

if the simjulation is to remain realistic.[2] The shape of the true error is also unknown to the retrieval community.

4.3 Interpolation of the Phillips data to standard levels

The numerical integration of equation (4.1.1) was done using a 64 level atmospheric pressure mesh shown in Table 4.2.1. Consequently, all the data from the Phillips radiosonde tape was converted to the 64 level mesh. The temperature was interpolated linearly in the log of the pressure from the Phillips significant pressure levels to the 64 pressure levels. The ozone distribution, given in column density per mb at the significant levels, was interpolated linearly in log P to the 64 levels. The humidity was given by Phillips as specific humidity at a subset of significant pressure levels, starting from the surface and going continuously to a pressure, P_L, typically in the mid-upper troposphere. The specific humidity was converted to relative humidity, which was interpolated linearly in log P to the sub-set of 64 levels at pressures greater than or equal P_L. The relative humidity was then converted to specific humidity and then to column density per mb. At pressures less than P_L, the humidity was extrapolated by assuming the specific humidity at pressures less than or equal to a stratospheric pressure, P_T, to be 2×10^{-6} gm/gm. P_T was taken as the lesser of either 100 mb or the pressure 5 levels higher in the atmosphere than P_L. The specific humidity was linearly interpolated in the log P between P_L and P_T, to define values at intermediate pressure values. The specific humidity values above P_L were then converted to column density per mb.

Table 4.2.1 Pressure mesh used in the radiance calculation

Level	Pressure	Increment
1-10	1 mb - 10 mb	1 mb
11, 12	15, 20 mb	5 mb
13-30	30 mb - 200 mb	10 mb
31-40	220 mb - 400 mb	20 mb
41-64	425 mb - 1000 mb	25 mb

4.4 Line-by-Line Calculations Used to Generate Rapid Algorithm Coefficients

The NASA rapid transmittance algorithm used in the radiative transfer calculations in the test is essentially identical to that used by GLA in analysis of TIROS-N HIRS2/MSU data, described in detail in Susskind et al., [12]. The atmospheric transmittance functions, $\tau_i(P)$, contain components coming from attenuation by discrete lines of absorbing gases, $\tau_{iL}(P)$, and

---

(2) It should be emphasized that the planned use of the NESDIS rapid transmittance model does not imply endorsement of that routine by NASA nor does the use of the NASA method imply endorsement of the NASA method by NESDIS.

also from broad-banded continuum absorption features. The component coming from discrete lines, which is modeled by the rapid algorithm, can be calculated by line-by-line calculations according to

$$\tau_{iL}(P,\theta) = \int d\nu F_i(\nu) \exp\left[-\int_{z(P)}^{\infty} \sum_L k_L(\nu,z) C_L(z) \pi(z)\, dz \sec\theta\right], \qquad (4.4.1)$$

where $F(\nu)$ is a normalized channel response function, $k_L(\nu,z)$ is the absorption coefficient of line L evaluated at the temperature and pressure of height z, $c_L(Z)$ is the molecular mixing ratio for the gas to which line L belongs, ρ is the density of air, and θ is the zenith angle of observation. The evaluation of $k_L(\nu,z)$ depends not only on the set of line parameters used [16] but also on assumptions regarding the temperature dependence of the Lorentz half width and the nature of the line shape.

All line-by-line calculations for the HIRS2 and AMTS channel transmittances were made as in Susskind and Searl [15] using the 1978 version of the AFGL line parameter tape [16]. The MSU transmittance functions were calculated in a similar manner, but using a Van Vleck-Weiskopf line shape and the overlapping line theory given by Rosenkranz [17] in the case of O_2 absorption. Computations were done with a 64 level atmosphere and a frequency spacing of .002 cm^{-1} for the HIRS2 channels and .00006 cm^{-1} for the MSU channels. HIRS2 calculations were done using the filter functions for HIRS2 on TIROS-N, truncated at frequencies on either side of the channel center where the filter function fell to 3% of its maximum value. These same truncated filter functions are used by GLA in analysis of TIROS-N data. The AMTS and MSU channels were treated as having triangular and rectangular response functions respectively, with specified half-widths and with the channel centers shown in Table 4.1.1.

The CO_2 line shape was taken to be sub-Lorentz as described by Susskind and Mo [18]. One significant modification made to the calculations of Susskind and Searl [15] was to include induced emission in the computation of the temperature dependence of the line strengths

$$\frac{S(T)}{S(T_s)} = \frac{Q_v(T_s)Q_R(T_s)}{Q_v(T)Q_R(T)} \times \frac{\exp(-1.439E''/T)[1-\exp(-1.439\nu/T)]}{\exp(-1.439E''/T_s)[1-\exp(-1.439\nu/T_s)]}, \qquad (4.4.2)$$

where E", Q_V and Q_R are defined in McClatchey, et. al. [14]. Neglect of the induced emission factor, $(1 - \exp(-1.439\nu/T))/(1 - \exp(-1.439\nu/T_s))$, as done in McClatchey, et. al. [14] and Susskind and Searl [15], decreases the intensity of lines at low temperatures relative to high temperature. For example, at ν = 650 cm^{-1}, the intensity of a line at 220K is underestimated relative to its intensity at 300 K by 3%. Such an error has the effect of broadening the weighting functions of channels sounding the tropopause region.

The total transmittance function $\tau_i(P)$ is taken as

$$\tau_i(P) = \bar{\tau}_{iL}(p)\tau_{iN}(p)\tau_{iW}(P), \qquad (4.4.3)$$

where τ_N and τ_W represent continuum absorption due to N_2, and water vapor. Water vapor continuum and nitrogen continuum absorption are treated as in Susskind and Searl [15]. $\bar{\tau}_L$ in equation (4.4.3) represents a rapid transmittance algorithm model for the line-by-line calculated transmittance, τ_{iL}, which is described in the next section.

4.5 The rapid transmittance algorithm

The averaged discrete line transmittance through the atmosphere from pressure P_ℓ to the top of the atmosphere, at a zenith θ, as seen by channel i, is modeled as

$$\bar{\tau}_{iL}(P_\ell,\theta) = \prod_{j=1}^{\ell} \bar{\tau}_{iF}(P_j,P_{j-1},\theta)\bar{\tau}_{iO}(P_j,P_{j-1},\theta)\bar{\tau}_{iW}(P_j,P_{j-1},\theta), \qquad (4.5.1)$$

where $\bar{\tau}_{iF}$, $\bar{\tau}_{iO}$, and $\bar{\tau}_{iW}$ represent models for effective layer transmittances from pressure P_j to P_{j-1} (P_j P_{j-1}) at zenith angle θ. The term τ_{iF} represents absorption by gases assumed to have a fixed mixing ratio, while $\bar{\tau}_{iO}$ and $\bar{\tau}_{iW}$ represent absorption due to ozone and water vapor respectively. $\bar{\tau}_{iL}(P_\ell,\theta)$ from equation (4.5.1) is used to model $\tau_{iL}(P,\theta)$ defined in equation (4.4.1) and used in equation (4.4.3).

Line-by-line calculations done at zenith angles of 0°, 50°, and 70°, are used to generate the coefficients for the effective transmittance models at the appropriate angle. Effective layer transmittances at other zenith angles are obtained by linear interpolation of the logarithm of the effective layer transmittance as a function of sec θ between two of the three angles.

Because a given channel is not monochromatic, the effective layer transmittances do not obey the multiplicative properties associated with monochromatic transmittances. Instead, given line-by-line transmittance calculations for $\tau_{iF}(P,\theta)$, $\tau_{iFO}(P,\theta)$, and $\tau_{iFOW}(P,\theta)$, corresponding respectively to absorption using only gases of fixed distribution, using fixed gases and ozone, and using all species, we define effective mean layer transmittances

$$\tau_i(P_j,P_{j-1},\theta) = \tau_i(P_j,\theta)/\tau_i(P_{j-1},\theta), \qquad (4.5.2)$$

$$\tau_{iO}(P_j,P_{j-1},\theta) = \tau_{iFO}(P_j,P_{j-1},\theta)/\tau_{iF}(P_j,P_{j-1},\theta), \qquad (4.5.3)$$

and

$$\tau_{iW}(P_j,P_{j-1},\theta) = \tau_{iFOW}(P_j,P_{j-1},\theta)/\tau_{iFO}(P_j,P_{j-1},\theta). \qquad (4.5.4)$$

Equation (4.5.2) defines an effective mean layer transmittance based on

line-by-line calculations using any combination of constituents [19]. The effective layer transmittances for ozone in equation (4.5.3) and water vapor in equation (4.5.4) are independent of calculations based on absorption of water vapor or ozone alone [20] and in fact, differ significantly from those defined in equation (4.5.2) based on the single species transmittances.

The magnitude of this effect is illustrated by table A2 of Halem and Susskind [19] which shows that the brightness temperatures computed for VTPR channel 7 using line-by-line transmittances, $\tau_{FO}\tau_{W}$, differ from those computed using line-by-line τ_{FOW}, by .4°C for a tropical temperature humidity profile. Since, the spectral response of VTPR channel 7 is very similar to that of HIRS channel 7, errors of similar magnitude are expected for HIRS2 channel 7.

The basic assumption of the models for water vapor and ozone transmittance is that the effective mean layer transmittances in equations (4.5.3, 4.5.4) can be treated as having the transmittance properties of a gas in a homogeneous layer having the mean temperature T, and pressure P, of the atmospheric layer, and vertical column density u of the absorbing gas in the layer. This assumption is reasonably valid because use of equation (4.5.2) removes most of the dependence of the mean layer transmittance on the properties of the atmosphere above the layer, and absorption due to water vapor and ozone has a second order effect on the radiances in the temperature sounding channels. We then expect the log of the mean layer transmittance to be proportional to u for weakly absorbing lines, and $u^{1/2}$ for strong lines. For a composite of lines, an effective exponent of intermediate value is obtained. The absorption coefficient depends on the pressure P and the temperature T.

The following form was therefore used to model the effective water and ozone transmittances for all channels and all layers:

$$\tau_{ic}(P_j,P_{j-1},\theta) = \exp-\{A_{i,j,c}(\theta)[1-B_{i,c}(T_j-273)]u_c(j,j-1)^{N_{i,c}}\}, \qquad (4.5.5)$$

where c stands for constituent, either ozone or water vapor, $u_c(j,j-1)$ is the integrated column density of the species in the layer between j and j-1, $N_{i,c}$ is a channel and species dependent constant between .5 and 1, $A_{i,j,c}$ is an effective channel, species, pressure, and angle dependent absorption coefficient, and $B_{i,c}$ is a channel and species dependent constant (percent change per degree). For simplicity, the temperature dependence, $B_{i,c}$, and exponent, $N_{i,c}$, are taken to be independent of pressure and angle. The coefficients A, B, and N are determined from the effective mean layer transmittances computed from the line-by-line calculations.

Most of the absorption for the temperature sounding channels is due to the gases of fixed distribution, primarily CO_2 and N_2O. The transmittance at a given angle depends only on the temperature profile. The effective mean layer transmittance for each reference angle is modelled according to

$$\tau_{iF}(P_j,P_{j-1},\theta) = D_{ij}(\theta)+E_{ij}(\theta)(T_j-T_j^{o})+F_{ij}(\theta)(\tilde{T}_{ij}(\theta)-\tilde{T}_{ij}^{o}(\theta)), \qquad (4.5.6)$$

where T_j is the mean temperature in the layer j, between P_{j-1}, for the temperature profile under consideration, T_j^o is the mean temperature in layer j in a standard temperature profile, and $\tilde{T}_{ij}$ and $\tilde{T}_{ij}^o$ are effective mean temperatures for the entire profile from P_j to the top of the atmosphere for the temperature profile under consideration and the standard temperature profile respectively. The effective mean temperature above pressure P for channel i is defined as the averaged temperature above pressure P weighted by the weighting function for channel i. The effective temperature is then channel and angle dependent and is defined as

$$\tilde{\tau}_{ij}(\theta) = \{1/[1-\tau_i^o(P_j,\theta)]\} \int_0^{P_j} T(P)[d\tau_i(\theta)/dP]dP, \qquad (4.5.7)$$

where $\tau_i^o(P,\theta)$ is the transmittance of channel i for the standard temperature profile.

The coefficients $D_{ij}(\theta)$, $E_{ij}(\theta)$, and $F_{ij}(\theta)$ are determined so as to give the best fit in the least squares sense to the values of τ_{iF} obtained from line-by-line calculations. As expected, the coefficient $D_{ij}(\theta)$ was found to be very close to $\tau_{iF}^o(P_j,P_{j-1},\theta)$, the effective layer transmittances for the standard profile.

This model is nearly identical to the model used by NESDIS and described by Eq. (14) of McMillin and Fleming [21]. Although details differ, the major difference of any significance in terms of accuracy is the number of terms used in the expression.

4.6 Radiances for the cloudy test

Radiances for the cloudy portion of the test were computed in the same manner as in the clear portion except that for infra-red channels, the surface terms in equation (1), T_S and P_S, were replaced by T_C and P_C, the temperature of the cloud top and the pressure of the cloud top. The microwave channels were treated as unaffected by clouds. In addition, all cases in the cloudy test were at night. This was done primarily to avoid the difficulty of modeling reflected solar radiation of clouds. The construction of the detailed radiance fields in the cloudy cases, consistent with the temperature, humidity, and cloud distributions and the scanning geometry of the instruments, is described in Chapter 7.

5. RETRIEVALS

5.1 GLA retrieval techniques (J. Susskind and M. Chahine)

5.1.1 The clear test

The retrieval methods used by GLA in the test are very similar to the procedures used in analysis of TIROS-N HIRS2/MSU data [12] at the time the test was conducted. The method is based on finding atmospheric and surface conditions, which, when substituted in the radiative transfer equation (4.1.1), match the observations to a specified amount. The procedure starts with an initial guess, computes the expected radiances, compares them with the observations, and modifies the guess in such a way as to decrease the difference in observed and computed brightness temperatures. Radiances are recomputed based on the next iterative profile and the procedure is repeated until sufficient agreement is obtained between observed and computed radiances.

The procedures used in the test differ from those used in analysis of TIROS-N data for two reasons:

1. A 6-hour forecast guess of temperature and humidity is used in analysis of TIROS-N data but is not available in the test.

2. The noise levels in the test are realistic assessments of instrumental noise but do not include the effects of scene noise.

As a result of these differences, the first guess temperature profile used in the analysis was based on a regression relationship between observed brightness temperatures and radiosonde temperature profiles. Also, the form of iterative relaxation equation was modified so as to decrease the smoothing applied to the solution. Climatology was used as a first guess humidity profile and this required a first order correction. This step is not employed when a forecast humidity initial guess is used for analysis of real data.

5.1.2 Steps in the processing system

The radiances in the clear part of the test were analyzed in a sequence of steps enumerated below. Before the iterative procedure to determine temperature profiles is started, a number of preliminary steps must be done. First, the radiances, which are observed at zenith angle , are corrected to hypothetical radiances expected to be seen under the same geophysical conditions viewed at nadir (Step 1 - Section 5.1.3). These radiances are then used to generate a first guess temperature profile via regression techniques (Step 2 - Section 5.1.4). Besides generation of the regression guess, an additional preliminary step involves tuning the observed radiances to remove systematic differences in brightness temperatures computed by Goldman, which represent the "true" physics, and those

computed by GLA, which represent "approximate" physics (Step 3 - Section 5.1.5). In order to begin calculations of expected brightness temperatures as a function of temperature profile, one still needs a first estimate of ground temperature (Step 4 - Section 5.1.6) and humidity profile (Step 5 - Section 5.1.7). Radiances at the observed zenith angle, expected for the initial guess temperature profile, ground temperature, and humidity profile, are now computed (Step 6) as described in Chapter 4. The iterative scheme now begins by comparing the observed radiances with radiances computed from the Nth guess (Step 7) and terminating the procedure if agreement is sufficiently close. Otherwise, an N+1 estimate of temperature profile is generated (Step 8 - Section 5.1.8) followed by an N+1 estimate of ground temperature (Step 9 - as in Step 4). Using these new N+1 estimate parameters, the N+1 estimate of observed radiances are computed (Step 10 as in Step 6) and the iterative procedure returns to Step 7 to check for convergence.

The steps are summarized below:

1. Angle correct observed radiances to predicted nadir observations in order to
2. Generate regression guess $T^{o}(P)$
3. Tune observed radiances to remove systematic differences between radiances computed by Goldman and GLA
4. Retrieve a ground temperature and solar radiation correction
5. Adjust humidity profile
6. Compute expected radiances using regression guess and ground temperature
7. Check differences between observed and expected radiances. If sufficiently accurate, terminate procedure
8. Adjust atmospheric temperature profile
9. Recompute ground temperature
10. Compute radiances using iterative atmospheric and ground temperature - return to step 7

Table 5.1.1 shows the channels of HIRS2 and AMTS and indicates which channels are involved in each of the steps.

The details of each step are given in the following sections.

5.1.3 The angle correction of radiances to generate the regression guess

The observations of HIRS2 and AMTS are generated at the specified satellite zenith angle for each sounding. In performing the physical

Table 5.1.1 Channels used in different steps

	HIRS	AMTS
Angle Correction	1-8, 13-16	3-10, 20-26
Regression Guess	1-8, 13-16	3-10, 20-26
Tuning	1-7, 13-16	1-10, 20-26
Ground Temperature	18, 19	26-28
Humidity Correction	8	11
Temperature Profile	1-4, 13-15	4-10, 20-24

retrieval, there is no need for an "angle correction" to the radiances. The computation of the radiative transfer equation 4.1.1 is done at the appropriate angle and no other correction is necessary. On the other hand, in order to generate an initial guess temperature profile based on regression relationships between observed brightness temperatures and atmospheric temperature profiles, it is desirable to remove to first order the angle dependence of the satellite brightness temperatures. To do this, observed satellite brightness temperatures at angle θ, $T_B(\theta)$, are corrected to $T_B(0)$, "their values if the observations were at nadir." In order to generate brightness temperatures expected at nadir, $T_B(0)$, given brightness temperatures computed at zenith angle θ, $T_B(\theta)$, we use the equation

$$T_B^S(0) = T_B^S(\theta) + A[(\sqrt{\sec\theta} - 1)/(\sqrt{\sec 50} - 1)]T_B^S(\theta). \qquad (5.1.1)$$

The superscript S means data simulated by GLA. The superscript G will be used to represent data generated by Goldman. A is 15 x 15 for AMTS and 12 x 12 for HIRS2 using channels shown in Table 5.1.1. A separate matrix was constructed for winter and summer.

The coefficients of the matrix A were determined by simulating radiances for the 800 profiles at a 50° zenith angle and at nadir as described in Chapter 4. The radiosonde temperature and humidity profiles were extrapolated from their values highest in the atmosphere to values at 1 mb according to climatology. Climatological ozone profiles were used in the analysis. The ground temperature was taken as the surface air temperature + a random 3° C difference. The matrix A was determined by a ridge regression.

$$A = [T_B^S(0) - T_B^S(50)]\, T_B^S(50)'\, [T_B^S(50)\, T_B^S(50)' + M_A\varepsilon_A^2 I]^{-1}, \qquad (5.1.2)$$

where M_A is the number of profiles in the sample used for angle correction, I is the identity, and A is the ridge parameter which was empirically optimized to be .05. In equation (5.1.2), $T_B^S(50)$ represents the matrix of brightness temperatures simulated for 50° zenith angle and $T_B^S(0)$, the brightness temperatures simulated at nadir. Once A is obtained, Eq. 5.1.1 is used to angle correct $T_B^G(\theta)$ to $T_B^G(0)$ to be used to generate the regression first guess.

5.1.4 Generation of the regression guess

Separate regression equations of the form

$$T(P) = \overline{T}(P) + B(T_B^G(0) - \overline{T}_B^G(0)] \qquad (5.1.3)$$

were constructed for each of the eight zones in the dependent set. In equation (5.1.3), T(P) is the (up to) 64 level temperature profile given by the truncated radiosonde profile provided by Phillips interpolated to the 64 standard levels shown in Table 4.3.1, and $\overline{T}(P)$ is the mean of all the profiles in the colocated data set (≈200 profiles per zone). $T_B^G(0)$ is the vector of brightness temperatures for the N_R channels used for regression constructed by angle correcting the data provided by Goldman for the particular profile to 0° according to equation (5.1.1). $\overline{T}_B^G(0)$ is the mean vector of all the resulting $T_B^G(0)$ in the dependent set. N_R = 15 for AMTS and 12 for HIRS with the channels shown in Table 5.1.1. Note that all humidity sounding channels and most window channels are excluded from the regression for both instruments.

Because the knowledge of the temperature profiles was incomplete, different profiles extend to different levels in the atmosphere. The regression equation (5.1.2) treats each level as independent of the others. The matrix B was truncated in the pressure index so as to include only those pressures where a sample of at least 30 temperatures were reported. This was typically in the range of 20-30 mb.

The solution to equation (5.1.3) was found by ridge regression

$$B = (T-\overline{T})[T_B^G(0)-\overline{T}_B^G(0)]'\{[T_B^G(0)-\overline{T}_B^G(0)][(T_B^G(0)-\overline{T}_B^G(0)]'+M_R\epsilon_R^2 I\}^{-1}, \qquad (5.1.4)$$

where R is the ridge parameter taken as .5°C, and M_R is the size of the dependent set sample at each level. B is evaluated at each pressure level based on the subset of M_R profiles for that level.

Given an array of angle corrected brightness temperatures $T_B^G(0)$, the initial guess to be used in the retrieval is constructed according to equation (5.1.3) with the values of $\overline{T}$, $\overline{T}_B^G(0)$, and B coming from the appropriate zone of the dependent set. The initial guess at pressures between 1 mb and the lowest pressure in the B matrix is constructed by extrapolation according to climatology.

5.1.5 Tuning of the observed radiances

In order to account for possible systematic differences in the calculation of observed brightness temperatures computed by Goldman, T_B^G, and simulated by GLA, T_B^S, a step was introduced to remove these differences to first order. This step is irrelevant with regard to the construction of the regression initial guess, but is significant for the physical retrieval solution, just as the angle correction to 0° was important for the regression guess but irrelevant for the physical retrieval.

The systematic differences are minimized by comparing the dependent set of "observed" brightness temperatures computed by Goldman T_B^G, with those simulated by GLA, T_B^S, and finding C and D which best fit the relation

$$T_B^S = C\ T_B^G + D \qquad (5.1.5)$$

where C is an $N_T \times N_T$ matrix for the N_T channels tuned and D is a $N_T \times 1$ vector. Once C and D are obtained from analysis of a dependent set, the observed brightness temperatures T_B^G in the independent set are modified according to

$$\tilde{T}_B^G = C\, T_B^G + D \tag{5.1.6}$$

so as to best match the brightness temperatures we would compute under the same conditions. Retrievals are performed using $\tilde{T}_B^G$ as data rather than T_B^G. Only those profiles which reached at least 40 mb in temperature and 625 mb in water vapor were used to generate C and D. The temperature profiles were extrapolated to 1 mb according to climatology, while the water vapor profiles were extrapolated by assuming the specific humidity was linear in ln P to 225 mb, above which climatological values for the water vapor specific humidity were used.

Four sets of C and D were found; one for each season for each instrument. Since only those profiles which reported temperature to at least 40 mb and water vapor to at least 625 mb were used, there were about 200 profiles for both summer and winter used to find C and D. The same channels were used on both sides of equation (5.1.5). These were channels 1-7 and 13-16 for HIRS and channels 1-10 and 20-26 for AMTS. Some channels used in the tuning are not used in the physical retrieval but aided in the systematic error removal. In addition, window channels were generally not tuned because their radiances are not sensitive to small changes in absorption coefficients.

In order to compute radiances given the radiosonde reports, it was necessary to determine a ground temperature and, in the day cases, a surface reflectivity for solar radiation. The ground temperature and surface reflectivity were determined from analysis of the untuned Goldman data as described in the next section.

5.1.6 Ground temperature and correction for solar radiation

The ground or sea surface temperatures are computed in an analogous manner to that of Susskind et al. [22], using only the shortwave window channels. The equations are simplified in the test because of the assumption of unit emissivity. At night, only one channel is necessary to determine a ground temperature. During the day, two channels are needed to obtain both a ground temperature and a correction for solar radiation reflected off the ground.

At night, all other terms in equation (4.1.1) but the ground temperature, T_S, are either observed or can be computed based on the estimated temperature-humidity profile. T_S can then be solved for using the observation in window channel i according to

$$T_S = B_i^{-1}\{R_i - \int_0^{\tau_i(P_S)} B_i[T(\tau)]d\tau\}/\tau_i(P_S). \tag{5.1.7}$$

For HIRS2, channels 18 and 19 are used to give two estimates of T_S, which are averaged together to give the final ground temperature. For AMTS, the same procedure is used with channels 27 and 28.

During the day, the effects of reflected solar radiation on the short wave window observations must be accounted for. As shown in equation (4.1.1), reflected solar radiation contributes a term $\rho_i H_i \tau'_i(P_S)$ to the observed radiances. H_i, the solar flux striking the top of the atmosphere, and $\tau_i'(P_S)$, the atmospheric transmittance of incident and reflected solar radiation, can be calculated given the solar zenith angle and an estimate of atmospheric conditions. If ρ_i were known, $R_i - \rho_i H_i \tau'_i(P_S)$ could be substituted directly into equation (5.1.7), in place of R_i, and T_S solved for immediately. The bi-directional reflectance ρ_i, is unknown, however, and must be solved for simultaneously with T_S. Instead of assuming ρ_i to be known, we use the less restrictive assumption that the reflectance is equal for all channels. Then we can write

$$[R_i - \int B_i d\tau]/\tau_i(P_S) = B_i(T_S) + \rho H_i \tau_i'(P_S)/\tau_i(P_S) = A_i. \qquad (5.1.8)$$

The left hand side of equation (5.1.8) can be treated as an "observed quantity", A_i, in an iteration. For two channels, equation (5.1.8) can be rewritten as

$$B_i(T_S) - \alpha B_j(T_S) = A_i - \alpha A_j = A \qquad (5.1.9)$$

where

$$\alpha = \frac{H_i}{H_j} \times \frac{\tau_i'(P_S)}{\tau_j'(P_S)} \times \frac{\tau_j(P_S)}{\tau_i(P_S)}.$$

Equation (5.1.9) is solved for iteratively according to

$$\frac{\exp(-h\bar{\nu}/T_S^{M+1})}{\exp(-h\bar{\nu}/T_S^{M})} = \frac{A}{B_i(T_S^M) - \alpha B_j(T_S^M)}, \qquad (5.1.10)$$

where $\bar{\nu}$ is the average frequency of the two window channels, $\bar{\nu} = (\nu_i + \nu_j)/2$. This procedure converges rapidly. Channels 18 and 19 are used for HIRS2 and 26 and 27 are used for AMTS to determine T_S during the day.

Once T_S is obtained, ρ is then determined from equation (5.1.8) and $\rho H_i \tau'_i(P_S)$ is then subtracted from all the observations in the 4.3 μm channels to remove to first order the smaller effects of reflected solar radiation on those channels.

The shortwave window channels were used to determine ground temperature rather than the longwave window channels 8 on HIRS2 and 11, 12 on AMTS, because the transmittances, and hence the brightness temperatures, of the longwave window channels are more sensitive to the humidity profile

than those of the shortwave window channels used. Nevertheless, the transmittances of the shortwave window channels do depend on the humidity profile and significant errors in retrieved ground temperature can occur, particularly during the day, if a poor estimate of humidity is used in calculation of the transmittances. For this purpose, we use the 11 μm window channel to determine whether the climatological estimate of humidity is reasonable, and, if not, to provide an improved humidity profile.

5.1.7 The humidity correction

The humidity correction is not employed in the analysis of TIROS-N data described in Susskind, et al. [12], because a forecast humidity profile is available for use in analysis of real data, while climatology is used in the test. The forecast humidity profile is considered to be accurate enough for use without modification.

Radiances in the 11 μm window channel depend primarily on the ground temperature and the temperature humidity profile. Given a ground temperature, determined from the 3.7 μm channels, and an estimate of the temperature-humidity profile, one can determine whether the humidity profile is reasonable by computing the expected brightness temperature $T_B(T_S, q)$ and comparing it with the observation $\tilde{T}_B$. If the agreement is close enough in the 11 μm window channel, it is assumed that the humidity profile is accurate enough so that significant errors in T_S did not occur from analysis of the 3.7 μm radiances, which are much less sensitive to the humidity profile than the 11 μm window radiances. If there is a significant difference between $\tilde{T}_B$ and $T_B(T_S, q)$, the sensitivity of $T_B(T_S, q)$ to the assumed humidity profile is determined by computation of $T_B(T_S, q')$ where $q'(P) = q(P)\ [1 + r]$. If T_B was greater than $T_B(T_S, q)$, it is assumed the guess humidity was too high and r is taken as -.5. Otherwise, r = .5. The modified humidity profile is taken as

$$q''(P) = q(P)\ (1 + Sr), \tag{5.1.11}$$

where S, the scaling factor is determined according to

$$S = \frac{.5\ [\tilde{T}_B - T_B(T_S,q)]}{[T_B(T_S,q') - T_B(T_S,q)]}. \tag{5.1.12}$$

If either the numerator is less than .5°, indicating that the guess is good enough, or the denominator is less than .5°C, indicating that the brightness temperature is not sensitive to humidity, S is taken as zero and no humidity correction is performed.

The modified humidities are used now to recalculate all transmittances and radiances, including those of the atmospheric sounding channels. The humidity correction is not iterated.

5.1.8 The temperature relaxation equation

The previous steps have provided the information necessary to retrieve

a temperature profile from the observations in the temperature sounding channels. We have now 1) obtained an initial guess temperature profile; 2) determined a ground temperature, updated humidity profile, and solar radiation correction term which are used to compute expected radiances for the first guess temperature profile; and 3) modified the observed radiances to minimize systematic differences between observed and computed radiances. We now compare the modified observed brightness temperatures for the temperature sounding channels $\tilde{T}_{B,i}$, with the computed brightness temperatures from the Nth guess, $T^N_{B,i}$, and modify the guess to produce an N+1th iterative temperature profile. Twelve temperature sounding channels are used for the AMTS and seven are used for HIRS2 as shown in Table 5.1.1.

The relaxation equations used almost identical to those described in Susskind et al. [12]. Temperatures at pressures between 30 and 1000 mb are treated differently than temperatures at pressures lower than 30 mb. The basis of the relaxation method lies in the approximation that a small constant shift in the entire temperature profile will produce an almost identical change in the brightness temperature computed for a sounding channel. Moreover, if the shift is applied only in the region of the atmosphere where the radiance of the channel is most sensitive to atmospheric temperature, a similar change in computed brightness temperatures will occur.

For channels sensitive to temperatures at pressures greater to 30 mb, we assign an atmospheric layer, P_{iL} to P_{iU}, representing the lower and upper pressure boundaries for sounding channel i, as shown in Table 5.1.2 for the sounding channels of AMTS and HIRS used in the analysis. Channels primarily sensitive to temperature changes above 30 mb are treated as representative of temperature changes at a specific pressure rather than in a layer. This pressure, P_i, is indicated in Table 5.1.2 for the appropriate channels.

For pressures greater than 30 mb, we write the relaxation equation

$$\bar{T}_i^{N+1} = \bar{T}_i^N + (\tilde{T}_{B,i} - T^N_{B,i}), \tag{5.1.13}$$

where $\bar{T}_i^N$ is the average temperature of the Nth iterative guess temperature profile in the atmospheric layer corresponding to channel i

$$\bar{T}_i^N = \left[\int_{P_{iL}}^{P_{iU}} T^N(P)\, d\ln(P)\right]/[\ln(P_{iU}/P_{iL}0)] \tag{5.1.14}$$

and $\bar{T}_i^{N+1}$ is the new estimate of the layer mean temperature in the appropriate atmospheric layer. In order to determine a N+1th iterative temperature profile at pressure P_k from estimates of layer mean temperatures, we constrain the solution to be given by

$$T^{N+1}(P_k) = T^0(P_k) + \sum A_j^{N+1} F_j(P_k), \tag{5.1.15}$$

Table 5.1.2 Assigned pressures for channels used in the temperature relaxation scheme

AMTS			HIRS		
CHANNEL	P	P_L-P_U	CHANNEL	P	P_L-P_U
9	3	-	1	10	-
10	15	-	2	-	30-90
8	-	30-50	3	-	90-200
7	-	30-80	4	-	200-380
6	-	50-150	15	-	380-625
5	-	100-220	14	-	625-875
4	-	200-400	13	-	875-1000
20	-	300-500			
21	-	400-600			
22	-	600-775			
23	-	775-1000			
24	-	925-1000			

where $T^0(P_k)$ is the initial guess, $F_j(P_k)$ are empirical orthogonal functions of temperature, given by the eigenvectors, with largest eigenvalues, of the covariance matrix of a set of global radiosonde profiles, sampled at the 52 pressure levels between 1000 and 30 mb, which are a subset of the 64 pressure levels used in the calculation, and A^{N+1} are the iterative coefficients which, together with the initial guess, completely determine the solution.

Equations (5.1.13) and (5.1.15) differ from those used in Susskind et al. [12] in that 1) observations in single channels are used to modify the estimated layer mean temperatures, rather than weighted sums of observations in different channels, and 2) the solution is expanded about the first guess rather than the global mean. Both changes introduced in the analysis of the simulated data were done to decrease the smoothing and increase the vertical resolution of the solution. These changes and the reasons for them were discussed in Section 5.1.1.

The coefficients, A^{N+1}, are solved for according

$$A^{N+1} = [\bar{F}'\bar{F} + \sigma H]^{-1}\ \bar{F}'[\bar{T}^{N+1} - \bar{T}^0], \qquad (5.1.16)$$

where $\bar{F}$ represents the matrix of layer averaged empirical orthogonal functions

$$\bar{F}_{ij} = [\int_{P_{iL}}^{P_{iU}} F_j(P)\ d\ln(P)]/[\ln(P_{iU}/P_{iL})], \qquad (5.1.17)$$

$\bar{F}'$ is the transpose of $\bar{F}$, H is a diagonal matrix with H_{jj} being the inverse of the fraction of the total variance arising from eigenvector j, and σ is a constant. The term H is added to $\bar{F}'\bar{F}$ in order to stabilize the solution, as in Susskind et al. [12].

For AMTS, mean temperatures in 10 layers, shown in Table 5.1.2, are used to estimate coefficients of 9 empirical orthogonal functions, with $\sigma = 1 \times 10^{-3}$. For HIRS2, 6 mean layer temperatures are used to estimate coefficients of 5 empirical orthogonal functions with $\sigma = 5 \times 10^{-4}$.

At pressures above 30 mb, the procedure is modified because the empirical orthogonal functions do not extend above that level and also because we did not want possible large errors in the initial guess above 30 mb, caused by sparsity of radiosonde data above that level, to filter down through the atmosphere through equations (5.1.15) and (5.1.16). Above 30 mb we used the equation

$$T^{N+1}(P_\ell) = T^N(P_\ell) + \tilde{T}_{B,i} - T^N_{B,i} \qquad (5.1.18)$$

At intermediate pressures above 30 mb, $T^{N+1}(P) - T^N(P)$ was linearly interpolated in the log of the pressure. At pressures lower than that corrected by the highest sounding channel, $T^{N+1}(P) - T^N(P)$ was taken to be the same as that of the highest sounding channel.

Given the $N+1^{th}$ estimate of temperature profile, we now recompute the brightness temperatures for the temperature sounding channels and compare with the observed brightness temperatures. If the root mean square difference of observed brightness temperatures and those computed from the $N+1^{th}$ iteration is not less than .95 of the root mean square difference computed from the N^{th} iteration, we terminate the procedure and call $T^{N+1}(P)$ the solution. If not, we retrieve a ground temperature and continue the iterative process. If the procedure is terminated and the root mean square difference of observed and computed brightness temperatures is less than .5°, the retrieval is accepted. Otherwise it is rejected. In the clear portion of the test, no retrievals were rejected, either in analysis of the dependent or independent sets.

5.1.9 The Cloudy Test

The cloudy portion of the test is a more realistic simulation than the clear portion because it takes into account not only multiple layer clouds but also three dimensional temperature fields and the detailed scan pattern of the instrument. This introduces two major new elements into analysis of the data; the selection of the proper area in which to perform a retrieval for a given scene, and the estimation of the clear column radiances which would have been observed if the selected area were cloud free. The techniques used by GLA to perform these two elements are basically the same, but somewhat more sophisticated than those used in analysis of HIRS2/MSU data from TIROS-N [12]. Given estimates of clear column radiances in a given iteration, the steps used to produce the estimated temperature profile in that iteration are essentially identical to those used in the clear part of the test.

5.1.10 Steps in the Processing System

The processing system is comprised of the following steps:

1. Select and prioritize sub-areas in the scene in which retrievals will be attempted. The following steps are attempted in the highest priority sub-area. If the retrieval fails, then the retrieval is attempted in the next sub-area. If the retrieval fails in five sub-areas, then no retrieval is produced for the scene.

2. Starting with a climatology guess, estimate clear column radiances, $\hat{R}_i^0$.

3. Using clear column radiances, determine ground temperature, T_S^0 (Eq. 5.1.7).

4. Re-estimate clear column radiances using T_S^0.

5. Using estimated clear column radiances, angle correct observations to nadir as in Eq. (5.1.1) for the purpose of generating the regression guess.

6. Generate regression $T^0(P)$, as in Eq. (5.1.3).

7. Using estimated clear column radiances, tune observations to give T_B as in Eq. (5.1.6). The iterative procedure now begins.

8. Using $T^N(P)$, T_S, and the tuned radiances, estimate $N+1^{th}$ iterative clear column radiances, $\hat{R}_i^{N+1}$ and, equivalently, clear column brightness temperature, $\hat{T}_{B,i}^{N+1}$.

9. Retrieve the $N+1^{th}$ ground temperature based on $N+1^{th}$ estimate clear column radiances.

10. Adjust atmospheric temperature profile to give $T^{N+1}(P)$ as in Eqs. (5.1.13) to (5.1.18), but replacing $\tilde{T}_{B,i}$ by $\hat{T}_{B,i}$.

11. Compare computed radiances from iterative solution, R_i^{N+1}, with estimated clear column radiances $\hat{R}_i^{N+1}$. If sufficient agreement is found, terminate iterative procedure. Otherwise return to step 8 to start $N+2^{nd}$ iteration with new estimate of clear column radiances.

The iterative procedure is identical to that used in the clear test, with the exception that the clear column radiances, R_i^{N+1}, are re-estimated every iteration. In addition, the climatological humidity profile was used, without change, to compute all transmittances in the cloudy test. The humidity scaling step, as in Eq. (5.1.12), was omitted in the cloudy test because the major effect of water vapor errors on retrieval errors occurs when handing the effect of reflected solar radiation in the determination of ground temperature during the day. The cloudy test was all night-time midlatitude cases. Therefore, reflected solar radiation was not a factor in the test. In addition, the atmospheres were all reasonably dry and the assumption of climatological humidity profiles was expected to be reasonable enough. The details of the new steps are given in the following two sections.

5.1.11 Selection and Prioritization of Sub-Areas

The scan pattern of the observations is shown in Figure 5.7. An AMTS scene is given as a 20 x 20 array of contiguous spots, 10 x 10 km at nadir. The HIRS scene is given as a 10 x 5 array of spots, 20 x 20 km at nadir. A multiple field of view approach is used to estimate clear column radiances in a given area. Two fields of view are needed to correct for one assumed cloud formation, three fields of view are needed to correct for two cloud formations, etc. In analysis of HIRS2/MSU TIROS-N data [12], two fields of view were used to account for one layer. In this test, three fields of view were used to account for two cloud formations. The fields of view are selected so as to maximize the contrast between them. To achieve maximum contrast, the spots in a sub-area are grouped according to increasing brightness temperature in an 11 m window channel, with each group being taken as a field of view.

Slightly different procedures were used for each instrument. In the case of HIRS2, each sub-area was comprised of 3 x 3 groups of spots, corresponding to roughly 60 km x 100 km at nadir. Twenty-four sub-areas, corresponding to all 3 x 8 possible groups of 3 x 3 spots, were considered. In each sub-area, the spots were ordered according to the brightness temperature for channel 8, the 11 μm window. Field of view 1 was taken as the three warmest spots, field of view 3 as the three coldest spots. The radiance for each channel in each field of view was taken as that of the spot containing the warmest 11 μm window observation in that field of view. The x, y coordinate of the sub-area was taken as that of the spot used in field of view 1. The MSU channel observations for the sub-area were taken as those of the spot used in field of view 1.

Each sub-area is given a priority number based on three parameters which should be reflections of cloudiness; (1) the 11 μm window brightness temperature in the warm field of view, (2) the difference between the 3.7 μm and 11 μm window channel brightness temperatures in the warm field of view, and (3) the standard deviation of the 11 μm window brightness temperatures in the warm field of view. The objective is to prioritize the spots according to decreasing cloudiness. Under clear conditions, one generally obtains a warm 11 μm window observation, a small difference between 11 μm and 3.7 μm window observations, and a small standard deviation of 11 μm window channel observations. With increasing cloudiness, the 11 μm window observation generally decreases, the difference between the 3.7 μm and 11 μm observations increases until almost full overcast and then begins to get small again, and the standard deviation in the 11 μm window increases, then, like the difference in the window channel observations, decreases as full overcast is approached. For each sub-area, we define the following quantities: A_0 is the difference between the 11 m window brightness temperature in field of view 1 and that of the single warmest field of view in the scene; A_1 is the difference between the difference of the 3.7 μm window brightness temperature and the 11 μm window brightness temperature in that sub-area, and that of the spot containing the closest 3.7 μm observation compared to the 11 μm observation; A_2 is the standard deviation of the 11 μm window brightness temperatures; and A_3 is the sum of the squares of the previous three quantities. The priority is

assigned according to decreasing values of A_3, with the sub-area having the lowest value of A_3 given the highest priority for a sounding location. In general, low values of A_0, which are used to prioritize sub-areas in analysis of TIROS-N HIRS2 data [12] also corresponds to low values of all the other quantities, that is, to small differences in 11 μm and 3.7 μm brightness temperatures and small standard deviations in the 11 μm observations. Nevertheless, a low A_0 (warm 11 μm window channel measurement) may be reflective of thermal gradients and not necessarily the clearest area, and the combined use of three indicators of an area which should be relatively clear was found to be more desirable. In the analysis of the 40 test cases, the retrieval attempted in the first priority area was always successful.

The AMTS data was treated in a slightly different manner than the HIRS2 data, primarily because of the higher spatial resolution of AMTS. For AMTS, each sub-area was made to consist of 6 x 6 contiguous spots corresponding to 60 x 60 km at nadir. This sub-area was broken into 4 fields of view each containing 9 spots, ordered and separated according to the radiances in the 11 μm window channel 12. Because AMTS spots are 10 x 10 km, and estimates based on a 20 x 20 km spot were used to generate the noise levels used in the clear part of the test, it was necessary to average at least 4 AMTS spots to achieve the same noise levels. In analysis of the data, we averaged the radiances for all 9 spots to give the radiances in each field of view for each channel. The corresponding MSU channel observations for the sub-area was the average of the observations in field of view 1. The zenith angle for each field of view was assigned as the angle whose cosine was the average of the cosines of all the spot zenith angles in the field of view. This procedure is identical to that done in analysis of HIRS2 TIROS-N data [12]. The x, y coordinates for each field of view are taken as the average of the x, y coordinates for all the spots in the field of view. Every other contiguous block of 6 x 6 spots was taken as a possible sub-area, resulting in 64 possible sub-areas for each scene. The sub-areas were assigned priorities in an identical fashion to those of HIRS2, using the averaged radiances to compute the brightness temperatures for the window channels. Channel 28, the most transparent 3.7 μm window channel, was used together with channel 12 in computing A_1. The analysis of the 40 test cases, the highest priority sub-area produced a successful retrieval in all but one scene, in which case the second priority sub-area was used. In some cases, the sub-area selected for AMTS by this objective approach was in a totally different part of the scene than that selected for HIRS2.

5.1.12 Estimation of Clear Column Radiances

The estimation or "reconstruction" of clear column radiances from a set of potentially cloud contaminated radiances is the single most important step in the retrieval of temperature profiles using infra-red observations. The approach we used in the test is a slightly generalized version of the approach used in Susskind et al., (1984). As shown by Chahine (1979), if one assumes M multiple cloud formations, the clear column radiances, $\hat{R}_i$, can be reconstructed by observations in M+1 fields of view according to

$$\hat{R}_i = R_{i,1} + \sum_{j=1}^{M} (R_{i,j+1} - R_{i,1}) \qquad (5.1.19)$$

where $R_{i,j}$ is the observed (tuned) radiance for channel i in field of view j. In analysis of TIROS-N data, a two field of view approach was used to determine one value of and to correct for one assumed cloud formation. In the test, three fields of view were used in analysis of both HIRS2 and AMTS data to correct for two assumed cloud formations. In the case of AMTS, radiances in the first, second, and fourth fields of view were used in analysis of the data. The data in the third field of view was not used.

First, we briefly review the procedure used to correct for clouds using one field of view. From Eq. (5.1.19), assuming only one cloud formation, we can estimate η according to

$$\eta_i^{N+1} = (R_{i,clr}^{N} - R_{i,1})/(R_{i,2} - R_{i,1}) \qquad (5.1.20)$$

where η_i^{N+1} is the value of η estimated from channel i using the value of $R_{i,CLR}^{N}$ computed for channel i from Eq. (4.1.1) using the N^{th} guess temperature profile and ground temperature. The iteration numbers N and N+1 are shown to be consistent with section 5.1.10. Henceforth, for simplicity, we will keep the superscripts the same for η and R (or T_B).

Errors in the N^{th} guess temperature profile will result in differences between $R_{i,CLR}^{N}$ and the true clear column radiance $R_{i,CLR}$. The effects of guess errors of a bias nature can be removed, to first order, by simultaneous use of a microwave channel sounding a similar portion of the atmosphere to that sounded by the infra-red channel used to estimate η, because a local bias error will cause roughly equivalent errors in the computed brightness temperature, T_B, for the two channels. We therefore estimate η according to

$$\eta_i^{N} = \{B_i[T_{B,i}^{N} + T_{B,M} - T_{B,M}^{N}] - R_{i,1}\}/(R_{i,2} - R_{i,1}) \qquad (5.1.21)$$

where $T_{B,M} - T_{B,M}^{N}$ represents the difference between observed and computed brightness temperatures for the microwave channels used in conjunction with infra-red channel i and $T_{B,i}^{N}$ is the brightness temperature corresponding to $R_{i,CLR}^{N}$. The quantity in brackets will be referred to as the microwave corrected brightness temperature $T_{B,i}^{'N}$. It is desirable to maximize the numerator and denominator in Eq. (5.1.21) to increase stability of the solution. Therefore, in analysis of TIROS-N data, Eq. (5.1.21) is used with HIRS2 channel 13, the lowest sounding 4.3 μm channel, in conjunction with MSU channel 2, the tropospheric sounding channel. Alternatively, HIRS2 channel 7, the lowest sounding 15 μm channel, could have been used in conjunction with MSU channel 2.

At least two infra-red channels must be used when attempting to correct for two cloud layers, as done in analysis of the test data. For HIRS2, channels 6 and 7, the two lowest sounding 15 μm channels, were used in conjunction with microwave channel 2, while for AMTS, channels 1 and 2, again the lowest sounding 15 μm channels, were used in conjunction with microwave channel 2. The clear column radiances for all channels were reconstructed according to

$$\hat{R}_i^N = R_{i,1} + \eta_1^N(R_{i,c} - R_{i,1}) + \eta_2^N(R_{i,2} - R_{i,1}) \qquad (5.1.22)$$

where field of view c is the field of view with the lowest 11 μm brightness temperatures, presumably the cloudiest field of view. In the case of HIRS2, this represents field of view 3 while for AMTS, it represents field of view 4. Once η_1 and η_2 are determined in a given iteration, the values of $\hat{R}_i$ obtained from Eq. (5.1.22) are used in the subsequent steps in the analysis for that iteration just as the tuned observed radiances, R_i, were used in the clear part of the test.

The approach to determine η_1 and η_2 involves first testing to see if the sub-area is thought to be clear, in which case η_1 and η_2 are set equal to zero. If not, a value of η_1 is estimated from Eq. (5.1.22) assuming only one cloud formation, that is, $\eta_2 = 0$. Once η_1 is solved for, η_2 is then determined from Eq. (5.1.22) using the previously obtained value of η_1. η_2 is usually at least one to two orders of magnitude smaller than η_1.

The sub-area is assumed to be clear if the following conditions hold: (1) the standard deviation of the 11 μm window observations in field of view 1 is less than .2°C; (2) the 11 μm brightness temperature is within .5°C of the warmest value in the scene; and (3) the microwave corrected estimate of the brightness temperature for the lowest sounding 15 μm channel computed from the N^{th} guess agrees with the observed brightness temperature for that channel to 1°C. If these conditions are not satisfied, two estimates of η_1 are obtained, using the two 15 μm cloud filtering channels according to

$$\eta_{i,1}^N = [B_i(T'^N_{B,i}) - R_{i,1}]/(R_{i,c} - R_{i,1}) \qquad (5.1.23)$$

and η_1^N is given by the average of the estimates from channel i and j, weighted by the square of the denominator in Eq. (5.1.23), representing the relative effect of clouds on each channel. The weighted value of η_1 is taken as

$$\eta_1^N = \frac{(R_{i,c} - R_{i,1})^2 \eta_{1,i}^N + (R_{j,c} - R_{j,1})^2 \eta_{1,j}^N}{(R_{i,c} - R_{i,1})^2 + (R_{j,c} - R_{j,1})^2 + \delta^2} \qquad (5.1.24)$$

where δ is a small damping parameter, taken as .25°C, which is close to the

uncertainty in calculating the denominator. If the estimate of η_1^N obtained in Eq. (5.1.24) is less than zero, it is set equal to zero.

If η_1^N is found to be zero, η_2^N is also set equal to zero. Otherwise, η_2^N is solved for in a completely analogous manner, using fields of view 1 and 2 with the term accounting for the inhomogenity due to cloud formation 1 subtracted from the estimated clear column radiances for each channel:

$$\eta_{2,i}^N = [B_i(T'^N_{B,i}) - R_{i,1} - \eta_i^N(R_{i,c} - R_{i,1})]/(R_{i,2} - R_{i,1}) \qquad (5.1.25)$$

$$\eta_2^N = \frac{(R_{i,2} - R_{i,1})^2 \eta_{2,i}^N + (R_{j,2} - R_{j,1})^2 \eta_{2,j}^N}{(R_{i,2} - R_{i,1})^2 + (R_{j,2} - R_{j,1})^2 + \delta^2} \qquad (5.1.26)$$

$\eta_{2,i}$ is set equal to zero in Eq. (5.1.25) if either the correction to the clear column radiance for the lowest 15 μm sounding channel from η_2, as obtained from Eq. (5.1.22), is less than 3% or more than 30% of that from η_1. In the first case, η_2 is thought to be insignificant, and in the second case, a potential problem is thought to exist. η_2 was found to be zero in all 40 cases for both HIRS2 and AMTS in the final estimate, but not necessarily in the intermediate estimates in the iterative system. η_1 was found to be zero in 23 cases for AMTS and in 19 cases for HIRS2. These cases were treated as clear in the final iteration, though they were not necessarily clear in actuality.

It is undesirable to perform a retrieval under very cloudy conditions when large extrapolations from observed radiances are necessary to give the clear column radiances. Therefore, the sub-area is called too cloudy to perform a retrieval if $\eta_1^2 + \eta_2^2 > 16$ or if the difference in the observed brightness temperatures for the lowest sounding 15 μm channel in the first and last fields of view is less than 1°C and the difference between the microwave corrected brightness temperature and the observed brightness temperature in field of view 1 is more than 2.5°C. Rejection according to these criteria never occurred in the highest priority spots but did occur in some of the cloudier areas.

5.1.13 Further Modifications to the Processing System

The major effect of clouds in the fields of view is to introduce a larger degree of uncertainty, or noise, in the clear column radiances than was represented by the instrumental noise levels used in the clear test, even after the cloud effects have been accounted for to first order. In addition, because of the clouds, steps had to be added to the procedures used in analysis of the data in the clear test because construction of the regression guess and tuning of the radiances require an estimate of clear column radiances. These clear column radiances, $\hat{R}_i$, can be estimated using Eqs. (5.1.22) to (5.1.26) but only after an initial guess of the

atmospheric temperature, and humidity profiles and the ground temperature are provided. To start the process, we used a zonally averaged climatology first guess for the temperature-humidity profile. The ground temperature to be used in Eq. (4.1.1) to compute channel radiances was set equal to the guess surface air temperature.

The microwave correction used to correct for initial guess errors in clear column radiances removes the effects of bias errors in the mid-lower troposphere but leaves residual errors in η due to errors in the structure of the guess and also, to even a larger extent, errors in the guess ground temperature. The estimates of both the atmospheric temperature profile and the ground temperature are expected to improve throughout the course of the iteration. Therefore, the reconstruction of clear column radiances becomes part of the iterative procedure.

Before the iterative procedure or even the generation of the regression guess begins, we use the estimated clear column radiances, $\hat{R}_i^0$, to compute an improved ground temperature, T_S^0, using Eq. (5.1.7). Using the estimated ground temperature, R_i^0, η_i^0, and $\hat{R}_i^0$ are re-estimated. At this point, we are ready to prepare to begin the iterative cycle, with the generation of the regression guess and the tuned observed radiances, as in Eqs. (5.1.1) to (5.1.4) and Eq. (5.1.6), using the 0^{th} estimate clear column brightness temperature $T_B^0{}_{,i}$ in the equations. The regression guess will, in general, be less accurate than that of the clear test because of residual uncertainties in the clear column brightness temperatures. The tuning will also be affected by uncertainties in clear column radiances but the tuning is small and therefore it is not iterated.

The iterative procedure begins with the estimation of the first iterative clear column radiances $\hat{R}_i^0$ using Eqs. (5.1.22) to (5.1.26). The brightness temperatures T_B^0 are computed from the regression guess, $T^0(P)$, and the initial retrieved ground temperature T_S^0. In the general iterative scheme, $\hat{R}_i^{N+1}$ is computed using T_B^N. The iterative ground temperature T_S^{N+1}, is now computed using $T^N(P)$ and $\hat{R}_i^{N+1}$. Based on T_S^{N+1} and $T^N(P)$, $T_B^N{}_{,i}$ is computed from Eq. (4.1.1). $T^{N+1}(P)$, the N+1th estimate of temperature profile, is now computed essentially as in Eqs. (5.1.13) to (5.1.17) in the clear test but in this case, $\hat{T}_B^{N+1}{}_{,i}$ the N+1th iterative estimate clear column brightness temperature based on the tuned observations, is used. As before, the expansion Eq. (5.15) is about the regression initial guess. The terms represented by the empirical orthogonal function expansion are now expected to be larger, however, because the guess may be poorer than in the clear part of the test. For the case of HIRS2, it was found that errors in the estimated clear column radiances produced sufficient noise so that additional smoothing had to be added in the temperature relaxation equation, in a manner completely analogous to that done in analysis of TIROS-N data [12]. For HIRS2, Eq. (5.1.13) was replaced by

$$\bar{T}_i^{N+1} = \bar{T}_i^N + \sum \bar{W}_{ij}(\hat{T}_{B,j}^{N+1} - T_{B,j}^{N+1}) \qquad (5.1.27)$$

where $\bar{W}_{ij}$ is the normalized slab average weighting function for temperature sounding channel j in layer i. This smoothing procedure was not found to be necessary for analysis of AMTS data, even under cloudy conditions, presumably because the clear column radiances were better accounted for in the cloud filtering procedure. The convergence requirement and rejection criteria in the cloudy test are identical to those in the clear test. In addition, once convergence has been reached, an additional check is added to test whether the retrieved temperature profile is consistent with the tropospheric sounding microwave observation. This is a final check to make sure that the cloud filtering has been done properly. After convergence, the profile is rejected if the brightness temperature computed for MSU channel 2, using the solution ground temperature and air temperature, differs from the observation in that channel by more than 1°C if the field of view was clear, and .5°C if the field of view was cloudy. The criterion is made more stringent under cloudy conditions because in these cases, MSU channel 2 affects the reconstructed clear column radiances and hence the solution. Under clear conditions, the observations in MSU channel 2 do not influence the solution in any way.

5.2 NESDIS Procedure

5.2.1 Clear cases

The NESDIS retrieval system used in the AMTS-HIRS test has two components. One is an angle correction procedure that adjusts all radiances to zero nadir. The second is the conversion of radiances to temperature.

This test is a comparison between an existing procedure and one that is being proposed. It started as a comparison between the NESDIS operational retrieval method and an approach proposed by M. Chahine. However, Chahine claimed that the advantages of his method would not be fully demonstrated by a HIRS instrument and for this reason the AMTS instrument was included in the test.

NESDIS's interest is in the potential for improving the operational approach so minimal changes have been made that are not duplicated in the operational system. However it should be noted that present HIRS instruments are considerably more noise-free than early instruments in the series. With less noise, more channels could be added to increase the vertical resolution through mathematical deconvolution of the weighting functions. Advances in cooling technology as proposed for the AMTS could be applied to the HIRS instrument to provide an additional decrease in noise with another increase in the number of channels that could be deconvoluted to increase the vertical resolution. These considerations were not part of the test.

Another factor to be considered in the test is that the HIRS instrument is used with two other instruments which compliment the HIRS in the upper atmosphere. These instruments lead to an increase in accuracy of TOVS soundings over HIRS alone in the upper atmosphere. In the future, an even more advanced microwave instrument is being proposed. Selection of a future infrared instrument should consider the marginal increase in

accuracy over microwave instruments which will likely be flying at that time.

The temperature retrieval for the NESDIS processing is easy to describe. It is the eigenvector regression described by Smith and Woolf [27]. In that regression, eigenvectors are found for both the radiances and the temperatures. The eigenvalues are checked and only those eigenvectors associated with eigenvalues larger than some minimum value are kept. Both the radiance and temperature profiles are then expressed as coefficients of the significant eigenvectors. Normal regression is used to predict the coefficients of the temperature eigenvectors from the coefficients of the radiance eigenvectors. These regression coefficients are then multiplied by the eigenvectors. This step transforms a regression which relates eigenvectors to eigenvectors to one which relates temperature to radiances. If all eigenvectors are used, the final result produces regression coefficients which agree with values produced by conventional methods. However, the radiances which serve as predictors have large correlations among themselves. When noise is present, the result of a normal regression tends to be unstable. Discarding the eigenvectors associated with the smaller eigenvalues tends to stabilize the regression and has an effect similar to ridge regression.

To summarize the regression, let

$$t=T^{*}a \tag{5.2.1}$$

and

$$t_B=T_B{}^{*}b, \tag{5.2.2}$$

where t and t_B are the vectors of temperature and brightness temperature, respectively, expressed as deviations from the sample mean, a and b are the coefficients of the eigenvectors, and T^{*} and $T_B{}^{*}$ are matrices containing the elements of the significant eigenvectors. Thus the dimension of a is less than the dimension of t and T^{*} is not a rectangular matrix because some eigenvectors have been deleted. Standard regression is used to find D in the relationship

$$a=Db, \tag{5.2.3}$$

where D is the matrix of regression coefficients. Finally, it is noted that

$$t=T^{*}Db \tag{5.2.4}$$

from Eqs. (5.2.1 and 5.2.2). Since the eigenvectors are orthogonal

$$b-T_B{}^{*}t_B \tag{5.2.5}$$

and substitution into Eq. (5.2.4) yields

$$t=T^{*}DT_B{}^{*}t_B \tag{5.2.6}$$

and

$$t = C t_B, \qquad (5.2.7)$$

where

$$C = T^* D T_B^*. \qquad (5.2.8)$$

The angle correction is more complicated because of various problems associated with the calculation of transmittances. NESDIS generates transmittances using a fast code which uses empirical coefficients generated, in turn, from line-by-line calculations. About four hours of computer time is required to generate the line-by-line data which are saved. Generation of empirical coefficients for a new instrument requires minutes of time since the line-by-line program has to be run only for major science changes. The original plan was to have an independent party (The University of Denver) calculate line-by-line transmittances. It turned out that the Denver line-by-line programs were too slow to calculate the coefficients. It would have taken weeks to run the data on the Cray. An alternative was needed and it was decided to use a Goddard fast transmittance that is similar to, but somewhat less accurate than, the NESDIS version. This code was selected because the Goddard physical retrieval method is more dependent on knowledge of the transmittance than the regression approach employed by NESDIS. In addition, fast coefficients were available for both the HIRS and AMTS instruments. Unfortunately, the Goddard fast coefficients had been generated with HIRS filters that had been truncated by chopping off the wings of the filters. This caused a discrepancy between Goddard and NESDIS fast coefficients. When this was discovered, it was also found that Goddard could not rerun the data because the basic data had not been saved and 150 hours of computer time would be required. Apparently the filters had been truncated because the Goddard system calculates each filter separately, even though there is appreciable overlap in the wings of the HIRS filters and a significant portion of the computer time can be saved by simply storing the line-by-line data from one filter to the next.

These factors had impacts on the angle correction procedure. In fact, given the small size of the angle effect and the relatively large changes due to differences in transmittance programs, the comparison would have been more reliable if the angle effects had been ignored.

In a regression procedure, angle adjustment coefficients are calculated from simulated data. This is because the adjustment requires cloudy radiances at two or more different angles for the same location, a physical impossibility for real data. A set of 1200 atmospheres are used to simulate clouds at various amounts and heights.

The use of Goddard transmittances was regarded as satisfactory until it became known that the HIRS filters had been truncated. At this point it was decided to produce a second run with data generated at zero angle. This was used to check the angle correction procedure for clear atmospheres. In addition, the data at zero angle provided a set of 400 atmospheres for which radiances were available at two angles. It was possible to generate angle data from these cases. Results of the various

angle corrections show that the error in the final angle correction is small, but the original NESDIS coefficients produced large errors due to the differences in the truncation of the weighting functions. To anticipate a question, the idea of truncating the weighting functions in the NESDIS calculations was considered, but there were uncertainties about the nature of the truncation that could not be resolved to everyone's satisfaction.

The AMTS corrections show slightly larger errors than the HIRS weighting functions. This is due to the fact that AMTS angle corrections were generated indirectly from the HIRS corrections. However, the increase in error due to this effect is less than 0.1K with the exception of a couple levels. The effect on the overall statistics was judged to be negligible.

Angle correction coefficients are calculated from the following relationship.

$$BT_j^o - BT_j^o = a_o + \sum_{i=1}^{N} a_i BT_i^o,$$

where BT_j is the brightness temperature for channel j at zero nadir angle, BT_j is the value at angle θ, and a_o and a_i are constants.

There was an attempt to evaluate the effect of noise on the retrievals by doubling the amount of noise present. However, the seed of the random number generator was not reset so the case with more noise had different noise from the original data, not the same noise with twice the amplitude. In a large sample, the difference should not be significant. The increase in accuracy with increased noise shown for the AMTS at some levels is in opposition to expectations and raises the possibility that there is some effect due to the fact that different random numbers were used. These results raise doubts about the validity of the results for the double noise test.

6. CLEAR COLUMN RESULTS (N. Phillips)

Appendix B contains a detailed tabulation of the results obtained by comparing the retrieved temperatures from the two instruments and two retrieval methods against the "original soundings." In doing this, each standardized original sounding T(p) defined as a sequence of connected straight line segments in log p, was first converted into a sequence of 22 temperature values defined as the mean value (with respect to log p) for the 18 verification layers between 1000 and 100 mb (the "troposphere"), and for the 4 layers between 100 and 16 mb (the "stratosphere"). Inspection of the individual continental and oceanic results showed little or no systematic difference. Therefore this distinction is ignored in this summary.[1]

A common measure will be a root mean square error. For a layer temperature this will be

$$dT_{jk\ell} = \sqrt{[1/N_k] \sum_{i=1}^{N_k} [T_{ijk}(ret_\ell) - T_{ijk}(ver)]^2}^{1/2}, \qquad (6.1)$$

where j (increasing upward) denotes the layer, k denotes the data base (latitude belt and/or season), N_k is the sample size, and denotes a particular choice of instrument and retrieval method. "ret" and "ver" denote the retrieved value and the verifying value. This measure is not sufficient by itself, however, since the vertical distribution of dT is meteorologically significant. Experience [22,23] has shown that dT has a vertical distribution such that it can be smaller for very thick layers than for thin layers.

As one aspect of this it is useful to examine the error in the height thickness error for pressure level j, obtained by replacing the two temperature values in the right side of (6.1) by the hydrostatic height of the pressure P_j relative to 1000 mb:

$$h_{iJk\ell} = (R/g) \sum_{j=1}^{J} T_{ijk\ell} \ln(p_{j-1}/p_j). \qquad (6.2)$$

(We ignore virtual temperature correction.)

Table 6.1 shows these measures as summary values of dT for the troposphere (1000>p>100) and stratosphere (100>p>16), and for the value of dh at two tropospheric pressure values. (STAT denotes the NESDIS statistical retrieval process and PHYS the NASA physical process described in Chapter 5.) The detailed vertical structure of dT, averaged for both latitude belts and both seasons, is shown in Figure 6.1. ("Averages" of dT are of

[1]The identity of the two instruments was coded in the retrieval tapes (HIRS = 1 and AMTS = 2) as was the retrieval method (STAT = 4, PHYS = 5) until this chapter was ready for final typing.

Table 6.1. Summary error measures of root mean square temperature and geopotential errors for different data sets, instruments, and retrieval methods. Units are degrees and meters.

Statistic	Data set	Inst: / Meth:	HIRS STAT	HIRS PHYS	AMTS STAT	AMTS PHYS	HIRS BOTH	AMTS BOTH	BOTH STAT	BOTH PHYS
dT over 18 layers (1000-100 mb)	Jan 30S-30N		1.74°	1.70°	1.29°	1.18°				
	Jun 30N-60N		2.64	2.48	2.10	1.72				
	Jun 30S-30N		1.77	1.66	1.32	1.16				
	Jun 30N-60N		2.28	2.06	1.62	1.43				
	Mean		2.14	2.00	1.62	1.39	2.07	1.51	1.90	1.72
dT over 4 layers (100-16 mb)	Jan 30S-30N		2.83°	2.78°	1.66°	1.85°				
	Jan 30N-60N		3.01	3.31	2.21	1.94				
	Jun 30S-30N		2.00	1.94	1.54	1.36				
	Jun 30N-60N		1.79	1.52	1.18	0.98				
	Mean		2.46	2.49	1.69	1.58	2.48	1.64	2.11	2.09
RMS of mean (bias) error over 18 layers (1000-100 mb)	Jan 30S-60N		0.44°	0.60°	0.27°	0.24°				
	Jun 30S-60N		0.25	0.47	0.22	0.18				
	Mean		0.36	0.54	0.25	0.21	0.46	0.23	0.31	0.41
dh (527 mb)	Jan 30S-30N		10.6m	7.7m	8.6m	4.0m				
	Jan 30N-60N		15.1	7.6	12.3	5.3				
	Jun 30S-30N		10.3	7.7	6.5	3.8				
	Jun 30N-60N		10.7	8.2	9.5	4.6				
	Mean		11.8	7.8	9.5	4.5	10.0	7.4	10.7	6.4
dh (245 mb)	Jan 30S-30N		14.6m	15.5m	13.6m	12.8m				
	Jan 30N-60N		34.0	37.4	30.5	33.1				
	Jun 30S-30N		14.5	17.8	11.1	11.0				
	Jun 30N-60N		25.7	21.0	19.5	15.6				
	Mean		23.7	24.5	20.1	20.2	24.1	20.1	22.0	22.4

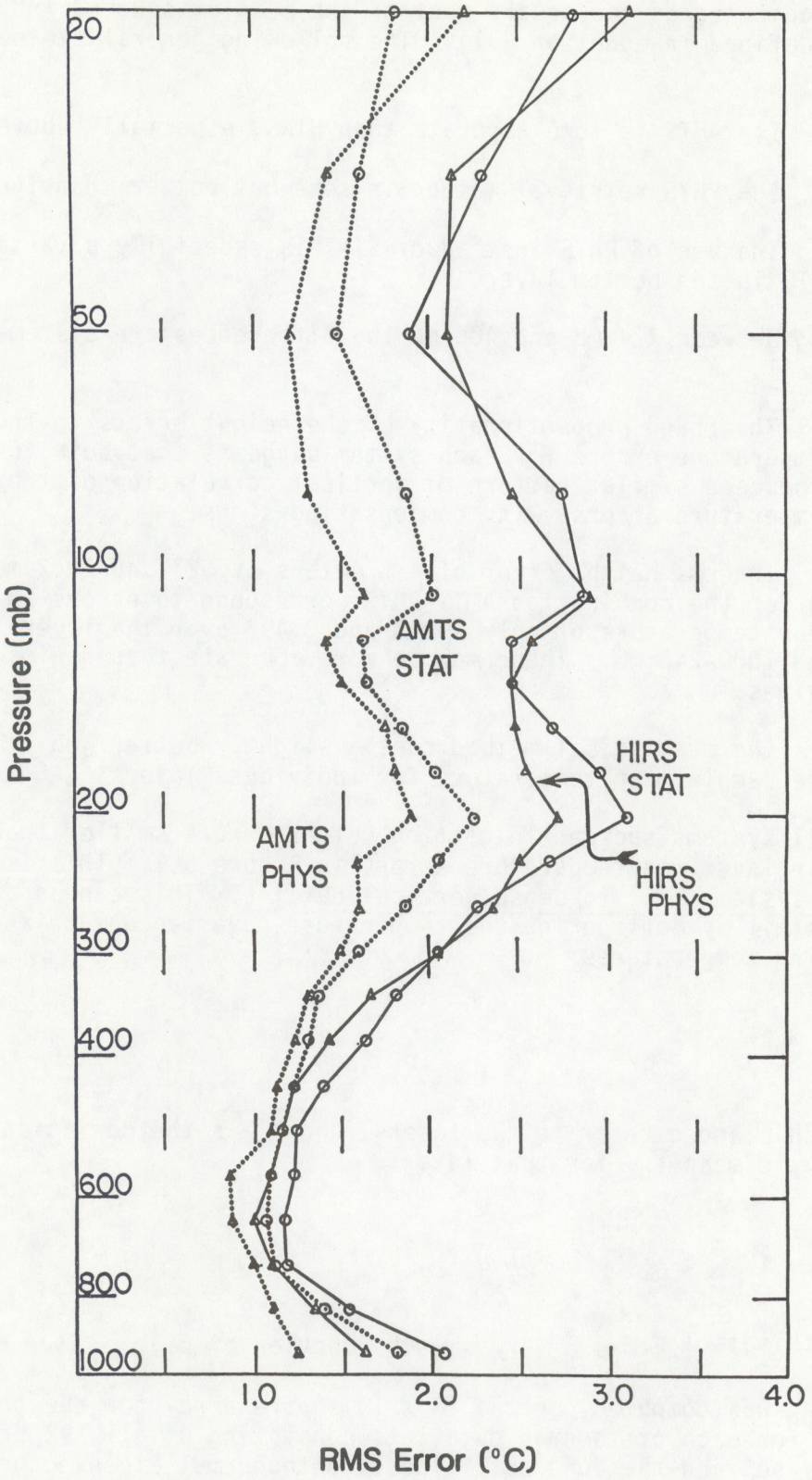

Figure 6.1 Vertical distribution of rms retrieval error averaged over all latitudes and both seasons. Values are plotted at the mean log p for each layer.

course computed as the square root of the mean of squared individual dT values defined in equation 6.1). The following general statements can be made.

A. The AMTS is more accurate than HIRS, especially above 300 mb.

B. The PHYS retrieval method is somewhat better than the STAT method.

C. The use of PHYS instead of STAT is especially advantageous for AMTS in the bottom layer.

D. Between 774 mb and 408 mb the differences are systematic but small.

E. The rough proportionality of the height errors to tropospheric temperature errors for each system suggests that both instruments produce a similar pattern of vertical correlation of tropospheric temperature errors, with compensating signs.

F. The rms height error of 4.5 meters at 527 and 20.2 meters at 245 mb for the combination AMTS-PHYS correspond to errors in vertical mean temperature of only 0.24° and 0.49° over the layers 1000-527 and 1000-245 mb. These may be more accurate than radiosonde values.

G. The statistical method does a slightly better job in retrieving the sample mean temperature for individual layers.

All systems succeed in getting height errors smaller than is suggested by their layer rms temperature errors in Figure 6.1. This is only possible if all systems fail to sense vertical details. This can be examined in more detail by considering the temperature covariance matrix of the verifying temperatures

$$C_{pqk} = (1/N_k) \sum_{i=1}^{n_k} T_{ipk}' T_{iqk}', \tag{6.3}$$

in which p and q refer to two layers, and T' is the deviation of T_{ipk} from the sample mean $\overline{T}_{pk}$ for that layer:

$$\overline{T}_{pk} = (1/N_k) \sum_{i=1}^{N_k} T_{ipk}(ver). \tag{6.4}$$

(In both sets $\overline{T}_{pk}$ was a very smooth function of p.)

C_{pq} was computed for the 18 x 18 square array for the troposphere layers for each of the two data sets consisting of all 192 profiles in the January set and the June set. The 18 orthonormal eigenvectors ε_{jn} of the symmetric matrix C_{pq} define "empirical orthogonal functions" for T' of this statistical sample, while the associated eigenvalues λ_n give the variance

of T' associated with each eigenvalue. The latter account for the total variance of T':

$$\sum_{p=1}^{18} C_{pp} = \sum_{n=1}^{18} \lambda_n. \tag{6.5}$$

The eigenvectors and eigenvalues are described in Table 6.2. The June and January values are very similar although the total variance in June (741 deg^2) is only about half that of the January set (1549 deg^2). This table (and the complete set) shows that the variance contributed by each eigenvector decreases as its vertical structure becomes more variable (i.e. more changes of sign). In winter 99.07 percent of the variance is in the first 5 eigenvectors. (These are shown graphically in Figure 6.2) In summer eigenvectors 1-5 account for 98.11 percent, with eigenvector 6 bringing the total to 98.89 percent.

A single profile of temperature deviation, either T'(ret) or T'(ver), can be analyzed into a linear combination of the ε_{jn},

$$T_{ij}' = \sum_{n=1}^{18} \alpha_{in}\varepsilon_{jn}, \tag{6.6}$$

where the expansion coefficient is given by

$$\alpha_{in} = \sum_{j=1}^{18} \varepsilon_{jn}T_j'. \tag{6.7}$$

The success of a particular system (ℓ) in retrieving vertical detail in T' below 100 mbs can then be examined by computing the error variance for each eigenvector

$$V_{nk\ell} = (1/N_k) \sum_{i=1}^{N_k} [\alpha_{ink}(ret_\ell) - \alpha_{ink}(ver)]^2. \tag{6.8}$$

[The sum of $V_{nk\ell}$ over all n would equal the sum of $(dT_{jk\ell})^2$ over j = 1,18 except that $V_{nk\ell}$ ignores errors in $\overline{T}$.] For example, if system ℓ = 1 has smaller values of dT at all levels than does system ℓ = 2, it might achieve this either by reducing $V_{nk\ell}$ for all or most values of n, or by only reducing $V_{nk\ell}$ for the first several values of n. In the former case it would do a better job of reproducing all vertical detail, while in the second case i would be doing so only for that vertical detail contained in the first several eigenvectors shown in Figure 6.2.

Table 6.3 describes this partitioning of squared error in T'. The sub-totals for vectors (1-5) and vectors (6-18) show clearly that:

H. All systems do equally poorly in eigenvectors 6-18, and the overall better performance of AMTS for dT and dh in Table 6.1

Table 6.2. Eigenvectors 1-6 plus 9, 12, and 18 (x 1000) for the winter and summer data sets, together with the fraction of the variance (parts per 1000) explained by each of them. The total mean variance was 1549 deg^2 for the winter set and 741 deg^2 for the summer set. In each set the eigenvectors are ordered according to decreasing eigenvalues.

RANK	1	2	3	4	5	6	9	12	18
				January					
VAR (0/00)	848	83	34	18	7	3	1	0.3	0.03
p(top)									
100	-240	303	426	-130	400	-165	258	-158	089
114	-208	314	344	-084	179	-040	-053	130	-311
129	-167	326	257	-039	-040	090	-271	245	418
147	-115	352	113	021	-251	203	-196	-169	-369
167	-044	393	-084	092	-363	144	181	-174	315
190	031	407	-250	141	-302	-010	323	111	-188
215	114	355	-357	078	004	-200	-151	181	061
245	185	275	-325	-057	317	-186	-327	-318	-056
278	234	187	-214	-167	369	-036	004	120	165
316	264	112	-088	-253	248	170	291	273	-332
359	283	052	044	-308	048	294	236	-278	415
408	290	020	138	-289	-112	289	-078	-199	-319
464	289	015	182	-224	-172	157	-338	404	157
527	287	019	209	-157	-225	-101	-083	038	-073
599	284	022	210	-046	-206	-391	181	-389	023
681	289	019	213	099	-116	-493	246	352	009
774	300	046	205	362	088	-144	-400	-209	-019
880	315	054	190	670	251	419	176	056	013
				June					
VAR (0/00)	805	97	41	28	10	8	1	0.5	0.05
p(top)									
100	-393	157	327	-267	227	-178	270	-254	019
114	-351	221	274	-226	141	-054	-156	387	-074
129	-295	284	190	-125	-023	095	-282	-003	111
147	-213	363	057	008	-209	214	-015	-297	-087
167	-096	445	-141	161	-301	157	289	166	066
190	023	452	-307	195	-159	-114	054	114	-069
215	128	347	-293	043	118	-317	-254	-250	106
245	202	246	-205	-118	324	-266	-126	-019	-198
278	241	178	-076	-251	366	-022	151	233	441
316	250	132	-002	-300	231	207	189	-013	-640
359	245	096	041	-297	068	322	072	-249	500
408	234	082	078	-272	-119	236	-141	-040	-231
464	220	057	105	-246	-328	105	-367	357	073
527	212	041	144	-192	-382	-042	-081	-148	-011
599	211	057	223	-090	-290	-266	423	-285	009
681	220	073	351	043	-121	-440	237	401	008
774	222	115	449	311	103	-196	-421	-271	-012
880	228	198	343	513	285	428	140	102	004

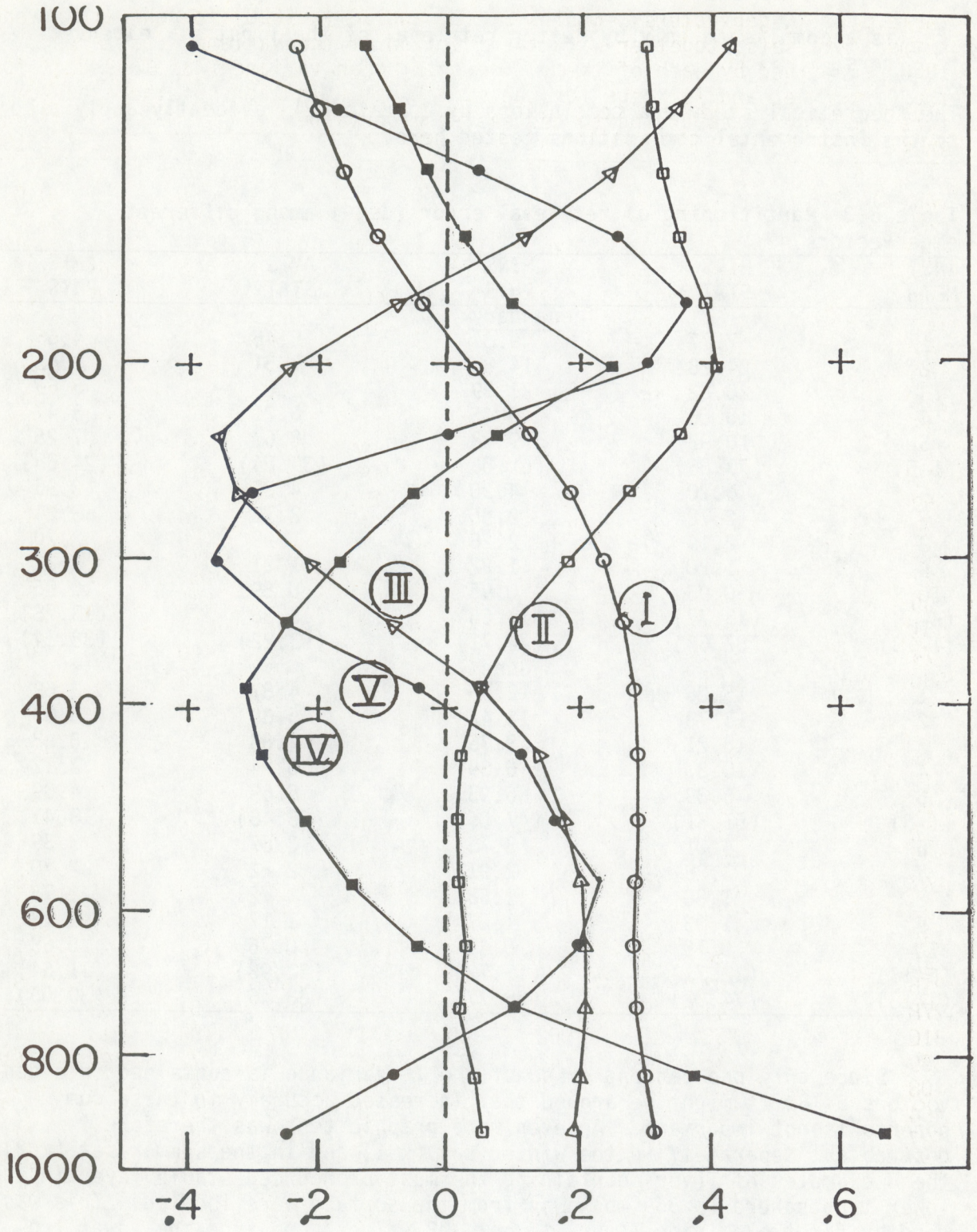

Figure 6.2 Variation with height of the first five eigenvectors (normalized) for the January data.

is accomplished only by better retrieval of the first six eigenvectors.

The theoretical study and conclusions by Conrath [24] evidently apply also to the instrumental combinations tested here.

Table 6.3 Partitioning of retrieval error (deg^2) among different eigenvectors.

INST METH	HIRS STAT	HIRS PHYS	AMTS STAT	AMTS PHYS
		January		
1	7.77	9.81	5.45	4.56
2	24.28	14.83	7.51	3.42
3	20.82	21.59	12.00	5.66
4	10.06	5.45	6.21	3.47
5	10.93	9.38	8.67	7.25
(1-5)	(73.86)	(61.06)	(39.84)	(24.36)
6	4.20	4.20	4.35	3.96
7	2.78	2.95	2.72	3.24
8	2.19	2.26	1.98	2.20
9	1.20	1.22	1.21	1.22
10	0.93	0.95	0.89	0.96
(6-18)	(13.77)	(13.65)	(13.38)	(13.78)
(1-18)	(87.63)	(74.71)	(53.22)	(38.14)
		June		
1	15.06	12.56	4.87	3.69
2	18.78	12.42	5.35	3.63
3	10.21	8.75	4.83	3.88
4	10.87	6.39	5.74	3.12
5	6.39	6.93	5.69	4.39
(1-5)	(61.31)	(47.05)	(26.48)	(18.41)
6	4.01	3.75	3.67	3.39
7	3.28	2.91	2.82	2.70
8	1.80	1.68	1.72	1.75
9	1.03	1.07	1.17	1.17
10	0.75	0.68	0.76	0.68
(6-18)	(12.71)	(11.72)	(11.98)	(11.64)
(1-18)	(74.02)	(58.77)	(38.46)	(30.05)

Since only one percent or so of the T' variance is contained in eigenvectors 6-18, it might be argued that increased accuracy in these components is not important. An even more graphic test was therefore desirable. Separately in the winter set (k=1) and in the summer set (k=2), the 6 examples of T(ver) containing the most pronounced stable layer in the lower troposphere (p>359 mb) away from the surface were located. This was done by first examining T(ver) to get 192 values, one from the lower troposphere of each profile, of the quantity

$$\Delta^2 T_{ik} = \max\ (j=3,8)\ \text{of}\ (T_{ij-ik} - 2T_{ijk} + T_{ij+ik}).$$

The 6 examples (i values) with the most negative Δ^2T were then selected for each k. Table 6.4 tabulates the 12 values of Δ^2T (ver) and the errors in retrieval values of this quantity. The latter are opposite in sign and almost equal in magnitude to Δ^2T (ver). All systems fail this test miserably, with errors large enough to reduce the large negative values of Δ^2T to zero.

Table 6.4 Errors in sensing inversions in the lower troposphere.

		Error in Δ^2T			
Data Set	Δ^2T(ver)	HIRS STAT	HIRS PHYS	AMTS STAT	AMTS PHYS
Jan	-8.3°	7.1°	7.1°	7.0°	6.2°
Jan	-7.7	6.2	5.6	6.0	4.7
Jan	-6.8	6.8	5.6	6.3	5.6
Jan	-6.1	6.2	6.9	6.2	6.4
Jan	-5.6	5.9	5.4	5.5	5.3
Jan	-5.6	4.1	4.5	4.8	4.5
Jun	-7.2	7.1	6.5	6.9	6.7
Jun	-5.7	4.9	4.7	5.2	4.1
Jun	-5.6	5.4	4.8	4.7	4.8
Jun	-5.6	5.2	4.7	5.1	4.4
Jun	-5.1	4.7	4.1	4.4	3.7
Jun	-4.7	4.2	3.7	4.6	3.5
Avg	-5.7	5.6	5.3	5.6	5.0

As described earlier in Chapter 4, the radiances from the extratropical winter set were recomputed with added noise, as a test of the sensitivity to the original noise values. Table 6.5 summarizes the results. The results do not change the relative skill, although it is puzzling why added noise slightly improved the performance of the AMTS-STAT combination. (Perhaps because of sampling uncertainties due to the limited sample size.)

Table 6.5 Effect of added noise on the winter 30°N-60°N retrievals (rms values in deg and meters). "Diff" is computed as the square root of the differences in the squares.

		HIRS STAT	HIRS PHYS	AMTS STAT	AMTS PHYS
dT	Noisy	2.82	2.55	2.08	1.96
over 18 lyrs	Orig	2.64	2.48	2.10	1.72
(1000-100 mb)	Diff	0.99	0.59	----	0.94
dT	Noisy	3.09	3.42	2.13	2.14
over 4 lyrs	Orig	3.01	3.31	2.21	1.94
(100-16 mb)	Diff	0.70	0.86	----	0.90
	Noisy	15.9	9.4	12.9	8.2
dh (527 mb)	Orig	15.1	7.6	12.3	5.3
	Diff	5.0	5.5	3.9	6.3
	Noisy	35.0	38.0	30.0	35.8
dh (245 mb)	Orig	34.0	37.4	30.5	33.1
	Diff	8.3	6.7	----	13.6

7. CLOUDS (L. Crone)

Many of the radiance measurements made by an atmospheric sounder are contaminated to some degree by clouds. Therefore, a simulation study would be seriously deficient if it did not include situations involving clouds. Radiances over an extended region of the earth's surface must be simulated since a sounding cannot be determined from a single cloud contaminated field of view. The present test has the additional complication that the fields of view and scan patterns of the two instruments are different.

7.1 Cloud fields

The cloudy test consists of 40 sets of simulated radiances for each of the two instruments. Each set of radiances represents the measurements made over an area which is nominally 200km x 200km at nadir, but actually covers a larger region on the earth's surface because of geometric effects. The 40 test cases are centered at four different scan angles: 0° (nadir), 13.5°, 27°, and 40.5°, with 10, 12, 10, and 8 cases, respectively, occurring at each angle.

Cloud fields were generated using a program written by Dr. L. Crone of NESDIS. This program allows up to four layers of clouds to be constructed, each layer composed of a number of overlapping ellipsoids. For each layer, the fraction of the region to be covered by clouds must be prescribed, as must the dimensions and orientation of the ellipsoids, and the height of the center of the ellipsoids above the ground. In addition, the user can request that the ellipsoids should tend to cluster together. The program then determines the locations of the cloud centers using a random number generator. Since each cloud layer is composed of many overlapping ellipsoidal elements, the upper surface is not flat, but is more or less bumpy depending on the dimensions of the ellipsoids.

In order to minimize any edge effects, the cloud field is actually simulated over an extended region which is nominally 240km x 240km at nadir. The center of an ellipsoidal cloud element at nadir can therefore be as far as 20km outside the target region in any direction.

Full details of the parameters used to determine the 40 cloud fields used in the test will be not released. The cloud fields will be available for future testing of algorithms or proposed sounders. However, the following broad description will show what kinds of cloud fields were used without revealing enough details to compromise future use of the data base.

The 40 cases were divided into seven groups based on a target total cloud cover C, as shown in Table 7.1.1. The fractional cloud covers C_1, C_2 and C_3 for three layers was chosen for each case so that if there were no correlations between the clouds in different layers, the total cloud cover would be C. In particular the relation

$$1 - \overline{C} = (1-C_1)\ (1-C_2)\ (1-C_3)$$

was satisfied. As a result the actual total cloud cover was in some cases greater than $\overline{C}$ and in some cases less.

Table 7.1.1 Distribution of cases by target cloud cover.

$\overline{C}$	.625	.675	.725	.775	.825	.875	.925
No. of Cases	2	4	6	8	9	8	3

The remaining cloud characteristics were determined by assigning for each case values for each of the vectors R, N, H and D. Tables 7.1.2-7.1.5 list the values which were used. The vector R determines the eccentricity of the ellipsoids at each of three cloud layers. That is, r_i is the ratio of the semi-major axis to the semi-minor axis of a cloud in layer i. The vector N determines the size of the cloud elements. In layer i, N_i is the number of cloud ellipsoids required to give the prescribed cloud cover if no overlapping occurred. This gives the product of the semi-major axis a_i and the semi-minor axis b_i by the formula

$$a_i\, b_i = (\text{Region Area}) \times C_i \,/\, (\ N_i).$$

The vector H describes the height of the cloud base and the thickness of the cloud, both in km. The vector D describes the orientation of the major axis of the ellipsoidal elements in each layer with respect to the East-West direction.

Finally, in order to ensure that there be no totally clear fields of view and to include the effects of minor variations in the atmosphere, the participants in the test decided that a thin cloud layer with emissivity .08 would be included at about 300 mb. This layer would consist of relatively small, non-clustering cloud elements covering approximately 50 percent of the region.

Table 7.1.2 Eccentricity of ellipsoids by layer.

	r_1	r_2	r_3
R_1	1	1	2
R_2	1	2	3
R_3	1	3	3
R_4	1	4	4

Table 7.1.3 Size of ellipsoids by layer.

	n_1	n_2	n_3
N_1	500	20	20
N_2	500	10	10
N_3	500	10	20
N_4	500	20	10

Table 7.4 Height of cloud bases and thickness of clouds.

	Layer 1 Base/Thickness	Layer 2 Base/Thickness	Layer 3 Base/Thickness
H_1	2/2	4/1	9/1
H_2	1/3	5/2	10/2
H_3	1/4	5/5	10/1
H_4	2/1	3/9	9/1

Table 7.5 Orientation of ellipsoids.

	Layer 1	Layer 2	Layer 3
D_1	0°	-70°	-70°
D_2	0°	20°	20°
D_3	0°	65°	20°

7.2 Scan patterns

The fields of view of the HIRS are modeled as rectangles 20km long in the direction of orbital motion and 1.35 degrees wide in scan angle from left to right. The fields of view are considered to be contiguous in the left to right direction but there is a 20km gap at nadir in the direction of orbital motion. The fields of view spread out in the direction of orbital motion as the instrument scans to the side because of increasing distance of the earth's surface from the satellite. Each test case contains 50 HIRS fields of view.

The fields of view of the AMTS are modeled as rectangles 10km long in the direction of orbital motion and 0.675 degrees wide in scan angle from left to right direction and in the direction of orbital motion. The model does not include a spread in the direction of orbital motion since the instantaneous field of view is tilted as the scan mirror turns. There are 400 AMTS fields of view in each test case.

Figure 7.2.1 shows the models used for the scan patterns of both instruments.

7.3 Radiances

Meteorological conditions were associated with each of the 40 test cases by specifying the temperature and humidity soundings at 16 locations distributed in a 4 x 4 array for each case. For each sounding and for each channel on both instruments a set of 17 radiances was computed by Murcray: one assuming a clear atmosphere, and 16 assuming a black cloud at 16 standard pressure levels in the atmosphere.

Each HIRS field of view was broken up into a 12 x 12 array of 144 pixels, and, independently, each AMTS field of view was broken up into a 6 x 6 array of 36 pixels. This made the HIRS pixels approximately the same size as the AMTS pixels. The conditions at the center of a pixel were assumed to exist across the entire pixel. Radiances from a pixel were computed by interpolating horizontally between the 16 soundings and vertically

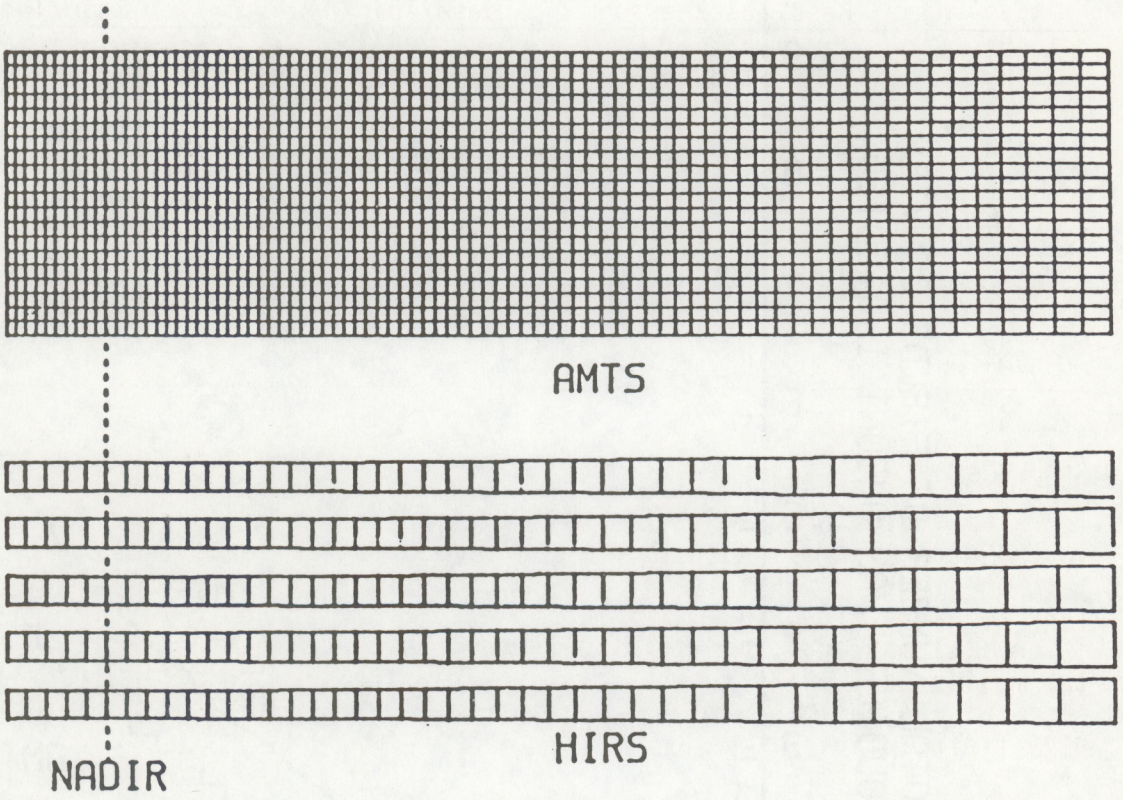

Figure 7.2.1 Modelled fields of view.

between the 16 standard pressure levels. Thus, simulated AMTS radiances are a sum of 36 pixel radiances, and simulated HIRS radiances are a sum of 144 pixel radiances.

Figure 7.3.1 shows the cumulative distribution of the cloudiness in each field of view for each instrument. There were 2,000 HIRS fields of view in the experiment (50 fields of view/case x 40 cases) and 16,000 AMTS fields of view (400 x 40). The ordinate in Figure 7.3.1 shows what fraction of the 2,000 HIRS or 16,000 AMTS fields of view had cloud cover less than or equal to the abscissa. For example, about 30 percent of the 16,000 AMTS fields of view had less than 70 percent cloud cover, but about 38 percent of the 2,000 HIRS cases were less than 70 percent cloudy. About 1 percent of the HIRS and 5 percent of the AMTS fields of view were clear, and 28 percent of the HIRS and 46 percent of the AMTS fields of view were totally cloudy. It should be noted that the statistics in Figure 7.3.1 do not include the thin cloud layer at 300mb. Also, these data are presented as a description of the simulated cloud cases used in the experiment. It is not clear whether real clouds would give smaller statistics.

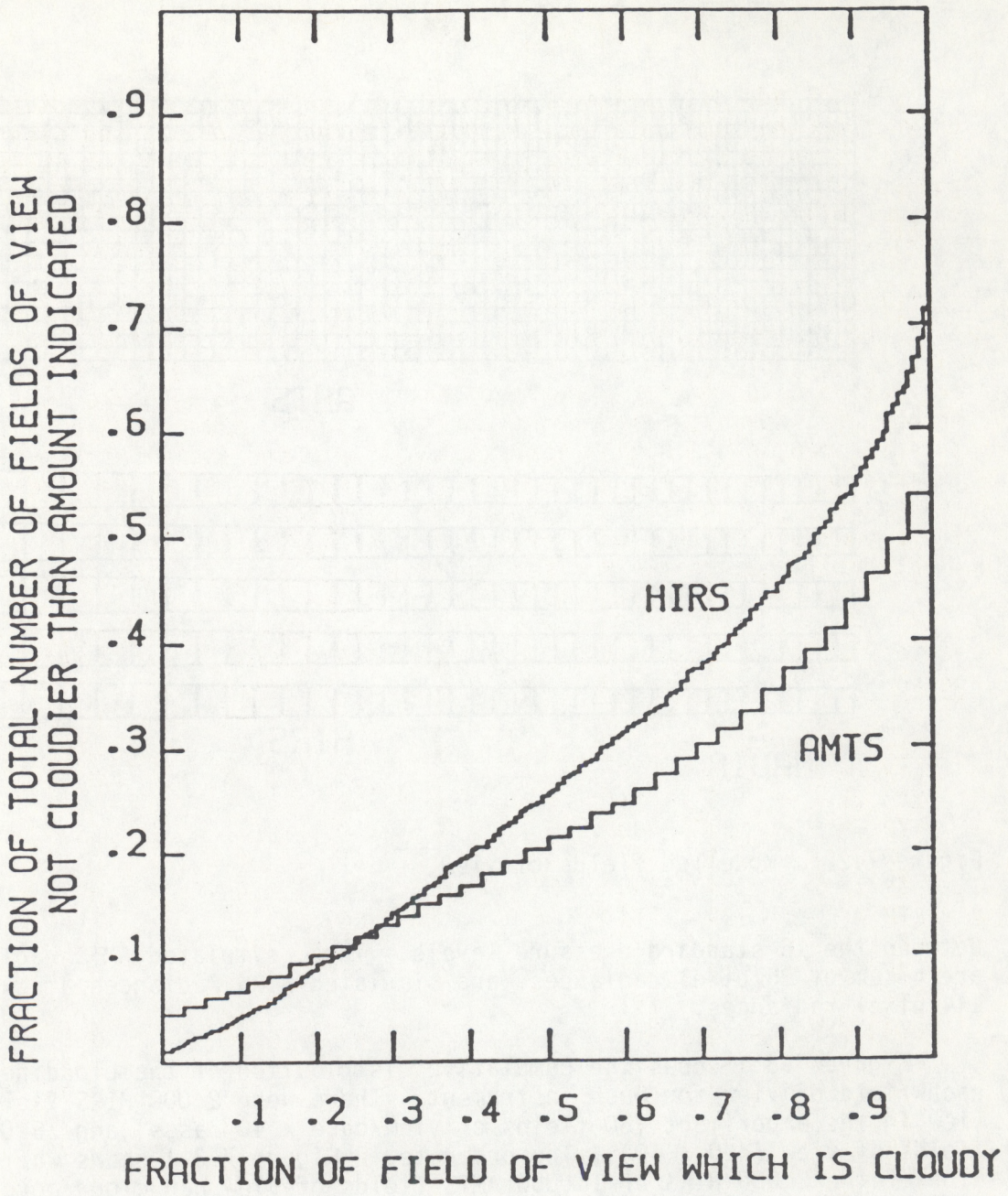

Figure 7.3.1. Cumulative distribution of 40 test cases.

8. Cloudy Results

The cloudy data set contained 40 test cases, based on radiosondes drawn from the same data base (January-February 1979) as the clear "winter" set. In the statistical retrieval method (NESDIS), 4 of the 40 cases were judged too difficult for a useful infrared retrieval. The emphasis in this chapter will therefore be on statistics of the 36 cases common to both retrieval methods.

Although drawn from the same data base, it turned out that the mean variance of temperature at fixed pressures in the troposphere was greater within the radiosondes of the clear winter sample than in the smaller collection selected for the cloudy set. It seems reasonable that retrieval errors are somewhat proportional to the 'signal' in a data set. If so, this accident of selection appears to explain the anomalous results (shown later) that the 36 cloudy retrievals were more accurate than the clear retrievals! Fortunately, there were 9 radiosondes that were used in both the cloudy and clear winter sets. This enabled a comparison to be made (Table 8.1) between the 9 clear and 9 cloudy cases for the physical

Table 8.1. Root-mean-square retrieval errors from physical retrieval method for 9 cases common to the cloudy and clear sets.

Layer	HIRS		AMTS	
	CLDY	CLR	CLDY	CLR
LYR 22 P = 25 - 16	2.42	3.02	2.02	2.50
LYR 21 P = 40 - 25	3.95	4.76	3.04	2.76
LYR 20 P = 63 - 40	2.96	3.01	1.70	1.79
LYR 19 P = 100 - 63	3.81	3.34	2.04	1.89
LYR 18 P = 114 - 100	3.86	3.50	2.75	2.35
LYR 17 P = 129 - 114	2.54	2.08	1.40	1.30
LYR 16 P = 147 - 129	2.29	1.94	1.50	1.67
LYR 15 P = 167 - 147	3.34	2.99	2.46	2.39
LYR 14 P = 190 - 167	4.44	3.91	2.85	2.53
LYR 13 P = 215 - 190	5.08	4.54	3.01	2.63
LYR 12 P = 245 - 215	4.25	3.85	2.19	1.97
LYR 11 P = 278 - 245	3.06	3.11	3.74	3.85
LYR 12 P = 245 - 215	4.25	3.85	2.19	1.97
LYR 11 P = 278 - 245	3.06	3.11	3.74	3.85
LYR 10 P = 316 - 278	2.72	2.51	2.93	3.10
LYR 9 P = 359 - 316	2.46	2.01	2.07	2.23
LYR 8 P = 408 - 359	2.19	1.75	1.67	1.79
LYR 7 P = 464 - 408	1.73	1.41	1.33	1.62
LYR 6 P = 527 - 464	1.34	1.22	1.23	1.55
LYR 5 P = 599 - 527	1.53	1.18	1.07	1.19
LYR 4 P = 681 - 599	1.22	0.77	0.96	0.79
LYR 3 P = 774 - 681	1.07	0.71	0.86	0.59
LYR 2 P = 880 - 774	1.77	1.38	1.03	1.34
LYR 1 P = 1000 - 880	2.20	0.64	1.71	0.87
TSKIN	0.85	0.27	0.81	0.12
LYRS 7-13	3.26	2.94	2.54	2.56
LYRS 1-6	1.57	1.02	1.18	1.11

retrieval method.[1] The table shows the clear retrievals to be slightly more accurate than the cloudy cases in the upper troposphere (layers 7-13), noticeably more accurate in the lower troposphere, and especially more accurate for the surface skin temperature (TSKIN). This agrees with intuition about the effect of clouds on retrievals. The smaller errors of the 36 (or 40) cloudy cases compared to the clear winter cases can therefore be ascribed confidently to an accident of the random selection process. In retrospect, cloudy tests should have been based on a larger sample and with additional attention to representativeness.

A. Amount of cloudiness
   1. Least clouds (12 cases) C = 61-74%
   2. Average clouds (14 cases) C = 75-84%
   3. Most clouds (10 cases) C = 85-91%

B. Elevation of verification layers
   1. High: 9 layers between 190-16 mb
   2. Middle: 7 layers between 464-190 mb
   3. Low: 6 layers between 1000-464 mb

The 464-mb pressure surface is near a height of 6 km. This was selected as a dividing level because the simulated cloud tops had one peak frequency of occurrence at about 4-5 km and another at about 10-12 km (close to the 190-mb level).

Physical reasoning would lead one to expect that retrieval errors in the high layers will be unaffected by clouds, and that in the middle and low layers, the retrieval errors will increase with increasing cloudiness. Table 8.2 summarizes the results. They show the expected dependence on cloudiness only in the 1000-464 mb layers. Of the 8 cloudiness changes in the middle layer, 6 show error decreasing with cloudiness, and 7 of the 8 cloudiness changes in the upper layer also show decreasing error with increasing cloudiness. Evidently the temperature structures were intrinsically more difficult to retrieve in the 12 least cloudy cases than in the 10 most cloudy cases.

The major conclusion that can be drawn from Table 8.2, however, is that the presence of clouds has not changed the relative ranking of instruments and of retrieval processes; AMTS outperforms HIRS, and the physical retrieval process used by GLAS outperforms the statistical regression process used by NESDIS.

Information on the degradation of retrieval accuracy by clouds is restricted to the physical retrieval process only, and only from the 9 cases reported in Table 8.1 that were common to both cloudy and clear cases. The smallness of the sample size is indicated by the anomalous showing that in these 9 cases, the clear HIRS results are slightly better than the clear AMTS results in the bottom 6 layers. This is completely contrary to the

[1]Unfortunately, the statistical retrieval tapes were destroyed before it was recognized that this comparison was desirable.

full clear sample of 96 cases. Apart from this caveat, Table 8.1 suggests that the simulated clouds generally produced only a small deterioration in retrieval accuracy.

Table 8.2 RMS temperature errors in cloudy cases averaged over each of three deep layers.

System	Lst Clds (12)	Avg Clds (14)	Most Clds (10)	All (36)
		LAYERS 14-22 (190-16 mb)		
HIRS + STAT	3.43	3.26	3.00	3.25
HIRS + PHYS	3.03	2.92	2.28	2.76
AMTS + STAT	2.25	2.04	1.90	2.08
AMTS + PHYS	1.89	1.94	1.61	1.82
All 4	2.72	2.50	2.26	2.54
		LAYERS 7-13 (464-190 mb)		
HIRS + STAT	3.11	3.53	2.79	3.20
HIRS + PHYS	3.02	3.04	1.85	2.69
AMTS + STAT	2.66	2.28	1.76	2.29
AMTS + PHYS	2.47	1.94	1.60	2.04
All 4	2.83	2.77	2.05	2.59
		LAYERS 1-6 (1000-464 mb)		
HIRS + STAT	1.71	1.46	1.82	1.65
HIRS + PHYS	1.27	1.47	1.69	1.49
AMTS + STAT	1.17	1.32	1.40	1.29
AMTS + PHYS	0.95	1.01	1.12	1.15
All 4	1.30	1.33	1.53	1.41

One minor point of interest in Table 8.2 is the benefit given HIRS by the physical rather than statistical retrieval method in the layer 190-16 mb. In the clear case this was the one region where the physical method failed to improve upon the statistical method (See Figure 6.1). This might reflect an ability of the physical method for stratospheric retrievals to be "distracted" less by tropospheric clouds than is the statistical retrieval method. (Because of meteorological correlations, clear radiances from tropospheric channels may be accepted as important statistical predictors of stratospheric temperatures, but lead to poor stratospheric results when tropospheric clouds are present to corrupt the tropospheric radiances.)

9. CONCLUSION (D. Wark)

The purpose of this study was to be a controlled simulation of comparative performance by an infrared satellite-based sounder having high spectral resolution and one having medium spectral resolution. The instruments were the proposed AMTS and the currently-operational HIRS-2, respectively. As the study progressed, design changes in the AMTS introduced other factors, including an increase in the number of spectral intervals and in the spatial resolution. Thus the experiment became a comparison of two instruments having several differences, and no attempt has been made to isolate the effects of the various factors. Nor was the experiment designed to evaluate the optimal spectral characteristics and spatial resolution of an infrared sounder.

An added aspect of the study was the use of different retrieval schemes by the participants. However, there was concern that the relative performances by the two instruments would be algorithm-dependent. To meet this problem, each was to be subjected to both retrieval schemes. In examining results, one must examine not only instruments but also retrieval techniques.

Before assessing the results form the study, a brief review is given of the factors which distinguish the two instruments and which contribute to the comparisons.

9.1. Instrumental differences

9.1.1 Spectral resolution

For a single frequency, the transmittance of the atmosphere is the exponential of the negative optical path, which is the product of an absorption coefficient and the mass of absorbing gas: $t=\exp(-c(m)m)$, where the product is understood to be the integrated quantity from the top of the atmosphere to the level at which the mass is m. For a uniformly mixed gas, m is proportional to atmospheric pressure, so transmittance takes the form $t=\exp(-a(p)p)$.

If the spectral interval of the observation is confined to a region between spectral lines in which c or a varies little with wavelength, the transmittance will closely resemble the monochromatic case and will be of the form $t=\exp(-a'p^2)$. If, on the other hand, the spectral interval is so broad as to encompass the entire region between spectral lines, the coefficient c or a can vary by orders of magnitude within the spectral interval and the mean transmittance within that spectral interval will be a more slowly changing function of altitude. These two cases represent the essential difference in the design of the AMTS and the HIRS-2.

Figure 9.1.1 shows on the left two curves representing the derivative of transmittance with respect to the logarithm of pressure for the two cases described above. The flatter curve is for equally spaced spectral lines characteristic of the absorption bands of carbon dioxide and is aver-

aged over the interval of the line spacing; the sharper curve is for the same transmittance pattern, but averaged over an interval between the lines with a triangular weight whose total width is one-fourth the line spacing. The widths at half-maximum of these two curves are 7.8 and 11.7 km in a Standard Atmosphere, with about 69 percent of each curve between those limits. The difference between these two curves is mainly in the depletion of the peak and the enhancement of the upper portion of the flatter curve, indicating that less of the radiance measured by the satellite comes from the vicinity of the maximum and more from the higher atmosphere and is therefore less representative of the temperature at a particular level.

The effect of the sharper weighting function is illustrated on the right in Fig. 9.1.1. Radiances were computed from the tropical profile shown as the dotted line and the weights on the left were shifted up or down in increments of 1/4 of a decade in pressure; these were then converted to radiance temperatures and plotted at the mean levels of origin, shown as the dashed and solid lines connecting the large dots. Radiance

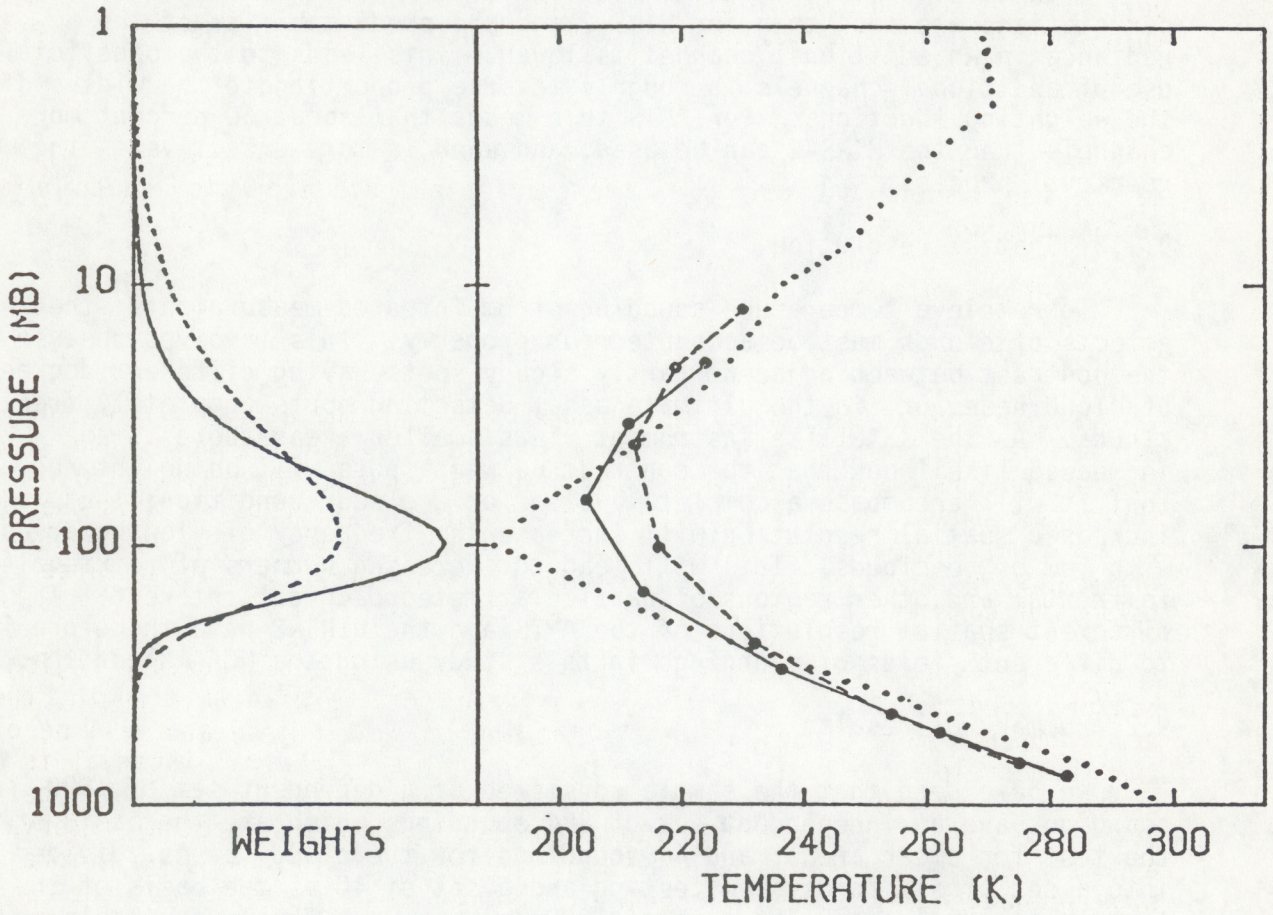

Fig. 9.1.1. Left: weighting functions typical of HIRS-2 (dashed line) and AMTS (solid line). Right: a tropical sounding (dotted line); and radiance temperatures for corresponding weighting functions (dashed and solid lines, resp.) shifted upward or downward in 1/4 decade increments.

temperatures given by the solid line, which represents the sharper weighting functions, more nearly approximate the shape and the temperatures of the profile, and in any retrieval scheme this is a benefit.

9.1.2 Number of spectral intervals

As the number of spectral intervals is increased, vertically adjacent weighting functions become more nearly the same. That is, they become more highly correlated. At the extreme, radiances in adjacent intervals differ by less than the noise of measurement and only the statistical advantage of numbers of intervals is achieved. But the number is really limited by the degree to which radiances in additional intervals can be predicted from a combination of the radiances in the other intervals. This, too, is limited by the noise of measurement. Weinreb and Crosby [8] have shown that for the HIRS-2 instrument the number of spectral intervals is optimum and could not profitably be increased.

With the sharper weighting functions of the AMTS the inter-channel correlations are less than for HIRS-2 and the predictability of the radiance in an additional channel is lower. This leads to the beneficial use of additional channels in roughly inverse proportion to the widths of the weighting functions. For AMTS this means that about 50 percent more channels than the HIRS-2 can be used, and each is more effective in the retrieval process.

9.1.3 Spatial resolution

To retrieve temperature soundings from infrared measurements, the effects of clouds must be accounted for properly. This involves the use of the contrast between adjacent partly cloudy spots having different degrees of cloudiness, or, in the ultimate case, detecting spots completely free of clouds. As the satellite instrument views smaller areas there is an increased likelihood that the contrast between spots will be heightened, or that it will encompass a completely clear or a cloudy condition; that is, increased spatial resolution will increase the frequency of viewing areas with few or no clouds. This will lead to increased numbers of retrievals in frontal and other regions of particular meteorological interest. The different spatial resolutions of the AMTS and the HIRS-2 have therefore led to different yields of soundings in this study using the NOAA algorithm.

9.2 Summary of results

We have seen that the sample consisted of a dependent set of 1600 soundings and an independent set of 384 soundings which are the basis of the test for clear areas; and 46 soundings for the cloudy cases, divided into a set of six for system testing and a set of 40 as the basis of the test in cloudy areas. The sets of 1600 and six were freely available to the participants, whereas the sets of 384 and 40 soundings were withheld. Only the statistics on the behavior of retrievals relative to the original profiles were revealed (chapters 6 and 8).

For the cloudy portion of the test, the scenes which were considered

to be too cloudy for producing effective retrievals could be bypassed, as is done in the normal operation for the HIRS-2. During the final computational phase of the test, four cloudy cases failed the HIRS-2 tests for clear radiances and were rejected. To give the results more meaning, those four soundings were also omitted from the AMTS statistics. In one other case the analysis of AMTS data exposed a clear spot in the cloudy test, so the process of "de-clouding" was bypassed. These five cases reveal the influence of spatial resolution in the instruments and emphasize its importance. The NASA chose to process clouds for all 40 cases for both instruments.

Before assessing the final results, one other factor must be considered. The TOVS system on the NOAA satellites includes two other instruments, the MSU and the SSU, which provide measurements to aid in the "de-clouding" process and to improve the retrievals near the tropopause and in the stratosphere. Therefore, the results of this study do not necessarily represent the capabilities of the HIRS-2 when used in combination with the other two instruments. In the stratosphere, particularly, the advantage of the more numerous AMTS channels is clear. A proper assessment of the stratospheric accuracy would have resulted from the incorporation of the three SSU channels encompassing the region of 2-30 mb.

The tropospheric results more closely reflect the operational performance of the HIRS-2. As suggested earlier, the sharper weighting functions of the AMTS and the effectiveness of more channels in the retrieval process lead to substantially better results in this portion of the atmosphere. A question that remains is the degree to which each of these factors contributes to these results. Unfortunately, the study of Weinreb and Crosby did not include weighting functions similar to those for the AMTS, so it is difficult to gauge the relative influences of the two factors. Certainly the present study did little to shed light on this question because the number of channels was not varied. So we may say only that the combination of sharper weighting functions and more channels provides a more effective design criterion, and more channels with narrower weighting functions must lead to better overall soundings. This is what the results of the study show.

The reader who wishes only to see the final results of this study should examine Table 6.1, which is shown pictorially in Figure 6.1, for the clear cases, and Table 8.2 for the cloudy cases. Figure 9.2 summarizes the results of the cloudy cases based on Appendix C. Table 8.1 is an important adjunct to Table 8.2 for reasons cited by the author of Chapter 8.

If we confine the region of interest to the troposphere (100-1000 mb) we see that for clear cases the AMTS has a slightly lower bias (0.23 versus 0.46 C), and a significantly better RMS difference (1.51 versus 2.07 C). However, this is tempered by the closer agreement in the range 400-800 mb, and much of the HIRS-2 result comes from the absence of the supportive microwave measurements normally employed in the operational retrievals; this effect is felt not only at 100 mb, where the microwave data are particularly useful, but also near 200 mb where the HIRS-2 has no channel

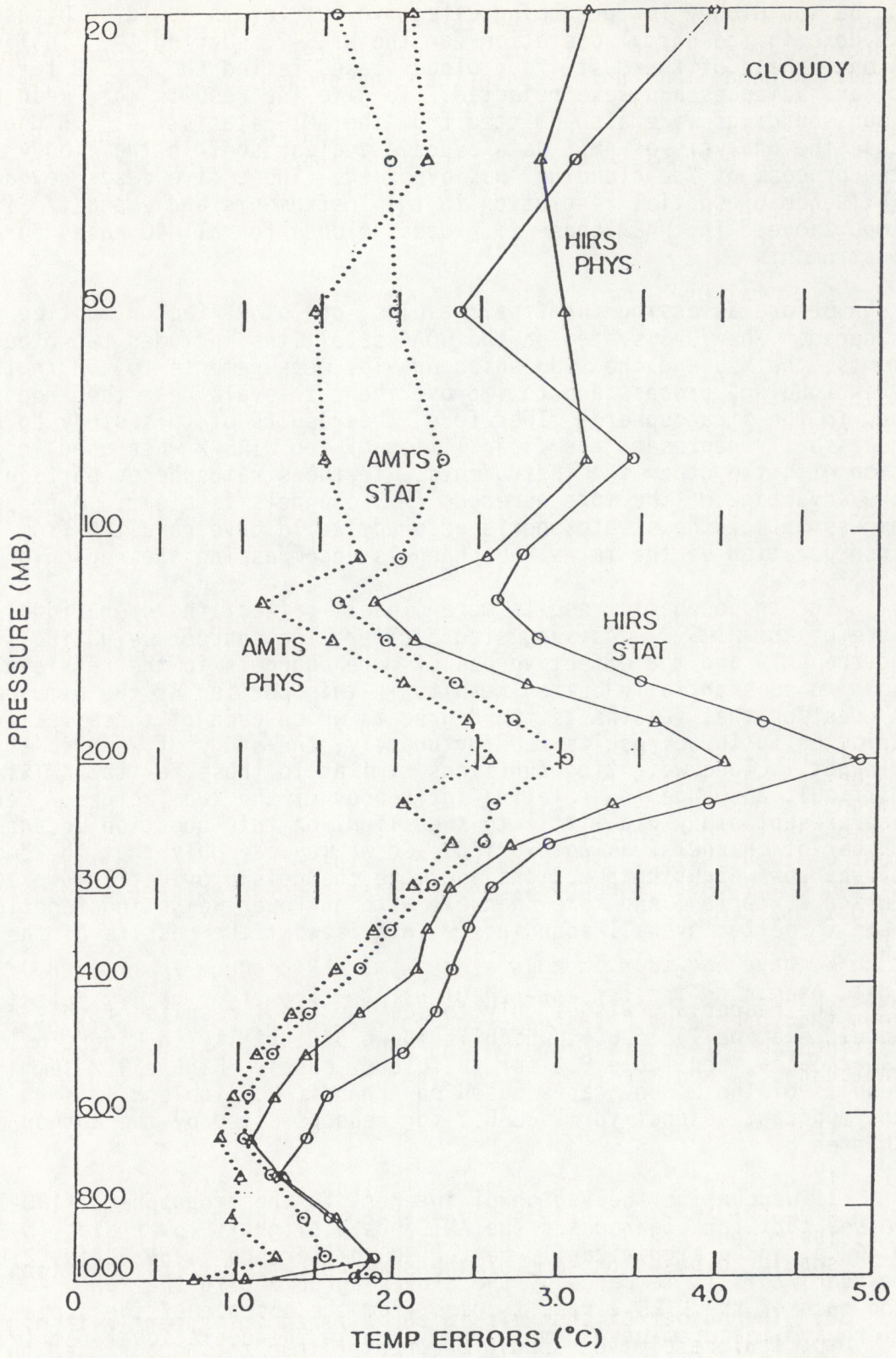

Figure 9.2 Vertical distribution of rms retrieval error for the cloudy cases. Values are plotted at the mean log (p) for each layer.

equivalent to the microwave or the AMTS. Nevertheless, part of the AMTS superiority at those levels may be attributed to the sharper weighting functions and it is unfortunate that the present test cannot give a good quantitative estimate to that influence. In the middle troposphere, where the lapse rates tend to be more constant than elsewhere, the HIRS-2 approaches in quality the AMTS because sharpness of weighting functions bears less relation to a retrieval's quality under those conditions. A slight increase in the AMTS advantage is seen near the surface, where lapse rates again become more diverse.

The test provided statistics for retrieved surface skin temperature as well. This is not a NOAA operational product from the HIRS-2, but it is produced by the NASA. Appendix A of Chapter 6 indicates that the AMTS physical retrievals gave this temperature with an accuracy of 0.28 C, compared with 0.78 C for the HIRS-2. This is the result of the cleaner windows and the added lower-troposphere channels of the AMTS.

The cloudy results should be seen not only as a test of weighting functions, but also of spatial resolution. Only differences between the two instruments should be considered for reasons cited in Chapter 8. In the layer 464-190 mb the AMTS shows an overall superiority of 0.62 C (2.32 versus 2.94 C), but in the layer 1000-464 mb this is reduced to 0.35 C (1.22 versus 1.57 C). Similar results are found in the nine special cases of Table 8.1, where the degradation introduced by clouds is less for the AMTS.

Overall, the AMTS suffers less than the HIRS-2 from the introduction of clouds by about 0.3 C, as shown in Table 8.1. From Figure 6.1 the AMTS is better by about 0.24 C in the layer 1000-464 mb, while in Table 8.2 the amount is 0.35 C. Similarly, in the 464-190 mb layer the comparable quantities are 0.48 C and 0.62 C, respectively, leading to an implied improvement of about 0.1 C. The conclusion is that the better spatial resolution of the AMTS, under the conditions of this study, improved cloudy retrievals by 0.1-0.3 C.

We have not seen in this study what would occur if only the first goal, examining the consequence of using narrower weighting functions, had been the sole focus. Instead, one must read the results with great care to distinguish influences of weighting functions, number and pressure range of the channels, and the spatial resolution.

Therefore, what are the lessons we have learned?

1. A future infrared sounding instrument should employ greater spectral resolution to achieve sharper weighting functions. That instrument need not be identical with the currently-designed AMTS, but should be based on some of the same conceptual considerations.

2. The number of channels in an infrared instrument with high spectral resolution should be greater than the number used in an instrument of medium spectral resolution. The optimum number of channels at either resolution has not been established by this study.

3. Meteorological requirements for accuracies of one degree Celsius have been approached but not met by the increase of spectral resolution and the number of channels. This suggests that an infrared sounding instrument having more channels than the AMTS may be required.

4. Spatial resolution is an important factor in the design of an infrared instrument. Every effort should be made to maximize it.

5. Although microwave instruments were not considered in this study, past experience and practice have shown that a combination of infrared and microwave measurements is vital to a sounding system, with the infrared contributing most effectively in the troposphere.

As we enter the planning stage for a successor to the HIRS-2, these guidelines should be factors in its design, and the benefit of this study with all its flaws, will be felt. Even though this study had the limited objective of comparing the performance of two sets of instrumental specifications rather than attempting to define an optimum set of specifications, it produced very revealing results in showing the combined benefits of increased spectral and spatial resolutions. Further studies will be needed to set the specifications for future operational flight programs.

Acknowledgement

The authors are indebted to K. LeFevre, who re-typed the manuscript and assisted in the final preparation for publication.

REFERENCES

1. L. D. Kaplan, "Inference of Atmospheric Structure from Remote Radiation Measurements," Journal of the Optical Society of America, vol. 49, 1959, pp. 1004-1007.

2. "The Nimbus III User's Guide," R. R. Sabatini, ed., National Aeronautics and Space Administration, Goddard Space Flight Center, Greenbelt, MD, 1969, 238 pp.

3. "The Nimbus IV User's Guide," R. R. Sabatini, ed., National Aeronautics and Space Administration, Goddard Space Flight Center, Greenbelt, MD, 1970, 214 pp.

4. The Nimbus 5 User's Guide," R. R. Sabatini, ed., National Aeronautics and Space Administration, Goddard Space Flight Center, Greenbelt, MD, 1972, 163 pp.

5. "The Nimbus 6 User's Guide," J. E. Sissala, ed., National Aeronautics and Space Administration, Goddard Space Flight Center, Greenbelt, MD, 1975, 227 pp.

6. L. M. McMillin, D. Q. Wark, J. M. Siomkajlo, P. G. Abel, A. Werbowetzki, L. A. Lauritson, J. Pritchard, D. S. Crosby, H. M. Woolf, R. C. Luebbe, M. P. Weinreb, H. E. Fleming, F. E. Bittner, and C. M. Hayden, "Satellite Infrared Soundings from NOAA Spacecraft," NOAA Technical Report NESS 65, U.S. Department of Commerce, National Oceanic and Atmospheric Administration, National Environmental Satellite Service, Washington, DC, September 1973, 112 pp.

7. W. L. Smith, "An Improved Method for Calculating Tropospheric Temperature and Moisture from Satellite Radiometer Measurements," Monthly Weather Review, vol. 96, 1968, pp. 387-396.

8. M. P. Weinreb and D. S. Crosby, "Optimization of Spectral Intervals for Remote Sensing of Atmospheric Temperature Profiles," Remote Sensing of Environment, vol. 2, 1972, pp. 193-201.

9. L. D. Kaplan, M. T. Chahine, J. Susskind, and J. E. Searl, "Spectral Band Passes for a High Precision Satellite Sounder," Applied Optics, vol. 16, 1977, p. 322.

10. M. T. Chahine, "Remote Sensing of Cloudy Atmospheres I. The Single Layer Cloud," Journal of the Atmospheric Sciences, vol. 31, 1974, pp. 233-243.

11. M. T. Chahine, "Remote Sensing of Cloudy Atmospheres II. Multiple Cloud Formation," Journal of the Atmospheric Sciences, vol. 34, 1977, pp. 744-757.

12. J. Susskind, J. Rosenfield, and D. Reuter, "An accurate radiative

transfer model for use in the direct physical inversion of HIRS2 and MSU temperature sounding data," Journal of Geophysical Research, vol. 88C, 1983, pp. 8550-8568.

13. M. P. Weinreb, H. E. Fleming, L. M. McMillin, and A. C. Neuendorffer, "Transmittances for the TIROS Operational Vertical Sounder," NOAA Technical Report NESS 85, U.S. Department of Commerce, National Oceanic and Atmospheric Administration, National Environmental Satellite Service, Washington, DC, September 1981, 60 pp.

14. R. McClatchey, W. S. Benedict, S. A. Clough, P. E. Burch, R. F. Calfee, K. Fox, L. S. Rothman and J. S. Garing, "AFCRL Atmospheric Absorption Line Parameter Compilation," AFCRL-TR-73-0096, Environmental Research Paper No. 434, Air Force Cambridge Research Laboratories, L. G. Hanscom Field, Bedford, MA, January 1973, 78 pp.

15. J. Susskind and J. E. Searl, "Synthetic Atmospheric Transmittance Spectra Near 15 and 4.3 ," Journal of Quantitative Spectroscopy and Radiative Transfer, vol. 19, 1978, pp. 195-215.

16. L. S. Rothman, "Update of the AFGL Atmospheric Absorption Line Parameters Compilation," Applied Optics, vol. 17, 1978, pp. 3517-3518.

17. P. W. Rosenkranz, "Shape of the 5 mm Oxygen Band in the Atmosphere," IEEE Transactions on Antennas and Propagation, vol. 23, 1975, pp. 498-506.

18. J. Susskind and T. Mo, "Atmospheric Absorption Spectral Near 2200 cm^{-1} and 2400 cm^{-1}," AMS Third Conference on Atmospheric Radiation, Davis, CA, June 28-30, 1978, American Meteorological Society, Boston, MA, June 1978, 387 pp.

19. M. Halem and J. Susskind, "The GISS VTPR Processing Manual," NASA Report X-130-77-53, National Aeronautics and Space Administration, Goddard Space Flight Center, Greenbelt, MD, March 1977, 165 pp.

20. J. Susskind, "Effective H_2O Transmittance in the 15 m Region," Remote Sensing of the Atmosphere Technical Digest, Anaheim, CA, March 19-21, 1975, Optical Society of America, Washington, DC, March 1975, 102 pp.

21. L. M. McMillin and H. E. Fleming, "Atmospheric Transmittance Model of an Absorbing Gas: A Computationally Fast and Accurate Transmittance Model for Absorbing Gases with Constant Mixing Ratios in Inhomogeneous Atmospheres," Applied Optics, vol. 15, 1976, pp. 358-363.

22. J. Susskind, J. Rosenfield, D. Reuter and M. T. Chahine, "Remote sensing of weather and climate parameters from HIRS2/MSU on TIROS-N," Journal of Geophysical Research, vol. 890, 1984, pp. 4677-4697.

23. N. Phillips, L. McMillin, A. Gruber and D. Wark, "An Evaluation of Early Operational Temperature Soundings from TIROS-N," Bulletin of the American Meteorological Society, vol. 60, 1979, pp. 1188-1197.

24. T. Schlatter, "An Assessment of Operational TIROS-N Temperature Retrievals Over the United States," Monthly Weather Review, vol. 109, 1981, pp. 110-119.

25. B. J. Conrath, "Vertical Resolution of Temperature Profiles Obtained from Remote Radiation Measurements," Journal of the Atmospheric Sciences, 29, pp. 1262-1271.

26. Susskind, J., J. Rosenfield, D. Reuter, and M. T. Chahine, 1983: The GLAS Physical Inversion Method for Analysis of HIRS2/MSU Sounding Data. NASA Technical Memorandum 84936. Goddard Space Flight Center, Greenbelt, MD 20771.

27. Smith, W. L. and H. M. Woolf, "The Use of Eigenvectors of Statistical Covariance Matrices for Interpreting Satellite Sounding Radiometer Measurements," Journal of the Atmospheric Sciences, vol. 33, 1976, pp. 1127-1140.

28. A. Goldman and R. S. Saunders, "Analysis of Atmospheric Infrared Spectra for Altitude Distribution of Atmospheric Trace Constituents - I. Method of Analysis," Journal of Quantitative Spectroscopy and Radiative Transfer, vol. 21, 1979, pp. 155-161.

Appendix A. Tape protocol and format for the AMTS/HIRS test.

Seven types of tapes were involved in the test. However, the reader of this document will have no application for most of these, as they are in many ways unique to the particular test described here. The tapes which are generally thought to be of interest are contained in those portions of types 1 and 4 which have been made known to all participants of the test. For other tapes, inquiries should be made through the originators of the tapes, as revealed in this appendix.

The types of tapes generated during the test are:

1. Original temperatures, moisture, and ozone profiles prepared by Phillips. Two "colocation" sets (winter and summer) were provided to all participants in the test. Two "test" sets, taken from radiosondes 1-2 weeks later than the colocation sets were provided to Goldman and were withheld from other participants (8 tapes plus 4 kept by Phillips).

2. Clear radiances for each instrument were prepared by Goldman from the colocation and test data sets and were provided to Susskind and McMillin (4 x 2 x 2 = 16 tapes).

3. Retrieved temperatures from the test sets were sent by Susskind (2 x 2) and McMillin (2 x 2) to Phillips (via A. Desmarais at NMC so that Phillips' evaluation could be unbiased) (8 tapes).

For cloudy tests:

4. Original temperature, moisture, and ozone for 16 columns in each of 46 scan arrays prepared by Phillips and sent to Goldman. These were constructed from the winter 30N-60N portion of the radiosonde base of 1-2 weeks that was used in the winter clear column test set. Abbreviated tapes containing the original profiles from the first six arrays were sent to Susskind and McMillin; the last 40 arrays were not sent to them (3 tapes).

5. Radiances for each instrument and with black-body clouds at a sequence of levels was sent to Crone by Goldman (2 tapes, one for each instrument).

6. Crone combined the data from the type 5 tapes for each array selectively according to his cloud models, giving 46 arrays of cloudy spot radiances. These were sent to Susskind and McMillin (2 apiece).

7. Retrieved temperatures at one location in each array were sent to Phillips (via Desmarais) by Susskind and McMillin (4 tapes altogether).

1. General tape structure

Although a variety of computers were involved, the following basic

tape conventions were followed:

a. All tapes are 9 track, 1600 bpi, odd parity, and EBCDIC.

b. There are no system generated tape labels.

c. All records on a tape are of the same length, although the record length will change from one tape type to another.

d. BLOCK SIZE is always the same as the record length.

e. The first record is always an identification record for that tape as a whole.

f. All data (including code integers in the identification record) are signed integers that are less than 32767 ($=2^{15}-1$) in magnitude. They are written and read under format control "I6" for each word.

g. Codes for data records (and thereby the uniform record length for the tape type) are defined by the originators identified in the next section.

h. Missing data (e.g., in an identification of data record) is written as the negative integer -32767.

2. Identification record (general) for each tape

The number of meaningful coded information integers in this record is invariably less than that of a data record on that tape. Therefore the last group of integers in this record will each be -32767 (i.e., coded as missing) in order that this record be the same length as the following data records.

The first words in a tape identification record are:

Word 1 Originator Code
1 - Phillips (tape types 1 and 4)
2 = Goldman (tape types 2 and 5)
3 = Crone (tape type 6)
4 and 5 = Susskind and McMillin, numbers assigned by A. Desmarais and not told to Phillips.

Word 2 Instrument Type
Tape types 1 and 4. Irrelevant, therefore -32767.
Tape types 2,3,5,6,7. The integers 1 and 2 denote each of the two instruments. The assignments were made by agreement between McMillin and Susskind and were communicated only to Goldman and Crone; Phillips and Desmarais did not know these assignments.

Note that between them, words 1 and 2, when carried through to the retrieved temperature tapes (types 3 and 7),

distinguish between retrieval methods (the statistical retrieval being done by McMillin and the physical inversion by Susskind) represented in word 1 and the instrument type recorded in word 2. Phillips was able to organize his evaluation of retrieval accuracy by the four pairs of coded integers (4,1), (4,2), (5,1), and (5,2) without knowing the meaning of these couplets. Their interpretation became common knowledge only after Phillips had written his final evaluation of the type 7 tapes.

Word 3 Data Period and Class Indicator
For tape types 1-3 (clear column):
1 = Winter colocation set
2 = Summer colocation set
3 = Winter test set
4 = Summer test set
For tape types 4-7 (cloudy):
5 = Cloudy test set (winter only 30N-58N)

Word 4 Number of data records that follow the identification record on tape

Word 5 N = Number of words in each record on tape

Words 6-10 Tape originators private code or -32767

Words 11-N Missing (-32767) or as defined by the originator for the next user of the tape.

3. Format and code for tape types 1 and 4. These are the "input" tapes of temperature, moisture, and ozone profiles. The record length is 220 words. The tape identification record is as follows:

	Meaning	Tape Type 1	Tape Type 4
Word 1	Originator	1	1
Word 2	Instrument type	-32767	-32767
Word 3	Data period	1,2,3, or 4	5
Word 4	Number of data records	(800 colocation sets) 192 (test sets)	736 Goldman 96 (NASA & NESDIS)
Word 5	Length of record (words)	220	220

In the clear column tapes 91) the first 400 data records of the colocation set is for latitude belt 30S-30N, and the last 400 are for latitude belt 30N-58N. In the clear column test sets, the first 96 records are for 30S-30N, and the last 96 are for 30N-58N. In the cloudy case there is only one tape, with 736 (or 96) data records.

Each data record contains information about one column (or profile). The first 20 words of each 220-word data record contains identifying information for that column (these 20 words are copied in each corresponding data

record on successive types of tapes generated by Goldman, Crone, McMillin, and Susskind, with the exception of Crone, who was permitted to alter words 2, 7, and 8). The first 20 words of each data record are as follows:

Word 1 Profile identification number one. In the clear column test this number is the integer 1000 x Data Period + n (n=1,..., 800 or 192). In the cloudy case this number defines the array n=1,...,46.

Word 2 Profile identification number two. In the clear column test this is irrelevant (-32767). In the cloudy case it is successively 1,...,16, denoting the 16 columns of temperature, moisture, and ozone necessary to define the "clear conditions" over one test array.

Word 3 0 for oceanic; 1 for continental

Word 4 Latitude rounded to nearest even number of degrees (-30 to 58).

Word 5 Local time in hours (0 through 23). In the cloudy case this is artificially set to 0.

Word 6 10^4 time the sine of the solar elevation angle. In the cloudy case this is artificially set to -10000 (night) for all profiles.

Word 7 Local zenith angle in 0.1 degrees (0 = vertical).

Word 8 Ground temperature in units of 0.1 K.

Word 9 N = number of pressure levels at which data are reported.

Words 10-20 Private code for Phillips.

The structure of words 21-220 is as follows:

Word 21 P (=10000) = first pressure level in 0.1 millibars

Word 22 T = temperature in 0.1 K at this level

Word 23 q = specific humidity at this level in units of grams of water vapor per 10^6 grams of moist air.

Word 24 O_3 = ozone at this level in units of molecules per cubic centimeter, multiplied by 10^{-9}

Words 25 to 28 Same information for the second data level.

Words 17+4n to 20+4n Same information for level n.

Words 17+4N to 20+4N Same information for the last level, N.

Words 21+4N to 220 Missing (-32767)

The last level is at 0.1 millibar. Specific humidity is reported as missing (-32767) if p is less than 200 mb. Ozone is reported at all levels. There is a maximum of 50 data levels for each column.

Appendix B - Detailed comparisons with "Correct" temperatures.

Numbers in parentheses identify instruments, retrieval processes and data sets.

Clear cases

Cloudy cases

INSTMNT 1 PROCESS 4 DATA SET 3
LAT BELT -30- 28 OCEANS ONLY
48 RETRIEVED SNDGS ARE INCLUDED IN THIS TABLE

LAYER	MN ERROR	RMS	TRU VAR	RET VAR	RATIO	RMS HT ERROR (METERS)
LYR 22 P= 25- 16	-0.82	3.61	187.08	185.77	1.00	64.86
LYR 21 P= 40- 25	0.00	2.67	136.50	143.77	1.06	68.65
LYR 20 P= 63- 40	0.41	1.89	63.87	68.98	1.08	75.69
LYR 19 P= 100- 63	0.07	3.82	38.63	19.23	0.50	69.44
LYR 18 P= 114-100	-0.25	3.22	30.88	14.37	0.47	37.61
LYR 17 P= 129-114	-0.14	2.42	22.58	14.05	0.63	34.13
LYR 16 P= 147-129	-0.24	2.36	16.26	9.71	0.60	30.84
LYR 15 P= 167-147	-0.32	2.13	10.11	6.36	0.63	28.22
LYR 14 P= 190-167	-0.28	1.82	5.84	4.28	0.74	26.37
LYR 13 P= 215-190	-0.41	1.87	5.93	3.93	0.67	22.84
LYR 12 P= 245-215	-0.13	1.83	8.56	4.10	0.48	19.04
LYR 11 P= 278-245	0.15	1.55	9.39	5.20	0.56	13.88
LYR 10 P= 316-278	0.43	1.29	10.25	6.66	0.65	10.05
LYR 9 P= 359-316	0.34	1.04	10.26	7.80	0.77	7.64
LYR 8 P= 408-359	0.24	0.98	10.43	8.78	0.85	7.35
LYR 7 P= 464-408	0.25	0.76	10.23	9.19	0.90	7.99
LYR 6 P= 527-464	0.15	0.83	9.69	9.35	0.97	8.84
LYR 5 P= 599-527	0.00	0.93	8.82	8.68	0.99	8.68
LYR 4 P= 681-599	0.03	0.73	8.42	8.43	1.01	9.25
LYR 3 P= 774-681	-0.32	0.98	11.21	9.13	0.82	9.83
LYR 2 P= 880-774	-0.05	1.52	14.22	12.21	0.86	9.24
LYR 1 P=1000-880	-0.08	1.43	14.08	12.62	0.90	5.34
TSKIN	-0.00	0.78	16.37	15.73	0.97	
STRATOSPHERIC RMS=	3.09 WITH AVG VAR RATIO=				0.92	
TROPOSPHERIC RMS=	1.67 WITH AVG VAR RATIO=				0.76	

INSTMNT 1 PROCESS 4 DATA SET 3
LAT BELT -30- 28 CONTINENTS ONLY
48 RETRIEVED SNDGS ARE INCLUDED IN THIS TABLE

LAYER	MN ERROR	RMS	TRU VAR	RET VAR	RATIO	RMS HT ERROR (METERS)
LYR 22 P= 25- 16	0.86	2.58	184.63	180.33	0.98	62.78
LYR 21 P= 40- 25	0.60	2.72	141.32	141.01	1.00	51.62
LYR 20 P= 63- 40	0.16	1.80	64.78	65.04	1.01	48.97
LYR 19 P= 100- 63	-0.83	2.96	25.55	17.28	0.68	52.72
LYR 18 P= 114-100	-0.71	2.67	15.78	11.13	0.71	42.90
LYR 17 P= 129-114	-0.39	1.92	9.83	8.07	0.83	41.40
LYR 16 P= 147-129	-0.36	2.27	8.09	4.27	0.53	38.59
LYR 15 P= 167-147	-0.02	2.52	5.91	2.12	0.36	33.83
LYR 14 P= 190-167	0.24	2.32	4.83	2.03	0.43	28.88
LYR 13 P= 215-190	0.28	2.15	6.95	3.81	0.55	24.08
LYR 12 P= 245-215	0.27	1.91	9.68	5.62	0.59	19.58
LYR 11 P= 278-245	0.01	1.76	11.69	7.78	0.67	15.30
LYR 10 P= 316-278	-0.21	1.73	12.21	9.71	0.80	11.96
LYR 9 P= 359-316	-0.12	1.46	11.75	11.15	0.95	9.99
LYR 8 P= 408-359	0.17	1.26	12.32	12.32	1.00	10.31
LYR 7 P= 464-408	0.05	1.18	13.12	12.32	0.94	11.14
LYR 6 P= 527-464	-0.17	0.96	12.39	12.03	0.98	11.92
LYR 5 P= 599-527	-0.11	0.92	12.76	11.34	0.89	12.16
LYR 4 P= 681-599	0.05	1.22	13.55	11.68	0.87	12.72
LYR 3 P= 774-681	0.21	1.08	15.32	14.07	0.92	13.38
LYR 2 P= 880-774	0.02	1.61	25.99	20.26	0.78	12.95
LYR 1 P=1000-880	-0.23	2.22	43.30	31.41	0.73	8.29
TSKIN	0.24	1.03	85.42	80.36	0.95	
STRATOSPHERIC RMS=	2.55 WITH AVG VAR RATIO=				0.92	
TROPOSPHERIC RMS=	1.81 WITH AVG VAR RATIO=				0.76	

INSTMNT 1 PROCESS 4 DATA SET 3
LAT BELT -30- 28 BOTH CONTINENT AND OCEAN
96 RETRIEVED SNDGS ARE INCLUDED IN THIS TABLE

LAYER	MN ERROR	RMS	TRU VAR	RET VAR	RATIO	RMS HT ERROR (METERS)
LYR 22 P= 25- 16	0.02	3.14	188.06	183.45	0.98	63.83
LYR 21 P= 40- 25	0.30	2.70	140.40	143.23	1.03	60.74
LYR 20 P= 63- 40	0.28	1.85	64.39	67.14	1.05	63.74
LYR 19 P= 100- 63	-0.38	3.41	32.52	18.32	0.57	61.65
LYR 18 P= 114-100	-0.48	2.96	23.65	12.87	0.55	40.34
LYR 17 P= 129-114	-0.26	2.19	16.61	11.33	0.69	37.94
LYR 16 P= 147-129	-0.30	2.32	12.59	7.33	0.59	34.93
LYR 15 P= 167-147	-0.17	2.33	8.22	4.62	0.57	31.15
LYR 14 P= 190-167	-0.02	2.09	5.47	3.57	0.66	27.66
LYR 13 P= 215-190	-0.06	2.01	6.54	4.30	0.66	23.47
LYR 12 P= 245-215	0.07	1.87	9.29	5.24	0.57	19.31
LYR 11 P= 278-245	0.08	1.66	10.92	6.79	0.63	14.61
LYR 10 P= 316-278	0.11	1.53	11.90	8.44	0.71	11.05
LYR 9 P= 359-316	0.11	1.27	11.46	9.67	0.85	8.89
LYR 8 P= 408-359	0.20	1.13	11.52	10.67	0.93	8.95
LYR 7 P= 464-408	0.15	0.99	11.76	10.80	0.92	9.70
LYR 6 P= 527-464	-0.01	0.90	11.09	10.69	0.97	10.50
LYR 5 P= 599-527	-0.05	0.92	10.81	10.01	0.93	10.57
LYR 4 P= 681-599	0.04	1.01	11.03	10.10	0.92	11.12
LYR 3 P= 774-681	-0.05	1.03	13.39	11.99	0.90	11.74
LYR 2 P= 880-774	-0.02	1.57	21.18	17.39	0.83	11.25
LYR 1 P=1000-880	-0.15	1.87	30.32	23.45	0.78	6.97
TSKIN	0.12	0.91	52.30	49.74	0.96	
STRATOSPHERIC RMS=	2.83 WITH AVG VAR RATIO=				0.91	
TROPOSPHERIC RMS=	1.74 WITH AVG VAR RATIO=				0.76	

INSTMNT 1 PROCESS 4 DATA SET 3
LAT BELT 30- 58 OCEANS ONLY
48 RETRIEVED SNDGS ARE INCLUDED IN THIS TABLE

LAYER	MN ERROR	RMS	TRU VAR	RET VAR	RATIO	RMS HT ERROR (METERS)
LYR 22 P= 25- 16	-1.33	3.03	81.08	77.43	0.96	73.39
LYR 21 P= 40- 25	-0.03	2.47	79.81	72.24	0.91	60.27
LYR 20 P= 63- 40	0.51	2.05	71.35	58.97	0.83	54.16
LYR 19 P= 100- 63	0.52	2.75	60.24	44.17	0.74	48.98
LYR 18 P= 114-100	-0.20	2.80	46.49	33.70	0.73	54.44
LYR 17 P= 129-114	-0.62	2.68	38.43	33.11	0.87	56.75
LYR 16 P= 147-129	-1.06	2.72	32.07	32.57	1.02	55.96
LYR 15 P= 167-147	-1.36	3.29	30.82	31.67	1.03	53.01
LYR 14 P= 190-167	-1.12	3.97	40.19	31.32	0.78	47.78
LYR 13 P= 215-190	-0.59	4.41	45.90	29.32	0.64	39.59
LYR 12 P= 245-215	0.59	4.08	35.81	21.87	0.62	32.14
LYR 11 P= 278-245	0.95	3.16	20.84	19.05	0.92	27.20
LYR 10 P= 316-278	0.65	2.53	15.78	19.62	1.25	23.69
LYR 9 P= 359-316	0.34	1.96	19.41	24.34	1.26	22.03
LYR 8 P= 408-359	0.23	1.82	29.66	30.86	1.05	20.39
LYR 7 P= 464-408	-0.11	1.63	36.72	35.98	0.98	17.94
LYR 6 P= 527-464	-0.26	1.47	39.18	38.67	0.99	15.26
LYR 5 P= 599-527	-0.16	1.43	43.13	37.64	0.88	13.33
LYR 4 P= 681-599	0.07	1.48	40.39	34.48	0.86	11.97
LYR 3 P= 774-681	0.33	1.39	36.24	30.13	0.84	11.00
LYR 2 P= 880-774	0.10	1.29	29.40	25.79	0.88	9.56
LYR 1 P=1000-880	-0.21	1.74	22.28	22.72	1.02	6.48
TSKIN	0.42	0.63	30.41	30.78	1.02	
STRATOSPHERIC RMS=	2.60	WITH AVG VAR RATIO=			0.86	
TROPOSPHERIC RMS=	2.62	WITH AVG VAR RATIO=			0.93	

INSTMNT 1 PROCESS 4 DATA SET 3
LAT BELT 30- 58 CONTINENTS ONLY
48 RETRIEVED SNDGS ARE INCLUDED IN THIS TABLE

LAYER	MN ERROR	RMS	TRU VAR	RET VAR	RATIO	RMS HT ERROR (METERS)
LYR 22 P= 25- 16	-1.76	4.38	86.74	68.14	0.79	88.82
LYR 21 P= 40- 25	0.41	3.07	67.92	57.01	0.84	91.49
LYR 20 P= 63- 40	1.24	2.63	54.40	45.83	0.85	85.05
LYR 19 P= 100- 63	1.08	3.22	46.50	38.64	0.84	70.90
LYR 18 P= 114-100	0.01	2.44	39.25	31.54	0.81	65.12
LYR 17 P= 129-114	-0.42	2.51	36.82	29.65	0.81	65.48
LYR 16 P= 147-129	-0.89	2.59	35.66	29.47	0.83	64.33
LYR 15 P= 167-147	-1.14	2.96	39.85	27.84	0.70	61.81
LYR 14 P= 190-167	-0.88	3.39	42.82	25.45	0.60	57.71
LYR 13 P= 215-190	-0.78	3.83	42.25	22.33	0.53	51.86
LYR 12 P= 245-215	-0.11	3.60	33.21	16.72	0.51	45.64
LYR 11 P= 278-245	0.48	3.49	28.05	17.01	0.61	39.61
LYR 10 p= 316-278	0.65	3.18	29.03	20.42	0.71	33.64
LYR 9 P= 359-316	0.68	2.85	34.40	26.05	0.76	27.50
LYR 8 P= 408-359	0.63	2.28	42.80	32.45	0.76	22.79
LYR 7 P= 464-408	0.47	1.93	48.40	37.36	0.78	19.84
LYR 6 P= 527-464	0.20	1.67	47.38	40.35	0.86	18.08
LYR 5 P= 599-527	0.12	1.65	45.98	41.93	0.92	16.71
LYR 4 P= 681-599	-0.25	1.55	46.69	43.25	0.93	15.48
LYR 3 P= 774-681	-0.58	1.54	50.12	45.51	0.91	14.35
LYR 2 P= 880-774	-0.11	1.63	49.91	50.98	1.03	14.09
LYR 1 P=1000-880	-0.35	2.71	63.03	69.30	1.10	10.14
TSKIN	1.21	1.52	129.75	113.69	0.88	
STRATOSPHERIC RMS=	3.38	WITH AVG VAR RATIO=			0.83	
TROPOSPHERIC RMS=	2.65	WITH AVG VAR RATIO=			0.79	

INSTMNT 1 PROCESS 4 DATA SET 3
LAT BELT 30- 58 BOTH CONTINENT AND OCEAN
96 RETRIEVED SNDGS ARE INCLUDED IN THIS TABLE

LAYER	MN ERROR	RMS	TRU VAR	RET VAR	RATIO	RMS HT ERROR (METERS)
LYR 22 P= 25- 16	-1.54	3.77	84.60	73.87	0.88	81.47
LYR 21 P= 40- 25	0.19	2.78	75.82	66.01	0.88	77.46
LYR 20 P= 63- 40	0.87	2.36	65.33	53.84	0.83	71.30
LYR 19 P= 100- 63	0.80	2.99	55.24	42.59	0.78	60.93
LYR 18 P= 114-100	-0.09	2.62	44.09	33.62	0.77	60.01
LYR 17 P= 129-114	-0.52	2.60	38.78	32.32	0.84	61.27
LYR 16 P= 147-129	-0.98	2.65	34.92	31.91	0.92	60.29
LYR 15 P= 167-147	-1.25	3.13	36.21	30.44	0.85	57.58
LYR 14 P= 190-167	-1,00	3.69	42.01	28.73	0.69	52.98
LYR 13 P= 215-190	-0.69	4.13	44.13	25.93	0.59	46.13
LYR 12 P= 245-215	0.24	3.85	34.62	19.28	0.56	39.47
LYR 11 P= 278-245	0.72	3.33	24.69	18.09	0.74	33.97
LYR 10 P= 316-278	0.65	2.87	22.54	20.16	0.90	29.09
LYR 9 P= 359-316	0.51	2.45	26.96	25.35	0.95	24.92
LYR 8 P= 408-359	0.43	2.07	36.26	31.79	0.88	21.62
LYR 7 P= 464-408	0.18	1.79	42.56	36.77	0.87	18.91
LYR 6 P= 527-464	-0.03	1.57	43.28	39.57	0.92	16.73
LYR 5 P= 599-527	-0.02	1.55	44.56	39.81	0.90	15.12
LYR 4 P= 681-599	-0.09	1.52	43.59	38.87	0.90	13.83
LYR 3 P= 774-681	-0.13	1.46	43.30	37.83	0.88	12.78
LYR 2 P= 880-774	-0.01	1.47	39.88	38.72	0.98	12.04
LYR 1 P=1000-880	-0.28	2.28	46.09	49.71	1.08	8.51
TSKIN	0.82	1.17	96.99	86.05	0.89	
STRATOSPHERIC RMS=	3.01	WITH AVG VAR RATIO=			0.84	
TROPOSPHERIC RMS=	2.64	WITH AVG VAR RATIO=			0.85	

INSTMNT 1 PROCESS 4 DATA SET 4
LAT BELT -30- 28 OCEANS ONLY
56 RETRIEVED SNDGS ARE INCLUDED IN THIS TABLE

LAYER	MN ERROR	RMS	TRU VAR	RET VAR	RATIO	RMS HT ERROR (METERS)
LYR 22 P= 25- 16	0.04	1.95	8.96	4.77	0.54	48.62
LYR 21 P= 40- 25	0.57	1.34	4.28	2.97	0.70	59.08
LYR 20 P= 63- 40	0.18	1.88	7.57	4.81	0.64	60.92
LYR 19 P= 100- 63	-0.26	2.17	12.19	6.68	0.55	58.44
LYR 18 P= 114-100	-0.20	3.63	24.77	5.30	0.22	38.29
LYR 17 P= 129-114	-0.59	2.78	17.79	5.39	0.31	29.51
LYR 16 P= 147-129	-0.47	2.38	10.39	3.30	0.32	24.25
LYR 15 P= 167-147	-0.37	2.27	6.53	1.99	0.31	20.11
LYR 14 P= 190-167	-0.18	1.82	4.32	1.99	0.47	17.95
LYR 13 P= 215-190	-0.11	1.47	5.50	3.58	0.66	17.00
LYR 12 P= 245-215	-0.07	1.22	8.44	5.90	0.70	15.57
LYR 11 P= 278-245	-0.03	1.32	12.89	8.64	0.68	13.77
LYR 10 P= 316-278	0.08	1.36	16.48	11.04	0.67	11.88
LYR 9 P= 359-316	0.09	1.20	16.99	12.05	0.71	10.32
LYR 8 P= 408-359	-0.01	1.02	15.37	12.77	0.84	9.57
LYR 7 P= 464-408	0.05	0.89	13.40	12.41	0.93	9.54
LYR 6 P= 527-464	0.10	0.91	11.33	11.07	0.98	9.24
LYR 5 P= 599-527	0.17	0.91	10.90	9.77	0.90	9.22
LYR 4 P= 681-599	0.10	0.77	11.17	9.88	0.89	10.56
LYR 3 P= 774-681	-0.19	0.92	12.77	12.82	1.01	11.69
LYR 2 P= 880-774	-0.05	1.62	13.75	17.43	1.27	10.59
LYR 1 P=1000-880	-0.14	1.55	15.06	17.63	1.18	5.77
TSKIN	-0.40	0.92	26.18	21.81	0.84	
STRATOSPHERIC RMS=	1.86 WITH AVG VAR RATIO=				0.61	
TROPOSPHERIC RMS=	1.72 WITH AVG VAR RATIO=				0.73	

INSTMNT 1 PROCESS 4 DATA SET 4
LAT BELT -30- 28 CONTINENTS ONLY
40 RETRIEVED SNDGS ARE INCLUDED IN THIS TABLE

LAYER	MN ERROR	RMS	TRU VAR	RET VAR	RATIO	RMS HT ERROR (METERS)
LYR 22 P= 25- 16	-0.10	2.24	12.01	8.55	0.72	59.38
LYR 21 P= 40- 25	0.36	1.67	8.69	5.95	0.69	63.02
LYR 20 P= 63- 40	0.29	2.12	13.69	8.38	0.62	57.81
LYR 19 P= 100- 63	0.21	2.60	21.66	10.57	0.49	51.52
LYR 18 P= 114-100	-0.38	3.40	22.86	6.39	0.28	35.65
LYR 17 P= 129-114	-0.75	2.99	14.62	4.71	0.33	29.90
LYR 16 P= 147-129	-1.04	2.58	9.49	4.15	0.44	25.60
LYR 15 P= 167-147	-0.70	2.01	7.43	4.49	0.61	24.56
LYR 14 P= 190-167	-0.06	1.43	10.25	6.22	0.61	24.80
LYR 13 P= 215-190	0.17	1.58	15.49	9.15	0.60	22.25
LYR 12 P= 245-215	0.39	1.66	19.90	12.33	0.62	18.91
LYR 11 P= 278-245	0.50	1.78	24.94	15.55	0.63	15.49
LYR 10 P= 316-278	0.45	1.63	28.03	17.81	0.64	13.02
LYR 9 P= 359-316	0.20	1.42	26.26	18.29	0.70	11.63
LYR 8 P= 408-359	0.08	1.26	23.50	18.83	0.81	11.37
LYR 7 P= 464-408	-0.03	1.05	19.79	17.41	0.88	11.70
LYR 6 P= 527-464	-0.09	1.04	15.71	14.63	0.94	11.88
LYR 5 P= 599-527	-0.28	1.32	11.05	12.76	1.16	11.72
LYR 4 P= 681-599	-0.01	1.31	13.21	13.64	1.04	11.25
LYR 3 P= 774-681	0.24	1.37	21.78	19.93	0.92	11.50
LYR 2 P= 880-774	-0.00	1.44	29.62	28.71	0.97	11.15
LYR 1 P=1000-880	-0.10	1.87	44.55	41.08	0.93	6.97
TSKIN	-0.05	1.13	89.12	81.13	0.92	
STRATOSPHERIC RMS=	2.18 WITH AVG VAR RATIO=				0.63	
TROPOSPHERIC RMS=	1.84 WITH AVG VAR RATIO=				0.73	

INSTMNT 1 PROCESS 4 DATA SET 4
LAT BELT -30- 28 BOTH CONTINENT AND OCEAN
96 RETRIEVED SNDGS ARE INCLUDED IN THIS TABLE

LAYER	MN ERROR	RMS	TRU VAR	RET VAR	RATIO	RMS HT ERROR (METERS)
LYR 22 P= 25- 16	-0.02	2.07	11.17	7.20	0.65	53.37
LYR 21 P= 40- 25	0.48	1.48	6.94	4.85	0.70	60.75
LYR 20 P= 63- 40	0.22	1.99	10.81	7.09	0.66	59.64
LYR 19 P= 100- 63	-0.06	2.36	16.63	9.17	0.56	55.66
LYR 18 P= 114-100	-0.27	3.54	24.90	6.52	0.27	37.21
LYR 17 P= 129-114	-0.66	2.87	17.41	5.90	0.34	29.67
LYR 16 P= 147-129	-0.71	2.47	11.34	4.41	0.39	24.82
LYR 15 P= 167-147	-0.51	2.17	7.83	3.67	0.47	22.07
LYR 14 P= 190-167	-0.13	1.67	7.20	4.25	0.60	21.07
LYR 13 P= 215-190	0.01	1.52	9.90	6.30	0.64	19.36
LYR 12 P= 245-215	0.12	1.42	13.33	8.90	0.67	17.04
LYR 11 P= 278-245	0.19	1.53	17.97	11.76	0.66	14.51
LYR 10 P= 316-278	0.23	1.48	21.34	14.03	0.66	12.36
LYR 9 P= 359-316	0.14	1.30	20.93	14.76	0.71	10.88
LYR 8 P= 408-359	0.03	1.13	18.82	15.38	0.82	10.36
LYR 7 P= 464-408	0.02	0.96	16.13	14.54	0.91	10.50
LYR 6 P= 527-464	0.02	0.97	13.22	12.58	0.96	10.42
LYR 5 P= 599-527	-0.02	1.10	11.15	11.06	1.00	10.33
LYR 4 P= 681-599	0.06	1.03	12.18	11.57	0.95	10.85
LYR 3 P= 774-681	-0.01	1.13	16.64	16.09	0.97	11.61
LYR 2 P= 880-774	-0.03	1.55	20.81	22.61	1.09	10.83
LYR 1 P=1000-880	-0.12	1.69	28.15	28.24	1.01	6.29
TSKIN	-0.26	1.01	53.40	47.89	0.90	
STRATOSPHERIC RMS=	2.00 WITH AVG VAR RATIO=				0.65	
TROPOSPHERIC RMS=	1.77 WITH AVG VAR RATIO=				0.73	

INSTMNT 1 PROCESS 4 DATA SET 4
LAT BELT 30- 58 OCEANS ONLY
48 RETRIEVED SNDGS ARE INCLUDED IN THIS TABLE

LAYER	MN ERROR	RMS	TRU VAR	RET VAR	RATIO	RMS HT ERROR (METERS)
LYR 22 P= 25- 16	0.17	1.36	7.07	6.41	0.91	54.12
LYR 21 P= 40- 25	0.27	1.66	9.73	6.50	0.67	46.87
LYR 20 P= 63- 40	-0.05	1.30	12.54	10.59	0.85	45.19
LYR 19 P= 100- 63	-0.02	1.60	20.26	18.67	0.93	47.45
LYR 18 P= 114-100	-0.30	1.84	22.26	21.47	0.97	45.31
LYR 17 P= 129-114	-0.63	1.87	20.35	21.76	1.07	43.79
LYR 16 P= 147-129	-0.64	2.39	20.31	20.60	1.02	41.66
LYR 15 P= 167-147	-0.17	3.11	23.16	18.16	0.79	37.56
LYR 14 P= 190-167	0.88	4.09	28.44	15.24	0.54	31.63
LYR 13 P= 215-190	1.35	4.29	27.05	12.88	0.48	25.49
LYR 12 P= 245-215	0.75	3.07	15.37	6.08	0.40	22.78
LYR 11 P= 278-245	-0.05	1.78	9.48	5.81	0.62	23.78
LYR 10 P= 316-278	-0.27	1.82	10.93	8.98	0.83	23.30
LYR 9 P= 359-316	-0.35	1.94	11.93	11.90	1.00	19.96
LYR 8 P= 408-359	-0.34	2.10	12.52	13.96	1.12	15.48
LYR 7 P= 464-408	-0.31	1.80	13.48	15.48	1.15	11.61
LYR 6 P= 527-464	-0.11	1.48	16.47	16.42	1.00	10.73
LYR 5 P= 599-527	-0.07	1.32	17.08	16.99	1.00	10.84
LYR 4 P= 681-599	-0.17	1.01	18.74	19.27	1.03	12.38
LYR 3 P= 774-681	-0.27	1.09	26.97	23.18	0.86	13.33
LYR 2 P= 880-774	0.18	1.72	34.07	25.46	0.75	12.31
LYR 1 P=1000-880	0.80	2.20	21.53	17.21	0.80	8.20
TSKIN	0.58	0.85	19.53	21.09	1.09	
STRATOSPHERIC RMS=	1.48	WITH AVG VAR RATIO=			0.85	
TROPOSPHERIC RMS=	2.34	WITH AVG VAR RATIO=			0.86	

INSTMNT 1 PROCESS 4 DATA SET 4
LAT BELT 30- 58 CONTINENTS ONLY
48 RETRIEVED SNDGS ARE INCLUDED IN THIS TABLE

LAYER	MN ERROR	RMS	TRU VAR	RET VAR	RATIO	RMS HT ERROR (METERS)
LYR 22 P= 25- 16	-0.56	2.27	11.00	13.58	1.24	52.33
LYR 21 P= 40- 25	-0.27	2.09	13.40	12.16	0.91	44.80
LYR 20 P= 63- 40	0.13	1.29	21.68	18.98	0.88	49.13
LYR 19 P= 100- 63	1.09	2.38	40.18	31.89	0.80	54.98
LYR 18 P= 114-100	0.92	2.89	48.38	36.00	0.75	44.36
LYR 17 P= 129-114	-0.04	2.19	39.56	33.38	0.85	40.80
LYR 16 P= 147-129	-0.56	2.50	33.94	28.90	0.86	37.92
LYR 15 P= 167-147	-0.89	2.87	28.69	21.17	0.74	34.02
LYR 14 P= 190-167	-0.81	3.42	25.28	13.61	0.54	30.73
LYR 13 P= 215-190	-0.41	3.47	23.50	11.75	0.50	28.63
LYR 12 P= 245-215	0.30	2.65	19.93	10.30	0.52	28.46
LYR 11 P= 278-245	0.28	2.27	25.63	15.18	0.60	27.54
LYR 10 P= 316-278	0.28	2.12	30.90	18.95	0.62	25.36
LYR 9 P= 359-316	0.02	1.91	29.66	20.65	0.70	21.18
LYR 8 P= 408-359	0.02	1.67	24.55	21.32	0.87	16.79
LYR 7 P= 464-408	0.21	1.39	21.45	21.51	1.01	12.95
LYR 6 P= 527-464	0.15	1.23	20.55	20.72	1.01	10.97
LYR 5 P= 599-527	0.02	1.22	20.55	19.36	0.95	10.56
LYR 4 P= 681-599	-0.03	1.06	20.97	20.10	0.96	11.55
LYR 3 P= 774-681	0.16	1.20	25.37	22.53	0.89	12.78
LYR 2 P= 880-774	-0.12	1.50	29.82	24.53	0.83	12.88
LYR 1 P=1000-880	-0.48	2.44	29.22	28.69	0.99	9.10
TSKIN	0.78	1.11	84.69	91.27	1.08	
STRATOSPHERIC RMS=	2.05	WITH AVG VAR RATIO=			0.96	
TROPOSPHERIC RMS=	2.23	WITH AVG VAR RATIO=			0.79	

INSTMNT 1 PROCESS 4 DATA SET 4
LAT BELT 30- 58 BOTH CONTINENT AND OCEAN
96 RETRIEVED SNDGS ARE INCLUDED IN THIS TABLE

LAYER	MN ERROR	RMS	TRU VAR	RET VAR	RATIO	RMS HT ERROR (METERS)
LYR 22 P= 25- 16	-0.20	1.87	9.44	10.07	1.07	53.24
LYR 21 P= 40- 25	-0.00	1.89	11.99	9.47	0.80	45.85
LYR 20 P= 63- 40	0.04	1.29	17.25	15.01	0.88	47.20
LYR 19 P= 100- 63	0.53	2.03	30.21	25.68	0.86	51.35
LYR 18 P= 114-100	0.31	2.42	35.30	29.11	0.83	44.84
LYR 17 P= 129-114	-0.34	2.04	30.02	27.89	0.93	42.32
LYR 16 P= 147-129	-0.60	2.44	27.46	25.14	0.92	39.83
LYR 15 P= 167-147	-0.53	2.99	27.06	20.16	0.75	35.83
LYR 14 P= 190-167	0.03	3.77	29.56	15.06	0.51	31.18
LYR 13 P= 215-190	0.47	3.90	28.22	13.01	0.47	27.10
LYR 12 P= 245-215	0.52	2.87	18.43	8.62	0.47	25.78
LYR 11 P= 278-245	0.11	2.04	17.65	10.71	0.61	25.73
LYR 10 P= 316-278	0.00	1.97	20.92	14.08	0.68	24.35
LYR 9 P= 359-316	-0.16	1.92	20.79	16.32	0.79	20.58
LYR 8 P= 408-359	-0.16	1.90	18.54	17.65	0.96	16.15
LYR 7 P= 464-408	-0.05	1.61	17.50	18.50	1.06	12.30
LYR 6 P= 527-464	0.02	1.36	18.51	18.57	1.01	10.85
LYR 5 P= 599-527	-0.02	1.27	18.82	18.18	0.97	10.70
LYR 4 P= 681-599	-0.10	1.03	19.86	19.70	1.00	11.97
LYR 3 P= 774-681	-0.05	1.14	26.17	22.91	0.88	13.06
LYR 2 P= 880-774	0.03	1.61	32.40	25.27	0.78	12.60
LYR 1 P=1000-880	0.16	2.32	30.12	25.31	0.85	8.66
TSKIN	0.68	0.99	66.84	71.71	1.08	
STRATOSPHERIC RMS=	1.79	WITH AVG VAR RATIO=			0.90	
TROPOSPHERIC RMS=	2.28	WITH AVG VAR RATIO=			0.81	

INSTMNT 1 PROCESS 4 DATA SET 3 (+ NOISE)
LAT BELT -30- 28 OCEANS ONLY
48 RETRIEVED SNDGS ARE INCLUDED IN THIS TABLE

LAYER	MN ERROR	RMS	TRU VAR	RET VAR	RATIO	RMS HT ERROR (METERS)
LYR 22 P= 25- 16	-0.80	2.92	81.08	75.10	0.93	82.39
LYR 21 P= 40- 25	0.12	2.54	79.81	69.58	0.88	75.38
LYR 20 P= 63- 40	0.53	2.20	71.35	58.90	0.83	72.37
LYR 19 P= 100- 63	0.55	3.06	60.24	44.95	0.75	63.16
LYR 18 P= 114-100	-0.12	3.05	46.49	33.14	0.72	61.69
LYR 17 P= 129-114	-0.57	3.00	38.43	32.46	0.85	62.55
LYR 16 P= 147-129	-1.01	3.07	32.07	32.00	1.00	60.00
LYR 15 P= 167-147	-1.30	3.59	30.82	31.05	1.01	55.51
LYR 14 P= 190-167	-1.06	4.16	40.19	30.66	0.77	49.13
LYR 13 P= 215-190	-0.52	4.50	45.90	28.79	0.63	40.34
LYR 12 P= 245-215	0.63	4.07	35.81	21.06	0.59	32.75
LYR 11 P= 278-245	0.97	3.11	20.84	18.18	0.88	27.65
LYR 10 P= 316-278	0.63	2.51	15.78	18.93	1.20	23.80
LYR 9 P= 359-316	0.29	2.00	19.41	24.01	1.24	21.88
LYR 8 P= 408-359	0.18	1.85	29.66	30.70	1.04	20.17
LYR 7 P= 464-408	-0.13	1.60	36.72	35.91	0.98	18.06
LYR 6 P= 527-464	-0.26	1.45	39.18	38.61	0.99	15.93
LYR 5 P= 599-527	-0.16	1.45	43.13	37.60	0.88	14.22
LYR 4 P= 681-599	0.07	1.51	40.39	34.47	0.86	12.76
LYR 3 P= 774-681	0.34	1.43	36.24	30.15	0.84	11.75
LYR 2 P= 880-774	0.12	1.37	29.40	25.73	0.88	10.10
LYR 1 P=1000-880	-0.19	1.81	22.28	22.87	1.03	6.76
TSKIN	0.45	0.65	30.41	30.92	1.02	
STRATOSPHERIC RMS=	2.69	WITH AVG VAR RATIO=			0.85	
TROPOSPHERIC RMS=	2.73	WITH AVG VAR RATIO=			0.92	

INSTMNT 1 PROCESS 4 DATA SET 3 (+ NOISE)
LAT BELT -30- 28 CONTINENTS ONLY
48 RETRIEVED SNDGS ARE INCLUDED IN THIS TABLE

LAYER	MN ERROR	RMS	TRU VAR	RET VAR	RATIO	RMS HT ERROR (METERS)
LYR 22 P= 25- 16	-1.53	4.22	86.74	64.72	0.75	112.88
LYR 21 P= 40- 25	0.32	3.20	67.92	55.01	0.81	120.49
LYR 20 P= 63- 40	1.24	2.74	54.40	44.47	0.82	114.28
LYR 19 P= 100- 63	1.27	3.49	46.50	36.01	0.78	98.53
LYR 18 P= 114-100	0.20	2.83	39.25	27.21	0.70	85.37
LYR 17 P= 129-114	-0.40	3.06	36.82	27.25	0.75	82.44
LYR 16 P= 147-129	-0.87	3.16	35.66	26.72	0.75	78.12
LYR 15 P= 167-147	-1.08	3.43	39.85	24.98	0.63	72.59
LYR 14 P= 190-167	-0.77	3.86	42.82	22.56	0.53	66.03
LYR 13 P= 215-190	-0.61	4.30	42.25	19.64	0.47	57.76
LYR 12 P= 245-215	0.09	4.05	33.21	14.57	0.44	49.24
LYR 11 P= 278-245	0.64	3.83	28.05	16.14	0.58	40.99
LYR 10 P= 316-278	0.76	3.39	29.03	20.51	0.71	33.65
LYR 9 P= 359-316	0.72	2.98	34.40	26.84	0.79	26.91
LYR 8 P= 408-359	0.62	2.33	42.80	33.39	0.79	22.01
LYR 7 P= 464-408	0.42	1.91	48.40	38.41	0.80	19.56
LYR 6 P= 527-464	0.15	1.65	47.38	41.50	0.88	18.41
LYR 5 P= 599-527	0.06	1.63	45.98	42.94	0.94	17.42
LYR 4 P= 681-599	-0.33	1.55	46.69	44.32	0.95	16.43
LYR 3 P= 774-681	-0.64	1.51	50.12	46.55	0.93	15.34
LYR 2 P= 880-774	-0.18	1.70	49.91	52.08	1.05	14.87
LYR 1 P=1000-880	-0.37	2.81	63.13	69.30	1.10	10.51
TSKIN	1.20	1.51	129.75	113.79	0.88	
STRATOSPHERIC RMS=	3.45	WITH AVG VAR RATIO=			0.80	
TROPOSPHERIC RMS=	2.92	WITH AVG VAR RATIO=			0.77	

INSTMNT 1 PROCESS 4 DATA SET 3 (+ NOISE)
LAT BELT -30- 28 BOTH CONTINENT AND OCEAN
96 RETRIEVED SNDGS ARE INCLUDED IN THIS TABLE

LAYER	MN ERROR	RMS	TRU VAR	RET VAR	RATIO	RMS HT ERROR (METERS)
LYR 22 P= 25- 16	-1.17	3.63	84.60	71.34	0.85	98.82
LYR 21 P= 40- 25	0.22	2.88	75.82	63.98	0.85	100.50
LYR 20 P= 63- 40	0.88	2.48	65.33	53.14	0.82	95.65
LYR 19 P= 100- 63	0.91	3.28	55.24	41.49	0.76	82.76
LYR 18 P= 114-100	0.03	2.94	44.09	31.06	0.71	74.47
LYR 17 P= 129-114	-0.48	3.03	38.78	30.83	0.80	73.17
LYR 16 P= 147-129	-0.94	3.12	34.92	30.28	0.87	69.65
LYR 15 P= 167-147	-1.19	3.51	36.21	28.69	0.80	64.62
LYR 14 P= 190-167	-0.91	4.01	42.01	26.93	0.65	58.20
LYR 13 P= 215-190	-0.56	4.40	44.13	24.28	0.56	49.82
LYR 12 P= 245-215	0.36	4.06	34.62	17.81	0.52	41.82
LYR 11 P= 278-245	0.81	3.49	24.69	17.27	0.70	34.96
LYR 10 P= 316-278	0.70	2.98	22.54	19.91	0.89	29.14
LYR 9 P= 359-316	0.51	2.54	26.96	25.62	0.96	24.52
LYR 8 P= 408-359	0.40	2.11	36.26	32.19	0.89	21.11
LYR 7 P= 464-408	0.15	1.76	42.56	37.26	0.88	18.82
LYR 6 P= 527-464	-0.06	1.55	43.28	40.10	0.93	17.21
LYR 5 P= 599-527	-0.05	1.55	44.56	40.29	0.91	15.90
LYR 4 P= 681-599	-0.13	1.53	43.59	39.39	0.91	14.71
LYR 3 P= 774-681	-0.15	1.47	43.30	38.37	0.89	13.66
LYR 2 P= 880-774	-0.03	1.54	39.88	39.29	0.99	12.71
LYR 1 P=1000-880	-0.28	2.36	46.19	49.87	1.09	8.84
TSKIN	0.83	1.17	96.99	86.34	0.90	
STRATOSPHERIC RMS=	3.09	WITH AVG VAR RATIO=			0.82	
TROPOSPHERIC RMS=	2.82	WITH AVG VAR RATIO=			0.83	

INSTMNT 1 PROCESS 5 DATA SET 3
LAT BELT -30- 28 OCEANS ONLY
48 RETRIEVED SNDGS ARE INCLUDED IN THIS TABLE

LAYER	MN ERROR	RMS	TRU VAR	RET VAR	RATIO	RMS HT ERROR (METERS)
LYR 22 P= 25- 16	0.44	2.53	187.08	165.66	0.89	55.09
LYR 21 P= 40- 25	1.09	2.33	136.50	134.86	0.99	61.04
LYR 20 P= 63- 40	0.47	1.81	63.87	67.83	1.07	60.65
LYR 19 P= 100- 63	-0.91	2.49	38.63	30.46	0.79	54.18
LYR 18 P= 114-100	-1.44	2.74	30.88	24.65	0.80	33.19
LYR 17 P= 129-114	-0.95	2.63	22.58	17.39	0.78	27.04
LYR 16 P= 147-129	-0.68	2,52	16.26	12.41	0.77	22.15
LYR 15 P= 167-147	-0.71	2.28	10.11	7.91	0.79	19.67
LYR 14 P= 190-167	-0.71	1.74	5.84	5.80	1.00	20.22
LYR 13 P= 215-190	-0.56	1.58	5.93	5.73	0.97	20.18
LYR 12 P= 245-215	-0.13	1.44	8.96	5.64	0.66	19.71
LYR 11 P= 278-245	0.25	1.42	9.39	6.13	0.66	16.60
LYR 10 P= 316-278	0.56	1.35	10.25	7.03	0.69	13.16
LYR 9 P= 359-316	0.44	1.09	10.26	7.80	0.77	9.93
LYR 8 P= 408-359	0.27	0.93	10.43	8.35	0.81	8.59
LYR 7 P= 464-408	0.15	0.78	10.23	8.25	0.81	7.91
LYR 6 P= 527-464	-0.08	0.91	9.69	8.50	0.88	7.44
LYR 5 P= 599-527	-0.04	0.95	8.82	8.52	0.97	7.66
LYR 4 P= 681-599	0.24	0.82	8.42	9.23	1.10	9.06
LYR 3 P= 774-681	-0.12	0.99	11.21	9.39	0.84	9.49
LYR 2 P= 880-774	-0.05	1.53	14.22	10.77	0.76	8.49
LYR 1 P=1000-880	0.43	1.24	14.08	13.02	0.93	4.62
TSKIN	-0.51	0.95	16.37	15.85	0.97	
STRATOSPHERIC RMS=	2.30	WITH AVG VAR RATIO=			0.94	
TROPOSPHERIC RMS=	1.62	WITH AVG VAR RATIO=			0.84	

INSTMNT 1 PROCESS 5 DATA SET 3
LAT BELT -30- 28 CONTINENTS ONLY
48 RETRIEVED SNDGS ARE INCLUDED IN THIS TABLE

LAYER	MN ERROR	RMS	TRU VAR	RET VAR	RATIO	RMS HT ERROR (METERS)
LYR 22 P= 25- 16	2.70	4.45	184.63	120.28	0.66	62.02
LYR 21 P= 40- 25	0.04	2.43	141.32	151.69	1.08	97.04
LYR 20 P= 63- 40	-0.60	2.34	64.78	81.82	1.27	83.36
LYR 19 P= 100- 63	-1.45	3.08	25.55	28.85	1.13	67.92
LYR 18 P= 114-100	-1.52	3.43	15.78	23.69	1.51	39.14
LYR 17 P= 129-114	-1.28	2.66	9.83	15.25	1.56	32.74
LYR 16 P= 147-129	-1.19	2.60	8.09	9.62	1.20	27.66
LYR 15 P= 167-147	-0.83	2.40	5.91	6.04	1.03	22.57
LYR 14 P= 190-167	-0.51	1.80	4.83	3.87	0.81	19.86
LYR 13 P= 215-190	-0.16	1.51	6.95	4.79	0.69	18.74
LYR 12 P= 245-215	0.02	1.38	9.68	6.69	0.70	16.92
LYR 11 P= 278-245	-0.05	1.39	11.69	9.47	0.82	14.36
LYR 10 P= 316-278	-0.11	1.51	12.21	12.14	1.00	11.78
LYR 9 P= 359-316	0.11	1.36	11.75	13.95	1.19	9.63
LYR 8 P= 408-359	0.47	1.18	12.32	14.88	1.21	8.79
LYR 7 P= 464-408	0.33	1.05	13.12	13.86	1.06	8.12
LYR 6 P= 527-464	-0.04	1.00	12.39	11.76	0.95	7.98
LYR 5 P= 599-527	-0.19	0.98	12.76	10.14	0.80	7.73
LYR 4 P= 681-599	-0.10	1.15	13.55	10.36	0.77	8.71
LYR 3 P= 774-681	0.25	0.99	15.32	13.80	0.91	10.08
LYR 2 P= 880-774	0.42	1.43	25.99	25.46	0.98	10.52
LYR 1 P=1000-880	0.11	1.93	43.30	36.72	0.85	7.20
TSKIN	-0.52	0.85	85.42	87.08	1.02	
STRATOSPHERIC RMS=	3.19	WITH AVG VAR RATIO=			1.04	
TROPOSPHERIC RMS=	1.78	WITH AVG VAR RATIO=			1.01	

INSTMNT 1 PROCESS 5 DATA SET 3
LAT BELT -30- 28 BOTH CONTINENT AND OCEAN
96 RETRIEVED SNDGS ARE INCLUDED IN THIS TABLE

LAYER	MN ERROR	RMS	TRU VAR	RET VAR	RATIO	RMS HT ERROR (METERS)
LYR 22 P= 25- 16	1.57	3.62	188.06	143.08	0.77	58.65
LYR 21 P= 40- 25	0.57	2.38	140.40	146.32	1.05	81.06
LYR 20 P= 63- 40	-0.07	2.09	64.39	75.42	1.18	72.90
LYR 19 P= 100- 63	-1.18	2.80	32.52	29.83	0.92	61.44
LYR 18 P= 114-100	-1.48	3.11	23.65	24.46	1.04	36.29
LYR 17 P= 129-114	-1.12	2.65	16.61	16.55	1.00	30.03
LYR 16 P= 147-129	-0.93	2.56	12.59	11.18	0.89	25.06
LYR 15 P= 167-147	-0.77	2.34	8.22	7.15	0.87	21.17
LYR 14 P= 190-167	-0.61	1.77	5.47	5.06	0.93	20.04
LYR 13 P= 215-190	-0.36	1.55	6.54	5.53	0.85	19.47
LYR 12 P= 245-215	-0.05	1.41	9.29	6.40	0.69	18.37
LYR 11 P= 278-245	0.10	1.41	10.92	8.02	0.74	15.52
LYR 10 P= 316-278	0.22	1.43	11.90	9.82	0.83	12.49
LYR 9 P= 359-316	0.28	1.23	11.46	11.13	0.98	9.78
LYR 8 P= 408-359	0.37	1.06	11.52	11.85	1.03	8.69
LYR 7 P= 464-408	0.24	0.93	11.76	11.20	0.96	8.01
LYR 6 P= 527-464	-0.06	0.96	11.09	10.19	0.92	7.72
LYR 5 P= 599-527	-0.11	0.97	10.81	9.33	0.87	7.69
LYR 4 P= 681-599	0.07	1.00	11.03	9.79	0.89	8.89
LYR 3 P= 774-681	0.07	0.99	13.39	11.89	0.89	9.79
LYR 2 P= 880-774	0.18	1.48	21.18	19.74	0.94	9.56
LYR 1 P=1000-880	0.27	1.62	30.32	26.11	0.87	6.05
TSKIN	-0.52	0.90	52.30	52.84	1.02	
STRATOSPHERIC RMS=	2.78	WITH AVG VAR RATIO=			0.98	
TROPOSPHERIC RMS=	1.70	WITH AVG VAR RATIO=			0.90	

INSTMNT 1 PROCESS 5 DATA SET 3
LAT BELT 30- 58 OCEANS ONLY
48 RETRIEVED SNDGS ARE INCLUDED IN THIS TABLE

LAYER	MN ERROR	RMS	TRU VAR	RET VAR	RATIO	RMS HT ERROR (METERS)
LYR 22 P= 25- 16	-1.09	3.77	81.08	80.62	1.00	67.37
LYR 21 P= 40- 25	-0.78	2.88	79.81	73.63	0.93	59.18
LYR 20 P= 63- 40	0.38	2.51	71.35	59.19	0.83	52.76
LYR 19 P= 100- 63	0.64	3.22	60.24	46.67	0.78	35.20
LYR 18 P= 114-100	0.03	3.20	46.49	38.42	0.83	37.55
LYR 17 P= 129-114	-0.48	2.61	38.43	35.04	0.92	43.85
LYR 16 P= 147-129	-0.97	2.42	32.07	32.40	1.02	48.54
LYR 15 P= 167-147	-1.40	2.79	30.82	30.25	0.99	51.83
LYR 14 P= 190-167	-1.26	3.28	40.19	27.62	0.69	52.98
LYR 13 P= 215-190	-0.67	3.85	45.90	25.97	0.57	50.56
LYR 12 P= 245-215	0.42	4.15	35.81	25.44	0.72	45.30
LYR 11 P= 278-245	1.15	3.83	20.84	24.84	1.20	36.56
LYR 10 P= 316-278	0.97	3.07	15.78	25.09	1.59	27.07
LYR 9 P= 359-316	0.75	2.28	19.41	28.33	1.46	20.81
LYR 8 P= 408-359	0.62	1.96	29.66	31.56	1.07	16.51
LYR 7 P= 464-408	0.08	1.69	36.72	34.80	0.95	12.46
LYR 6 P= 527-464	-0.22	1.52	39.18	36.62	0.94	9.39
LYR 5 P= 599-527	-0.18	1.35	43.13	37.43	0.87	8.12
LYR 4 P= 681-599	0.10	1.36	40.39	36.72	0.91	8.75
LYR 3 P= 774-681	0.37	1.37	36.24	34.73	0.96	8.10
LYR 2 P= 880-774	0.02	1.08	29.40	29.86	1.02	6.90
LYR 1 P=1000-880	-0.02	1.42	22.28	26.13	1.18	5.28
TSKIN	-0.22	0.36	30.41	29.03	0.96	
STRATOSPHERIC RMS=	3.13	WITH AVG VAR RATIO=			0.89	
TROPOSPHERIC RMS=	2.58	WITH AVG VAR RATIO=			1.00	

INSTMNT 1 PROCESS 5 DATA SET 3
LAT BELT 30- 58 CONTINENTS ONLY
48 RETRIEVED SNDGS ARE INCLUDED IN THIS TABLE

LAYER	MN ERROR	RMS	TRU VAR	RET VAR	RATIO	RMS HT ERROR (METERS)
LYR 22 P= 25- 16	-0.35	4.85	86.74	55.57	0.65	74.56
LYR 21 P= 40- 25	0.85	2.81	67.92	52.99	0.79	104.52
LYR 20 P= 63- 40	0.63	2.82	54.40	46.13	0.85	85.13
LYR 19 P= 100- 63	-0.05	3.05	46.50	39.11	0.85	58.00
LYR 18 P= 114-100	-1.14	2.85	39.25	34.70	0.89	43.68
LYR 17 P= 129-114	-1.31	2.53	36.82	32.84	0.90	45.29
LYR 16 P= 147-129	-1.38	2.50	35.66	30.42	0.86	47.39
LYR 15 P= 167-147	-1.30	2.59	39.85	28.73	0.73	48.93
LYR 14 P= 190-167	-0.71	2.76	42.82	29.25	0.69	49.42
LYR 13 P= 215-190	-0.23	3.29	42.25	27.56	0.66	47.56
LYR 12 P= 245-215	0.38	3.25	33.21	25.45	0.77	43.94
LYR 11 P= 278-245	0.98	3.43	28.05	24.93	0.89	38.25
LYR 10 P= 316-278	0.85	2.88	29.03	27.71	0.96	31.58
LYR 9 P= 359-316	0.86	2.41	34.40	31.87	0.93	26.37
LYR 8 P= 408-359	0.91	2.04	42.80	37.30	0.88	21.39
LYR 7 P= 464-408	0.88	1.96	48.40	42.56	0.88	16.06
LYR 6 P= 527-464	0.65	1.58	47.38	46.02	0.98	10.39
LYR 5 P= 599-527	0.51	1.15	45.98	46.19	1.01	7.00
LYR 4 P= 681-599	-0.06	0.90	46.69	46.70	1.01	6.88
LYR 3 P= 774-681	-0.39	1.08	50.12	48.94	0.98	6.99
LYR 2 P= 880-774	-0.02	1.33	49.91	52.04	1.05	8.20
LYR 1 P=1000-880	-0.18	1.78	63.03	67.06	1.07	6.64
TSKIN	-0.16	0.33	129.75	127.03	0.98	
STRATOSPHERIC RMS=	3.49	WITH AVG VAR RATIO=			0.79	
TROPOSPHERIC RMS=	2.37	WITH AVG VAR RATIO=			0.90	

INSTMNT 1 PROCESS 5 DATA SET 3
LAT BELT 30- 58 BOTH CONTINENT AND OCEAN
96 RETRIEVED SNDGS ARE INCLUDED IN THIS TABLE

LAYER	MN ERROR	RMS	TRU VAR	RET VAR	RATIO	RMS HT ERROR (METERS)
LYR 22 P= 25- 16	-0.72	4.35	84.60	68.31	0.81	71.06
LYR 21 P= 40- 25	0.03	2.85	75.82	63.64	0.84	84.93
LYR 20 P= 63- 40	0.51	2.67	65.33	54.74	0.84	70.82
LYR 19 P= 100- 63	0.30	3.14	55.24	45.83	0.83	47.97
LYR 18 P= 114-100	-0.55	3.03	44.09	39.42	0.90	40.73
LYR 17 P= 129-114	-0.89	2.57	38.78	36.16	0.94	44.58
LYR 16 P= 147-129	-1.17	2.46	34.92	32.94	0.95	47.97
LYR 15 P= 167-147	-1.35	2.69	36.21	30.27	0.84	50.40
LYR 14 P= 190-167	-0.98	3.03	42.01	28.62	0.69	51.23
LYR 13 P= 215-190	-0.45	3.58	44.13	26.75	0.61	49.08
LYR 12 P= 245-215	0.40	3.73	34.62	25.54	0.74	44.62
LYR 11 P= 278-245	1.07	3.64	24.69	25.05	1.02	37.42
LYR 10 P= 316-278	0.91	2.97	22.54	26.49	1.18	29.41
LYR 9 P= 359-316	0.81	2.35	26.96	30.18	1.12	23.75
LYR 8 P= 408-359	0.77	2.00	36.26	34.53	0.96	19.11
LYR 7 P= 464-408	0.48	1.83	42.56	38.86	0.92	14.37
LYR 6 P= 527-464	0.21	1.55	43.28	41.51	0.96	9.90
LYR 5 P= 599-527	0.16	1.26	44.56	41.95	0.95	7.58
LYR 4 P= 681-599	0.02	1.16	43.59	41.73	0.96	7.87
LYR 3 P= 774-681	-0.01	1.23	43.30	41.83	0.97	7.56
LYR 2 P= 880-774	-0.00	1.21	39.88	41.19	1.04	7.58
LYR 1 P=1000-880	-0.10	1.61	46.09	50.34	1.10	6.00
TSKIN	-0.19	0.34	96.99	94.72	0.98	
STRATOSPHERIC RMS=	3.31	WITH AVG VAR RATIO=			0.84	
TROPOSPHERIC RMS=	2.48	WITH AVG VAR RATIO=			0.94	

INSTMNT 1 PROCESS 5 DATA SET 4
LAT BELT -30- 28 OCEANS ONLY
56 RETRIEVED SNDGS ARE INCLUDED IN THIS TABLE

LAYER	MN ERROR	RMS	TRU VAR	RET VAR	RATIO	RMS HT ERROR (METERS)
LYR 22 P= 25- 16	-0.30	2.21	8.86	4.43	0.50	49.92
LYR 21 P= 40- 25	0.15	1.15	4.28	3.28	0.77	52.11
LYR 20 P= 63- 40	-0.19	1.95	7.57	4.98	0.66	49.71
LYR 19 P= 100- 63	-0.83	1.61	12.19	10.50	0.87	44.91
LYR 18 P= 114-100	-0.93	2.91	24.77	12.67	0.52	33.19
LYR 17 P= 129-114	-1.07	2.61	17.79	8.21	0.47	26.14
LYR 16 P= 147-129	-0.90	2.12	10.39	4.29	0.42	22.37
LYR 15 P= 167-147	-0.78	2.04	6.53	1.91	0.30	21.23
LYR 14 P= 190-167	-0.49	1.72	4.32	2.06	0.48	21.51
LYR 13 P= 215-190	-0.11	1.49	5.50	4.54	0.83	21.53
LYR 12 P= 245-215	0.08	1.29	8.44	7.33	0.87	19.90
LYR 11 P= 278-245	0.22	1.39	12.89	10.03	0.78	17.30
LYR 10 P= 316-278	0.31	1.41	16.48	12.09	0.74	14.15
LYR 9 P= 359-316	0.33	1.16	16.99	12.91	0.77	11.04
LYR 8 P= 408-359	0.26	0.93	15.37	12.58	0.82	8.94
LYR 7 P= 464-408	0.24	0.72	13.40	11.37	0.85	8.29
LYR 6 P= 527-464	0.07	0.90	11.33	10.40	0.92	7.58
LYR 5 P= 599-527	0.04	0.90	10.90	9.23	0.85	7.61
LYR 4 P= 681-599	0.10	0.66	11.17	9.29	0.84	8.80
LYR 3 P= 774-681	0.10	0.97	12.77	9.86	0.78	9.43
LYR 2 P= 880-774	0.19	1.39	13.75	12.59	0.92	7.96
LYR 1 P=1000-880	0.30	1.21	15.06	18.25	1.22	4.50
TSKIN	-0.47	0.89	26.18	24.10	0.93	
STRATOSPHERIC RMS=	1.77	WITH AVG VAR RATIO=			0.71	
TROPOSPHERIC RMS=	1.55	WITH AVG VAR RATIO=			0.75	

INSTMNT 1 PROCESS 5 DATA SET 4
LAT BELT -30- 28 CONTINENTS ONLY
40 RETRIEVED SNDGS ARE INCLUDED IN THIS TABLE

LAYER	MN ERROR	RMS	TRU VAR	RET VAR	RATIO	RMS HT ERROR (METERS)
LYR 22 P= 25- 16	-0.46	2.41	12.01	5.16	0.43	52.67
LYR 21 P= 40- 25	0.37	1.60	8.69	6.14	0.71	54.48
LYR 20 P= 63- 40	0.06	2.13	13.69	9.13	0.67	51.04
LYR 19 P= 100- 63	-0.42	2.37	21.66	13.40	0.62	43.96
LYR 18 P= 114-100	-1.16	3.21	22.86	9.23	0.41	29.99
LYR 17 P= 129-114	-1.31	3.09	14.62	6.55	0.45	25.58
LYR 16 P= 147-129	-1.39	2.60	9.49	5.34	0.57	24.26
LYR 15 P= 167-147	-1.05	2.02	7.43	5.37	0.73	26.49
LYR 14 P= 190-167	-0.32	1.39	10.25	7.60	0.75	28.61
LYR 13 P= 215-190	0.15	1.56	15.49	10.21	0.66	26.70
LYR 12 P= 245-215	0.38	1.56	19.90	12.56	0.64	23.01
LYR 11 P= 278-245	0.56	1.79	24.94	15.20	0.61	18.46
LYR 10 P= 316-278	0.56	1.63	28.03	17.97	0.65	13.81
LYR 9 P= 359-316	0.37	1.35	26.26	18.76	0.72	10.42
LYR 8 P= 408-359	0.20	1.07	23.50	20.62	0.88	9.10
LYR 7 P= 464-408	0.02	0.83	19.79	20.83	1.06	8.74
LYR 6 P= 527-464	0.08	1.15	15.71	17.02	1.09	8.32
LYR 5 P= 599-527	-0.08	1.31	11.05	13.75	1.25	7.87
LYR 4 P= 681-599	0.15	1.27	13.21	12.85	0.98	8.47
LYR 3 P= 774-681	0.16	1.31	21.78	19.56	0.90	9.30
LYR 2 P= 880-774	0.09	1.16	29.62	24.98	0.85	9.96
LYR 1 P=1000-880	0.26	1.84	44.55	35.27	0.80	6.86
TSKIN	-0.46	0.78	89.12	87.35	0.99	
STRATOSPHERIC RMS=	2.15	WITH AVG VAR RATIO=			0.62	
TROPOSPHERIC RMS=	1.79	WITH AVG VAR RATIO=			0.78	

INSTMNT 1 PROCESS 5 DATA SET 4
LAT BELT -30- 28 BOTH CONTINENT AND OCEAN
96 RETRIEVED SNDGS ARE INCLUDED IN THIS TABLE

LAYER	MN ERROR	RMS	TRU VAR	RET VAR	RATIO	RMS HT ERROR (METERS)
LYR 22 P= 25- 16	-0.36	2.30	11.17	5.57	0.50	51.08
LYR 21 P= 40- 25	0.24	1.36	6.94	5.50	0.80	53.11
LYR 20 P= 63- 40	-0.09	2.02	10.81	7.62	0.71	50.26
LYR 19 P= 100- 63	-0.66	1.96	16.63	12.51	0.76	44.52
LYR 18 P= 114-100	-1.02	3.04	24.90	11.96	0.49	31.89
LYR 17 P= 129-114	-1.17	2.82	17.41	8.25	0.48	25.91
LYR 16 P= 147-129	-1.10	2.33	11.34	5.55	0.49	23.18
LYR 15 P= 167-147	-0.89	2.03	7.83	4.04	0.52	23.57
LYR 14 P= 190-167	-0.42	1.59	7.20	4.91	0.69	24.72
LYR 13 P= 215-190	-0.00	1.52	9.90	7.29	0.74	23.82
LYR 12 P= 245-215	0.20	1.41	13.33	9.75	0.74	21.25
LYR 11 P= 278-245	0.36	1.57	17.97	12.35	0.69	17.80
LYR 10 P= 316-278	0.42	1.50	21.34	14.66	0.69	14.01
LYR 9 P= 359-316	0.35	1.24	20.93	15.44	0.74	10.79
LYR 8 P= 408-359	0.24	0.99	18.82	15.98	0.85	9.01
LYR 7 P= 464-408	0.15	0.77	16.13	15.34	0.96	8.48
LYR 6 P= 527-464	0.08	1.01	13.22	13.22	1.01	7.90
LYR 5 P= 599-527	-0.01	1.09	11.15	11.26	1.01	7.72
LYR 4 P= 681-599	0.12	0.96	12.18	10.96	0.90	8.66
LYR 3 P= 774-681	0.13	1.12	16.64	14.04	0.85	9.38
LYR 2 P= 880-774	0.15	1.30	20.81	18.14	0.88	8.85
LYR 1 P=1000-880	0.28	1.50	28.15	26.11	0.93	5.61
TSKIN	-0.46	0.84	53.40	51.46	0.97	
STRATOSPHERIC RMS=	1.94	WITH AVG VAR RATIO=			0.70	
TROPOSPHERIC RMS=	1.66	WITH AVG VAR RATIO=			0.76	

INSTMNT 1 PROCESS 5 DATA SET 4
LAT BELT 30- 58 OCEANS ONLY
48 RETRIEVED SNDGS ARE INCLUDED IN THIS TABLE

LAYER	MN ERROR	RMS	TRU VAR	RET VAR	RATIO	RMS HT ERROR (METERS)
LYR 22 P= 25- 16	0.19	1.12	7.07	5.34	0.76	44.51
LYR 21 P= 40- 25	-0.08	1.42	9.73	5.79	0.60	41.62
LYR 20 P= 63- 40	-0.25	1.28	12.54	9.83	0.79	36.37
LYR 19 P= 100- 63	-0.54	1.69	20.26	15.73	0.78	36.74
LYR 18 P= 114-100	-1.04	2.09	22.26	19.17	0.87	37.30
LYR 17 P= 129-114	-1.13	2.14	20.35	19.06	0.94	37.16
LYR 16 P= 147-129	-1.12	2.54	20.31	19.21	0.95	36.02
LYR 15 P= 167-147	-0.71	3.05	23.16	18.16	0.79	33.53
LYR 14 P= 190-167	0.26	3.79	28.44	15.75	0.56	29.94
LYR 13 P= 215-190	1.17	4.02	27.05	11.81	0.44	25.60
LYR 12 P= 245-215	0.78	2.86	15.37	6.71	0.44	21.46
LYR 11 P= 278-245	0.32	1.78	9.48	6.77	0.72	20.40
LYR 10 P= 316-278	0.10	1.79	10.93	9.59	0.88	18.98
LYR 9 P= 359-316	0.12	1.66	11.93	11.64	0.98	15.42
LYR 8 P= 408-359	0.09	1.61	12.52	13.03	1.05	11.57
LYR 7 P= 464-408	0.05	1.23	13.48	14.07	1.05	8.95
LYR 6 P= 527-464	0.18	1.10	16.47	14.72	0.90	8.55
LYR 5 P= 599-527	0.14	1.07	17.08	15.13	0.89	7.89
LYR 4 P= 681-599	0.05	0.86	18.74	17.37	0.93	8.40
LYR 3 P= 774-681	-0.04	1.01	26.97	22.20	0.83	8.38
LYR 2 P= 880-774	0.03	1.35	34.07	28.74	0.85	7.46
LYR 1 P=1000-880	0.06	1.51	21.53	22.09	1.03	5.63
TSKIN	-0.24	0.65	19.53	17.76	0.91	
STRATOSPHERIC RMS=	1.39 WITH AVG VAR RATIO=				0.74	
TROPOSPHERIC RMS=	2.17 WITH AVG VAR RATIO=				0.84	

INSTMNT 1 PROCESS 5 DATA SET 4
LAT BELT 30- 58 CONTINENTS ONLY
48 RETRIEVED SNDGS ARE INCLUDED IN THIS TABLE

LAYER	MN ERROR	RMS	TRU VAR	RET VAR	RATIO	RMS HT ERROR (METERS)
LYR 22 P= 25- 16	-0.16	1.64	11.00	6.45	0.59	43.45
LYR 21 P= 40- 25	-0.05	1.87	13.40	8.63	0.65	35.74
LYR 20 P= 63- 40	-0.03	1.30	21.68	17.91	0.83	32.59
LYR 19 P= 100- 63	0.09	1.74	40.18	37.23	0.93	37.24
LYR 18 P= 114-100	0.04	2.29	48.38	45.87	0.95	31.88
LYR 17 P= 129-114	-0.39	2.25	39.56	39.57	1.01	29.54
LYR 16 P= 147-129	-0.77	2.41	33.94	30.08	0.89	27.86
LYR 15 P= 167-147	-1.08	2.54	28.69	20.60	0.72	26.40
LYR 14 P= 190-167	-1.09	2.82	25.28	12.65	0.51	25.74
LYR 13 P= 215-190	-0.71	2.94	23.50	10.40	0.45	25.07
LYR 12 P= 245-215	-0.20	2.44	19.93	12.68	0.64	24.26
LYR 11 P= 278-245	0.17	2.30	25.63	18.74	0.74	21.54
LYR 10 P= 316-278	0.23	1.93	30.90	22.40	0.73	17.90
LYR 9 P= 359-316	0.01	1.48	29.66	22.88	0.78	14.05
LYR 8 P= 408-359	0.04	1.17	24.55	23.06	0.94	11.89
LYR 7 P= 464-408	0.29	0.97	21.45	22.55	1.06	10.05
LYR 6 P= 527-464	0.28	0.92	20.55	21.46	1.05	8.74
LYR 5 P= 599-527	0.19	0.99	20.55	19.83	0.97	8.59
LYR 4 P= 681-599	0.07	0.96	20.97	20.78	1.00	9.65
LYR 3 P= 774-681	0.26	1.09	25.37	23.88	0.95	10.57
LYR 2 P= 880-774	0.26	1.34	29.82	25.98	0.88	10.24
LYR 1 P=1000-880	0.15	1.90	29.22	25.82	1.03	7.09
TSKIN	-0.46	0.69	84.69	80.18	0.95	
STRATOSPHERIC RMS=	1.65 WITH AVG VAR RATIO=				0.76	
TROPOSPHERIC RMS=	1.94 WITH AVG VAR RATIO=				0.85	

INSTMNT 1 PROCESS 5 DATA SET 4
LAT BELT 30- 58 BOTH CONTINENT AND OCEAN
96 RETRIEVED SNDGS ARE INCLUDED IN THIS TABLE

LAYER	MN ERROR	RMS	TRU VAR	RET VAR	RATIO	RMS HT ERROR (METERS)
LYR 22 P= 25- 16	0.01	1.40	9.44	6.11	0.65	43.99
LYR 21 P= 40- 25	-0.06	1.66	11.99	7.65	0.64	38.79
LYR 20 P= 63- 40	-0.14	1.29	17.25	14.11	0.82	34.53
LYR 19 P= 100- 63	-0.23	1.71	30.21	26.63	0.89	36.99
LYR 18 P= 114-100	-0.50	2.19	35.30	32.82	0.93	34.70
LYR 17 P= 129-114	-0.76	2.20	30.02	29.74	1.00	33.57
LYR 16 P= 147-129	-0.95	2.48	27.46	25.23	0.92	32.20
LYR 15 P= 167-147	-0.89	2.80	27.06	20.15	0.75	30.18
LYR 14 P= 190-167	-0.42	3.34	29.56	15.13	0.52	27.92
LYR 13 P= 215-190	0.23	3.52	28.22	11.70	0.42	25.33
LYR 12 P= 245-215	0.29	2.66	18.43	9.85	0.54	22.90
LYR 11 P= 278-245	0.24	2.06	17.65	12.81	0.73	20.97
LYR 10 P= 316-278	0.17	1.86	20.92	16.01	0.77	18.45
LYR 9 P= 359-316	0.07	1.57	20.79	17.26	0.84	14.75
LYR 8 P= 408-359	0.07	1.41	18.54	18.06	0.98	11.73
LYR 7 P= 464-408	0.17	1.11	17.50	18.31	1.05	9.52
LYR 6 P= 527-464	0.23	1.02	18.51	18.09	0.98	8.65
LYR 5 P= 599-527	0.17	1.03	18.82	17.48	0.93	8.25
LYR 4 P= 681-599	0.06	0.91	19.86	19.08	0.97	9.04
LYR 3 P= 774-681	0.11	1.05	26.17	23.07	0.89	9.54
LYR 2 P= 880-774	0.14	1.35	32.40	27.99	0.87	8.96
LYR 1 P=1000-880	0.10	1.71	30.12	30.89	1.03	6.40
TSKIN	-0.35	0.67	66.84	62.84	0.95	
STRATOSPHERIC RMS=	1.52 WITH AVG VAR RATIO=				0.76	
TROPOSPHERIC RMS=	2.06 WITH AVG VAR RATIO=				0.84	

INSTMNT 1 PROCESS 5 DATA SET 3 (+ NOISE)
LAT BELT -30- 28 OCEANS ONLY
48 RETRIEVED SNDGS ARE INCLUDED IN THIS TABLE

LAYER	MN ERROR	RMS	TRU VAR	RET VAR	RATIO	RMS HT ERROR (METERS)
LYR 22 P= 25- 16	-0.87	4.21	81.08	80.55	1.00	80.06
LYR 21 P= 40- 25	-0.87	3.14	79.81	76.80	0.97	69.89
LYR 20 P= 63- 40	0.28	2.50	71.35	62.00	0.87	63.59
LYR 19 P= 100- 63	0.66	3.33	60.24	50.95	0.85	48.46
LYR 18 P= 114-100	0.00	3.44	46.49	43.06	0.93	40.05
LYR 17 P= 129-114	-0.56	2.93	38.43	40.14	1.05	43.37
LYR 16 P= 147-129	-1.10	2.90	32.07	37.61	1.18	46.19
LYR 15 P= 167-147	-1.53	3.24	30.82	34.63	1.13	48.35
LYR 14 P= 190-167	-1.43	3.33	40.19	30.86	0.77	49.50
LYR 13 P= 215-190	-0.92	3.63	45.90	27.66	0.61	48.19
LYR 12 P= 245-215	0.11	3.92	35.81	25.75	0.72	44.12
LYR 11 P= 278-245	0.85	3.74	20.84	24.89	1.20	36.21
LYR 10 P= 316-278	0.72	3.09	15.78	25.12	1.60	26.74
LYR 9 P= 359-316	0.55	2.29	19.41	28.47	1.47	20.23
LYR 8 P= 408-359	0.48	1.95	29.66	31.91	1.08	16.11
LYR 7 P= 464-408	0.02	1.74	36.72	34.49	0.94	12.57
LYR 6 P= 527-464	-0.19	1.57	39.18	35.94	0.92	10.11
LYR 5 P= 599-527	-0.14	1.36	43.13	36.54	0.85	9.42
LYR 4 P= 681-599	0.16	1.32	40.39	36.17	0.90	10.07
LYR 3 P= 774-681	0.44	1.46	36.24	34.16	0.95	9.05
LYR 2 P= 880-774	0.06	1.09	29.40	29.71	1.02	7.22
LYR 1 P=1000-880	-0.12	1.50	22.28	27.00	1.22	5.61
TSKIN	-0.22	0.36	30.41	29.10	0.96	
STRATOSPHERIC RMS=	3.34 WITH AVG VAR RATIO=				0.93	
TROPOSPHERIC RMS=	2.64 WITH AVG VAR RATIO=				1.03	

INSTMNT 1 PROCESS 5 DATA SET 3 (+ NOISE)
LAT BELT -30- 28 CONTINENTS ONLY
48 RETRIEVED SNDGS ARE INCLUDED IN THIS TABLE

LAYER	MN ERROR	RMS	TRU VAR	RET VAR	RATIO	RMS HT ERROR (METERS)
LYR 22 P= 25- 16	-0.48	4.84	86.74	58.68	0.68	78.10
LYR 21 P= 40- 25	0.74	3.30	67.92	58.54	0.87	101.23
LYR 20 P= 63- 40	0.35	2.80	54.40	45.33	0.84	82.41
LYR 19 P= 100- 63	-0.08	2.93	46.50	37.44	0.81	61.75
LYR 18 P= 114-100	-1.02	2.82	39.25	32.64	0.84	48.78
LYR 17 P= 129-114	-1.18	2.50	36.82	31.46	0.86	50.01
LYR 16 P= 147-129	-1.23	2.45	35.66	29.81	0.84	51.56
LYR 15 P= 167-147	-1.16	2.56	39.85	29.37	0.74	52.58
LYR 14 P= 190-167	-0.60	2.96	42.82	30.04	0.71	52.42
LYR 13 P= 215-190	-0.11	3.54	42.25	29.22	0.70	49.84
LYR 12 P= 245-215	0.47	3.44	33.21	27.46	0.83	45.61
LYR 11 P= 278-245	1.08	3.47	28.05	27.14	0.97	39.77
LYR 10 P= 316-278	0.97	2.94	29.03	30.28	1.05	33.29
LYR 9 P= 359-316	0.98	2.57	34.40	33.52	0.98	27.41
LYR 8 P= 408-359	0.97	2.18	42.80	37.85	0.89	21.38
LYR 7 P= 464-408	0.91	2.03	48.40	42.40	0.88	15.98
LYR 6 P= 527-464	0.65	1.63	47.38	45.84	0.97	11.30
LYR 5 P= 599-527	0.45	1.19	45.98	46.16	1.01	9.42
LYR 4 P= 681-599	-0.14	0.97	46.69	47.48	1.02	10.10
LYR 3 P= 774-681	-0.51	1.18	50.12	51.20	1.03	10.18
LYR 2 P= 880-774	-0.17	1.57	49.91	57.14	1.15	10.56
LYR 1 P=1000-880	-0.29	2.04	63.03	71.38	1.14	7.60
TSKIN	-0.11	0.35	129.75	125.34	0.97	
STRATOSPHERIC RMS=	3.50 WITH AVG VAR RATIO=				0.80	
TROPOSPHERIC RMS=	2.46 WITH AVG VAR RATIO=				0.93	

INSTMNT 1 PROCESS 5 DATA SET 3 (+NOISE)
LAT BELT -30- 28 BOTH CONTINENT AND OCEAN
96 RETRIEVED SNDGS ARE INCLUDED IN THIS TABLE

LAYER	MN ERROR	RMS	TRU VAR	RET VAR	RATIO	RMS HT ERROR (METERS)
LYR 22 P= 25- 16	-0.67	4.54	84.60	70.02	0.83	79.08
LYR 21 P= 40- 25	-0.07	3.09	75.82	68.01	0.90	86.98
LYR 20 P= 63- 40	0.31	2.65	65.33	56.01	0.86	73.60
LYR 19 P= 100- 63	0.29	3.13	55.24	47.22	0.86	55.50
LYR 18 P= 114-100	-0.51	3.15	44.09	40.47	0.92	44.63
LYR 17 P= 129-114	-0.87	2.72	38.78	37.72	0.98	46.81
LYR 16 P= 147-129	-1.16	2.68	34.92	34.91	1.00	48.95
LYR 15 P= 167-147	-1.35	2.92	36.21	32.57	0.90	50.51
LYR 14 P= 190-167	-1.01	3.15	42.01	30.53	0.73	50.98
LYR 13 P= 215-190	-0.51	3.59	44.13	28.45	0.65	49.02
LYR 12 P= 245-215	0.29	3.69	34.62	26.87	0.78	44.87
LYR 11 P= 278-245	0.97	3.61	24.69	26.39	1.07	38.03
LYR 10 P= 316-278	0.85	3.02	22.54	27.95	1.24	30.19
LYR 9 P= 359-316	0.76	2.43	26.96	31.19	1.16	24.09
LYR 8 P= 408-359	0.72	2.07	36.26	35.05	0.97	18.93
LYR 7 P= 464-408	0.46	1.89	42.56	38.67	0.91	14.38
LYR 6 P= 527-464	0.23	1.60	43.28	41.08	0.95	10.72
LYR 5 P= 599-527	0.16	1.28	44.56	41.45	0.94	9.42
LYR 4 P= 681-599	0.01	1.16	43.59	41.83	0.96	10.09
LYR 3 P= 774-681	-0.03	1.32	43.30	42.70	0.99	9.63
LYR 2 P= 880-774	-0.06	1.35	39.88	43.78	1.10	9.05
LYR 1 P=1000-880	-0.20	1.79	46.09	52.94	1.15	6.68
TSKIN	-0.17	0.35	96.99	93.68	0.97	
STRATOSPHERIC RMS=	3.42 WITH AVG VAR RATIO=				0.87	
TROPOSPHERIC RMS=	2.55 WITH AVG VAR RATIO=				0.97	

INSTMNT 2 PROCESS 4 DATA SET 3
LAT BELT -30- 28 OCEANS ONLY
48 RETRIEVED SNDGS ARE INCLUDED IN THIS TABLE

LAYER	MN ERROR	RMS	TRU VAR	RET VAR	RATIO	RMS HT ERROR (METERS)
LYR 22 P= 25- 16	0.01	1.68	187.08	190.68	1.02	39.21
LYR 21 P= 40- 25	0.24	1.65	136.50	142.33	1.05	34.74
LYR 20 P= 63- 40	0.35	1.39	63.87	67.97	1.07	29.17
LYR 19 P= 100- 63	-0.25	1.64	38.63	33.56	0.87	27.83
LYR 18 P= 114-100	-0.30	1.80	30.88	28.32	0.92	23.09
LYR 17 P= 129-114	0.21	1.53	22.58	19.97	0.89	23.26
LYR 16 P= 147-129	0.18	1.64	16.26	13.66	0.85	23.04
LYR 15 P= 167-147	0.12	1.64	10.11	9.03	0.90	22.85
LYR 14 P= 190-167	0.12	1.33	5.84	6.03	1.04	22.65
LYR 13 P= 215-190	-0.07	1.47	5.93	5.45	0.92	20.83
LYR 12 P= 245-215	0.11	1.37	8.56	5.82	0.69	17.96
LYR 11 P= 278-245	0.26	1.22	9.39	7.21	0.77	14.16
LYR 10 P= 316-278	0.44	1.06	10.25	8.72	0.86	11.33
LYR 9 P= 359-316	0.24	0.79	10.26	9.53	0.93	9.31
LYR 8 P= 408-359	0.03	0.73	10.43	9.90	0.95	8.17
LYR 7 P= 464-408	-0.01	0.72	10.23	9.76	0.96	7.68
LYR 6 P= 527-464	-0.12	0.93	9.69	9.53	0.99	7.69
LYR 5 P= 599-527	-0.15	0.82	8.82	8.69	0.99	8.16
LYR 4 P= 681-599	0.03	0.68	8.42	8.60	1.03	9.01
LYR 3 P= 774-681	-0.23	1.02	11.21	9.16	0.82	9.25
LYR 2 P= 880-774	0.05	1.32	14.22	11.61	0.82	8.62
LYR 1 P=1000-880	-0.04	1.43	14.08	11.96	0.85	5.35
TSKIN	-0.09	0.75	16.37	16.03	0.98	
STRATOSPHERIC RMS=	1.59 WITH AVG VAR RATIO=				1.01	
TROPOSPHERIC RMS=	1.24 WITH AVG VAR RATIO=				0.90	

INSTMNT 2 PROCESS 4 DATA SET 3
LAT BELT -30- 28 CONTINENTS ONLY
48 RETRIEVED SNDGS ARE INCLUDED IN THIS TABLE

LAYER	MN ERROR	RMS	TRU VAR	RET VAR	RATIO	RMS HT ERROR (METERS)
LYR 22 P= 25- 16	0.39	1.74	184.63	194.57	1.06	40.07
LYR 21 P= 40- 25	0.15	1.76	141.32	142.78	1.02	32.22
LYR 20 P= 63- 40	0.34	1.55	64.78	62.74	0.97	27.87
LYR 19 P= 100- 63	0.24	1.91	25.55	17.91	0.71	27.10
LYR 18 P= 114-100	0.08	1.87	15.78	14.17	0.90	24.21
LYR 17 P= 129-114	-0.13	1.44	9.83	10.65	1.09	23.60
LYR 16 P= 147-129	-0.35	1.55	8.09	6.67	0.83	23.18
LYR 15 P= 167-147	-0.23	1.74	5.91	4.29	0.73	21.19
LYR 14 P= 190-167	-0.11	1.47	4.83	3.44	0.72	19.65
LYR 13 P= 215-190	-0.18	1.39	6.95	4.46	0.65	18.17
LYR 12 P= 245-215	-0.16	1.32	9.68	5.67	0.59	15.76
LYR 11 P= 278-245	-0.35	1.28	11.69	7.54	0.65	13.02
LYR 10 P= 316-278	-0.45	1.18	12.21	9.71	0.80	10.92
LYR 9 P= 359-316	-0.25	0.92	11.75	11.73	1.00	9.71
LYR 8 P= 408-359	0.19	0.93	12.32	13.58	1.11	9.44
LYR 7 P= 464-408	0.22	1.07	13.12	14.29	1.09	9.10
LYR 6 P= 527-464	0.09	1.01	12.39	14.15	1.15	9.02
LYR 5 P= 599-527	0.10	0.82	12.76	13.06	1.03	9.01
LYR 4 P= 681-599	0.13	1.14	13.55	13.05	0.97	9.40
LYR 3 P= 774-681	0.18	0.97	15.32	15.08	0.99	10.26
LYR 2 P= 880-774	-0.12	1.27	25.99	22.32	0.86	10.77
LYR 1 P=1000-880	-0.37	2.01	43.30	32.77	0.76	7.51
TSKIN	0.16	0.94	85.42	81.45	0.96	
STRATOSPHERIC RMS=	1.74 WITH AVG VAR RATIO=				0.94	
TROPOSPHERIC RMS=	1.34 WITH AVG VAR RATIO=				0.89	

INSTMNT 2 PROCESS 4 DATA SET 3
LAT BELT -30- 28 BOTH CONTINENT AND OCEAN
96 RETRIEVED SNDGS ARE INCLUDED IN THIS TABLE

LAYER	MN ERROR	RMS	TRU VAR	RET VAR	RATIO	RMS HT ERROR (METERS)
LYR 22 P= 25- 16	0.20	1.71	188.06	194.29	1.04	39.64
LYR 21 P= 40- 25	0.20	1.71	140.40	144.16	1.03	33.50
LYR 20 P= 63- 40	0.34	1.47	64.39	65.42	1.02	28.53
LYR 19 P= 100- 63	-0.01	1.78	32.52	26.55	0.82	27.46
LYR 18 P= 114-100	-0.11	1.84	23.65	21.80	0.93	23.66
LYR 17 P= 129-114	0.04	1.48	16.61	15.53	0.94	23.43
LYR 16 P= 147-129	-0.08	1.60	12.59	10.31	0.82	23.11
LYR 15 P= 167-147	-0.06	1.69	8.22	6.74	0.82	22.03
LYR 14 P= 190-167	0.01	1.40	5.47	4.80	0.88	21.20
LYR 13 P= 215-190	-0.13	1.43	6.54	5.02	0.77	19.55
LYR 12 P= 245-215	-0.03	1.35	9.29	5.82	0.63	16.89
LYR 11 P= 278-245	-0.04	1.25	10.92	7.48	0.69	13.60
LYR 10 P= 316-278	-0.01	1.12	11.90	9.36	0.79	11.13
LYR 9 P= 359-316	-0.00	0.86	11.46	10.81	0.95	9.51
LYR 8 P= 408-359	0.11	0.83	11.52	11.95	1.04	8.83
LYR 7 P= 464-408	0.10	0.91	11.76	12.20	1.04	8.42
LYR 6 P= 527-464	-0.02	0.97	11.09	11.94	1.08	8.38
LYR 5 P= 599-527	-0.03	0.82	10.81	10.93	1.02	8.60
LYR 4 P= 681-599	0.08	0.94	11.03	10.89	0.99	9.21
LYR 3 P= 774-681	-0.02	0.99	13.39	12.44	0.93	9.77
LYR 2 P= 880-774	-0.03	1.30	21.18	17.88	0.85	9.76
LYR 1 P=1000-880	-0.21	1.75	30.32	23.59	0.78	6.52
TSKIN	0.04	0.85	52.30	50.44	0.97	
STRATOSPHERIC RMS=	1.66 WITH AVG VAR RATIO=				0.98	
TROPOSPHERIC RMS=	1.29 WITH AVG VAR RATIO=				0.89	

INSTMNT 2 PROCESS 4 DATA SET 3
LAT BELT 30- 58 OCEANS ONLY
48 RETRIEVED SNDGS ARE INCLUDED IN THIS TABLE

LAYER	MN ERROR	RMS	TRU VAR	RET VAR	RATIO	RMS HT ERROR (METERS)
LYR 22 P= 25- 16	-0.89	2.04	81.08	77.18	0.96	31.93
LYR 21 P= 40- 25	0.08	1.57	79.81	74.22	0.93	34.88
LYR 20 P= 63- 40	0.52	1.58	71.35	59.58	0.84	34.40
LYR 19 P= 100- 63	0.36	2.19	60.24	44.31	0.74	32.20
LYR 18 P= 114-100	-0.22	2.20	46.49	36.12	0.78	33.15
LYR 17 P= 129-114	-0.22	1.53	38.43	36.05	0.94	36.63
LYR 16 P= 147-129	-0.61	1.66	32.07	36.07	1.13	38.69
LYR 15 P= 167-147	-0.85	2.27	30.82	35.27	1.15	38.39
LYR 14 P= 190-167	-0.61	2.80	40.19	35.31	0.88	36.18
LYR 13 P= 215-190	-0.10	3.11	45.90	35.02	0.77	32.03
LYR 12 P= 245-215	0.91	3.17	35.81	29.22	0.82	28.63
LYR 11 P= 278-245	1.08	2.78	20.84	24.75	1.19	27.92
LYR 10 P= 316-278	0.56	2.08	15.78	19.35	1.23	27.56
LYR 9 P= 359-316	0.13	1.65	19.41	19.12	0.99	27.69
LYR 8 P= 408-359	-0.00	1.96	29.66	22.07	0.75	25.45
LYR 7 P= 464-408	-0.34	1.92	36.72	26.18	0.72	20.93
LYR 6 P= 527-464	-0.47	1.64	39.18	29.78	0.77	16.03
LYR 5 P= 599-527	-0.28	1.64	43.13	30.90	0.72	12.28
LYR 4 P= 681-599	0.02	1.54	40.39	31.46	0.78	9.76
LYR 3 P= 774-681	0.38	1.38	36.24	31.67	0.88	9.10
LYR 2 P= 880-774	0.19	1.17	29.40	30.91	1.06	8.14
LYR 1 P=1000-880	-0.13	1.54	22.28	25.40	1.14	5.74
TSKIN	0.26	0.82	30.41	31.32	1.04	
STRATOSPHERIC RMS=	1.86 WITH AVG VAR RATIO=				0.87	
TROPOSPHERIC RMS=	2.08 WITH AVG VAR RATIO=				0.93	

INSTMNT 2 PROCESS 4 DATA SET 3
LAT BELT 30- 58 CONTINENTS ONLY
48 RETRIEVED SNDGS ARE INCLUDED IN THIS TABLE

LAYER	MN ERROR	RMS	TRU VAR	RET VAR	RATIO	RMS HT ERROR (METERS)
LYR 22 P= 25- 16	-0.89	2.95	86.74	65.84	0.76	40.36
LYR 21 P= 40- 25	0.39	2.61	67.92	52.73	0.78	50.96
LYR 20 P= 63- 40	0.65	1.95	54.40	46.32	0.86	46.03
LYR 19 P= 100- 63	0.27	2.47	46.50	46.71	1.01	36.62
LYR 18 P= 114-100	-0.53	2.25	39.25	41.49	1.06	32.97
LYR 17 P= 129-114	-0.64	1.74	36.82	39.61	1.08	35.79
LYR 16 P= 147-129	-0.92	1.83	35.66	39.46	1.11	38.10
LYR 15 P= 167-147	-0.98	2.04	39.85	37.80	0.95	39.93
LYR 14 P= 190-167	-0.59	2.35	42.82	35.46	0.83	40.89
LYR 13 P= 215-190	-0.36	2.87	42.25	32.35	0.77	39.65
LYR 12 P= 245-215	0.43	2.74	33.21	23.02	0.70	36.95
LYR 11 P= 278-245	1.01	2.90	28.05	19.79	0.71	32.82
LYR 10 P= 316-278	0.98	2.61	29.03	19.78	0.69	27.99
LYR 9 P= 359-316	0.92	2.37	34.40	24.38	0.71	23.77
LYR 8 P= 408-359	0.81	2.09	42.80	31.37	0.74	19.39
LYR 7 P= 464-408	0.60	1.87	48.40	37.79	0.79	15.19
LYR 6 P= 527-464	0.32	1.46	47.38	42.74	0.91	12.83
LYR 5 P= 599-527	0.28	1.27	45.98	44.13	0.96	12.30
LYR 4 P= 681-599	-0.09	1.25	46.69	45.32	0.98	12.09
LYR 3 P= 774-681	-0.49	1.33	50.12	47.73	0.96	11.85
LYR 2 P= 880-774	-0.04	1.53	49.91	54.06	1.09	11.86
LYR 1 P=1000-880	-0.22	2.39	63.03	68.15	1.09	8.94
TSKIN	1.14	1.48	129.75	116.17	0.90	
STRATOSPHERIC RMS=	2.52 WITH AVG VAR RATIO=				0.86	
TROPOSPHERIC RMS=	2.11 WITH AVG VAR RATIO=				0.90	

INSTMNT 2 PROCESS 4 DATA SET 3
LAT BELT 30- 58 BOTH CONTINENT AND OCEAN
96 RETRIEVED SNDGS ARE INCLUDED IN THIS TABLE

LAYER	MN ERROR	RMS	TRU VAR	RET VAR	RATIO	RMS HT ERROR (METERS)
LYR 22 P= 25- 16	-0.89	2.54	84.60	72.19	0.86	36.39
LYR 21 P= 40- 25	0.24	2.15	75.82	65.03	0.86	43.67
LYR 20 P= 63- 40	0.58	1.78	65.33	55.20	0.85	40.63
LYR 19 P= 100- 63	0.31	2.33	55.24	47.50	0.86	34.48
LYR 18 P= 114-100	-0.38	2.22	44.09	40.40	0.92	33.06
LYR 17 P= 129-114	-0.43	1.64	38.78	39.49	1.02	36.21
LYR 16 P= 147-129	-0.77	1.74	34.92	39.18	1.13	38.40
LYR 15 P= 167-147	-0.92	2.16	36.21	37.55	1.04	39.17
LYR 14 P= 190-167	-0.60	2.58	42.01	35.88	0.86	38.61
LYR 13 P= 215-190	-0.23	2.99	44.13	33.82	0.77	36.04
LYR 12 P= 245-215	0.67	2.97	34.62	26.12	0.76	33.05
LYR 11 P= 278-245	1.05	2.84	24.69	22.48	0.92	30.47
LYR 10 P= 316-278	0.77	2.36	22.54	19.90	0.89	27.78
LYR 9 P= 359-316	0.52	2.04	26.96	22.13	0.83	25.80
LYR 8 P= 408-359	0.40	2.03	36.26	27.05	0.75	22.63
LYR 7 P= 464-408	0.13	1.90	42.56	32.24	0.76	18.28
LYR 6 P= 527-464	-0.08	1.55	43.28	36.42	0.85	14.52
LYR 5 P= 599-527	0.00	1.46	44.56	37.61	0.85	12.29
LYR 4 P= 681-599	-0.03	1.40	43.59	38.41	0.89	10.99
LYR 3 P= 774-681	-0.05	1.35	43.30	39.71	0.92	10.56
LYR 2 P= 880-774	0.08	1.36	39.88	42.83	1.08	10.17
LYR 1 P=1000-880	-0.18	2.01	46.09	50.39	1.10	7.51
TSKIN	0.70	1.20	96.99	87.23	0.90	
STRATOSPHERIC RMS=	2.21 WITH AVG VAR RATIO=				0.86	
TROPOSPHERIC RMS=	2.10 WITH AVG VAR RATIO=				0.91	

INSTMNT 2 PROCESS 4 DATA SET 4
LAT BELT -30- 28 OCEANS ONLY
56 RETRIEVED SNDGS ARE INCLUDED IN THIS TABLE

LAYER	MN ERROR	RMS	TRU VAR	RET VAR	RATIO	RMS HT ERROR (METERS)
LYR 22 P= 25- 16	0.03	1.65	8.86	7.99	0.91	38.02
LYR 21 P= 40- 25	0.44	1.06	4.28	3.10	0.73	30.16
LYR 20 P= 63- 40	0.04	1.58	7.57	4.43	0.59	24.67
LYR 19 P= 100- 63	-0.12	1.48	12.19	8.97	0.74	25.93
LYR 18 P= 114-100	0.29	2.26	24.77	12.44	0.51	23.53
LYR 17 P= 129-114	0.02	1.53	17.79	13.01	0.74	22.29
LYR 16 P= 147-129	0.14	1.55	10.39	8.98	0.87	20.81
LYR 15 P= 167-147	0.17	1.85	6.53	5.05	0.78	18.44
LYR 14 P= 190-167	0.24	1.56	4.32	2.82	0.66	16.03
LYR 13 P= 215-190	0.21	1.36	5.50	3.41	0.62	14.05
LYR 12 P= 245-215	0.16	1.13	8.44	5.95	0.71	12.23
LYR 11 P= 278-245	0.12	1.09	12.89	10.08	0.79	10.88
LYR 10 P= 316-278	0.17	1.03	16.48	12.98	0.85	9.87
LYR 9 P= 359-316	0.13	0.82	16.99	15.48	0.92	9.08
LYR 8 P= 408-359	-0.00	0.72	15.37	15.71	1.03	8.26
LYR 7 P= 464-408	-0.01	0.66	13.40	13.77	1.03	7.47
LYR 6 P= 527-464	-0.02	0.90	11.33	10.81	0.96	6.60
LYR 5 P= 599-527	0.05	0.90	10.90	9.04	0.83	6.20
LYR 4 P= 681-599	0.08	0.76	11.17	9.25	0.83	7.39
LYR 3 P= 774-681	-0.12	0.95	12.77	11.58	0.91	8.43
LYR 2 P= 880-774	0.06	1.28	13.75	15.16	1.11	8.07
LYR 1 P=1000-880	-0.07	1.31	15.06	17.07	1.14	4.89
TSKIN	-0.44	1.06	26.18	21.39	0.82	
STRATOSPHERIC RMS=	1.45	WITH AVG VAR RATIO=			0.75	
TROPOSPHERIC RMS=	1.27	WITH AVG VAR RATIO=			0.85	

INSTMNT 2 PROCESS 4 DATA SET 4
LAT BELT -30- 28 CONTINENTS ONLY
40 RETRIEVED SNDGS ARE INCLUDED IN THIS TABLE

LAYER	MN ERROR	RMS	TRU VAR	RET VAR	RATIO	RMS HT ERROR (METERS)
LYR 22 P= 25- 16	-0.08	1.64	12.01	10.02	0.84	41.49
LYR 21 P= 40- 25	0.15	1.28	8.69	5.86	0.68	36.82
LYR 20 P= 63- 40	0.16	1.59	13.69	10.53	0.77	30.17
LYR 19 P= 100- 63	0.39	2.03	21.66	17.22	0.80	30.62
LYR 18 P= 114-100	0.10	2.40	22.86	15.17	0.67	26.44
LYR 17 P= 129-114	-0.06	2.34	14.62	9.71	0.67	22.16
LYR 16 P= 147-129	-0.49	1.92	9.49	6.57	0.70	18.07
LYR 15 P= 167-147	-0.30	1.56	7.43	5.42	0.73	17.04
LYR 14 P= 190-167	0.18	1.26	10.25	7.10	0.70	17.51
LYR 13 P= 215-190	0.23	1.35	15.49	11.45	0.74	15.54
LYR 12 P= 245-215	0.28	1.20	19.90	16.25	0.82	13.34
LYR 11 P= 278-245	0.23	1.18	24.94	21.24	0.86	11.53
LYR 10 P= 316-278	0.11	0.94	28.03	24.27	0.87	10.44
LYR 9 P= 359-316	-0.12	0.83	26.26	23.88	0.91	9.70
LYR 8 P= 408-359	-0.12	0.77	23.50	22.42	0.96	8.91
LYR 7 P= 464-408	-0.03	0.80	19.79	18.67	0.95	8.00
LYR 6 P= 527-464	0.08	1.11	15.71	14.36	0.92	7.23
LYR 5 P= 599-527	-0.07	1.01	11.05	12.02	1.09	6.98
LYR 4 P= 681-599	0.20	1.09	13.21	12.02	0.92	7.62
LYR 3 P= 774-681	0.29	1.27	21.78	17.51	0.81	8.57
LYR 2 P= 880-774	-0.18	1.05	29.62	27.86	0.95	9.00
LYR 1 P=1000-880	-0.39	1.71	44.55	42.46	0.96	6.37
TSKIN	-0.15	1.28	89.12	80.40	0.91	
STRATOSPHERIC RMS=	1.65	WITH AVG VAR RATIO=			0.78	
TROPOSPHERIC RMS=	1.40	WITH AVG VAR RATIO=			0.85	

INSTMNT 2 PROCESS 4 DATA SET 4
LAT BELT -30- 28 BOTH CONTINENT AND OCEAN
96 RETRIEVED SNDGS ARE INCLUDED IN THIS TABLE

LAYER	MN ERROR	RMS	TRU VAR	RET VAR	RATIO	RMS HT ERROR (METERS)
LYR 22 P= 25- 16	-0.02	1.64	11.17	9.72	0.88	39.51
LYR 21 P= 40- 25	0.32	1.16	6.94	4.83	0.70	33.10
LYR 20 P= 63- 40	0.09	1.59	10.81	7.77	0.72	27.10
LYR 19 P= 100- 63	0.09	1.73	16.63	13.31	0.81	27.98
LYR 18 P= 114-100	0.21	2.32	24.90	14.34	0.58	24.78
LYR 17 P= 129-114	-0.01	1.91	17.41	12.49	0.72	22.24
LYR 16 P= 147-129	-0.12	1.72	11.34	8.68	0.77	19.72
LYR 15 P= 167-147	-0.02	1.73	7.83	5.74	0.74	17.87
LYR 14 P= 190-167	0.21	1.45	7.20	4.98	0.70	16.66
LYR 13 P= 215-190	0.22	1.35	9.90	7.02	0.71	14.69
LYR 12 P= 245-215	0.21	1.16	13.33	10.40	0.78	12.70
LYR 11 P= 278-245	0.16	1.12	17.97	14.81	0.83	11.15
LYR 10 P= 316-278	0.14	0.99	21.34	18.31	0.86	10.11
LYR 9 P= 359-316	0.03	0.83	20.93	19.00	0.91	9.35
LYR 8 P= 408-359	-0.05	0.74	18.82	18.54	0.99	8.54
LYR 7 P= 464-408	-0.01	0.72	16.13	15.87	0.99	7.69
LYR 6 P= 527-464	0.02	1.00	13.22	12.38	0.94	6.87
LYR 5 P= 599-527	0.00	0.95	11.15	10.42	0.94	6.53
LYR 4 P= 681-599	0.13	0.91	12.18	10.62	0.88	7.49
LYR 3 P= 774-681	0.05	1.10	16.64	14.35	0.87	8.49
LYR 2 P= 880-774	-0.04	1.19	20.81	20.75	1.00	8.47
LYR 1 P=1000-880	-0.20	1.49	28.15	28.19	1.01	5.55
TSKIN	-0.32	1.16	53.40	47.28	0.89	
STRATOSPHERIC RMS=	1.54	WITH AVG VAR RATIO=			0.78	
TROPOSPHERIC RMS=	1.32	WITH AVG VAR RATIO=			0.85	

INSTMNT 2 PROCESS 4 DATA SET 4
LAT BELT 30- 58 OCEANS ONLY
48 RETRIEVED SNDGS ARE INCLUDED IN THIS TABLE

LAYER	MN ERROR	RMS	TRU VAR	RET VAR	RATIO	RMS HT ERROR (METERS)
LYR 22 P= 25- 16	0.05	1.18	7.07	8.15	1.16	26.74
LYR 21 P= 40- 25	0.05	0.94	9.73	8.65	0.89	23.15
LYR 20 P= 63- 40	-0.08	0.79	12.54	12.14	0.97	20.64
LYR 19 P= 100- 63	0.19	1.37	20.26	19.09	0.95	20.40
LYR 18 P= 114-100	0.00	1.70	22.26	20.62	0.93	24.20
LYR 17 P= 129-114	-0.40	1.39	20.35	18.81	0.93	24.73
LYR 16 P= 147-129	-0.43	1.52	20.31	18.30	0.91	24.82
LYR 15 P= 167-147	-0.00	1.76	23.16	18.09	0.79	23.85
LYR 14 P= 190-167	0.99	2.56	28.44	20.27	0.72	21.69
LYR 13 P= 215-190	1.39	3.09	27.05	23.05	0.86	18.53
LYR 12 P= 245-215	0.73	2.24	15.37	13.38	0.88	16.08
LYR 11 P= 278-245	-0.14	1.36	9.48	8.58	0.91	16.78
LYR 10 P= 316-278	-0.36	1.50	10.93	7.92	0.73	16.54
LYR 9 P= 359-316	-0.41	1.41	11.93	9.39	0.79	14.25
LYR 8 P= 408-359	-0.37	1.40	12.52	11.18	0.90	11.51
LYR 7 P= 464-408	-0.28	1.18	13.48	12.80	0.95	9.29
LYR 6 P= 527-464	-0.01	1.02	16.47	14.15	0.86	8.50
LYR 5 P= 599-527	0.06	1.02	17.08	15.64	0.92	8.24
LYR 4 P= 681-599	-0.02	0.95	18.74	18.68	1.00	9.22
LYR 3 P= 774-681	-0.21	0.99	26.97	24.82	0.93	9.63
LYR 2 P= 880-774	0.09	1.37	34.07	31.71	0.94	8.51
LYR 1 P=1000-880	0.54	1.67	21.53	22.20	1.04	6.23
TSKIN	0.47	0.92	19.53	22.23	1.14	

STRATOSPHERIC RMS= 1.09 WITH AVG VAR RATIO= 1.00
TROPOSPHERIC RMS= 1.65 WITH AVG VAR RATIO= 0.89

INSTMNT 2 PROCESS 4 DATA SET 4
LAT BELT 30- 58 CONTINENTS ONLY
48 RETRIEVED SNDGS ARE INCLUDED IN THIS TABLE

LAYER	MN ERROR	RMS	TRU VAR	RET VAR	RATIO	RMS HT ERROR (METERS)
LYR 22 P= 25- 16	-0.16	1.05	11.00	14.42	1.32	32.34
LYR 21 P= 40- 25	-0.16	1.12	13.40	13.94	1.05	32.49
LYR 20 P= 63- 40	0.12	1.03	21.68	18.45	0.86	31.07
LYR 19 P= 100- 63	0.56	1.73	40.18	30.42	0.76	27.54
LYR 18 P= 114-100	0.50	1.70	48.38	40.69	0.85	24.68
LYR 17 P= 129-114	-0.07	1.28	39.56	39.17	1.00	24.76
LYR 16 P= 147-129	-0.46	1.41	33.94	33.61	1.00	24.63
LYR 15 P= 167-147	-0.62	1.78	28.69	25.02	0.88	23.97
LYR 14 P= 190-167	-0.30	2.22	25.28	18.35	0.73	23.73
LYR 13 P= 215-190	0.31	2.33	23.50	19.45	0.83	24.24
LYR 12 P= 245-215	0.94	2.11	19.93	16.99	0.86	23.89
LYR 11 P= 278-245	0.73	1.91	25.63	20.78	0.82	21.85
LYR 10 P= 316-278	0.43	1.60	30.90	22.27	0.73	19.41
LYR 9 P= 359-316	0.00	1.32	29.66	22.81	0.77	15.87
LYR 8 P= 408-359	-0.06	1.08	24.55	23.00	0.94	12.96
LYR 7 P= 464-408	0.09	0.94	21.45	22.69	1.06	11.35
LYR 6 P= 527-464	0.05	0.92	20.55	21.52	1.05	10.72
LYR 5 P= 599-527	-0.03	1.11	20.55	20.00	0.98	10.55
LYR 4 P= 681-599	-0.09	1.09	20.97	19.82	0.95	10.88
LYR 3 P= 774-681	0.11	1.11	25.37	22.13	0.88	11.71
LYR 2 P= 880-774	-0.16	1.27	29.82	24.53	0.83	11.52
LYR 1 P=1000-880	-0.46	2.20	29.22	27.94	0.96	8.22
TSKIN	0.52	0.93	84.69	90.12	1.07	

STRATOSPHERIC RMS= 1.26 WITH AVG VAR RATIO= 1.00
TROPOSPHERIC RMS= 1.58 WITH AVG VAR RATIO= 0.90

INSTMNT 2 PROCESS 4 DATA SET 4
LAT BELT 30- 58 BOTH CONTINENT AND OCEAN
96 RETRIEVED SNDGS ARE INCLUDED IN THIS TABLE

LAYER	MN ERROR	RMS	TRU VAR	RET VAR	RATIO	RMS HT ERROR (METERS)
LYR 22 P= 25- 16	-0.05	1.11	9.44	11.57	1.23	29.67
LYR 21 P= 40- 25	-0.05	1.03	11.99	11.60	0.97	28.21
LYR 20 P= 63- 40	0.02	0.92	17.25	15.52	0.90	26.38
LYR 19 P= 100- 63	0.38	1.56	30.21	24.82	0.83	24.23
LYR 18 P= 114-100	0.25	1.70	35.30	30.70	0.87	24.44
LYR 17 P= 129-114	-0.24	1.34	30.02	29.18	0.98	24.74
LYR 16 P= 147-129	-0.45	1.47	27.46	26.27	0.96	24.73
LYR 15 P= 167-147	-0.31	1.77	27.06	22.13	0.82	23.91
LYR 14 P= 190-167	0.34	2.40	29.56	20.31	0.69	22.73
LYR 13 P= 215-190	0.85	2.74	28.22	22.61	0.81	21.57
LYR 12 P= 245-215	0.83	2.18	18.43	16.16	0.88	20.36
LYR 11 P= 278-245	0.30	1.66	17.65	15.22	0.87	19.48
LYR 10 P= 316-278	0.03	1.55	20.92	15.30	0.74	18.03
LYR 9 P= 359-316	-0.20	1.36	20.79	16.15	0.78	15.08
LYR 8 P= 408-359	-0.22	1.25	18.54	17.10	0.93	12.26
LYR 7 P= 464-408	-0.09	1.07	17.50	17.75	1.02	10.37
LYR 6 P= 527-464	0.02	0.97	18.51	17.84	0.97	9.68
LYR 5 P= 599-527	0.01	1.07	18.82	17.82	0.95	9.47
LYR 4 P= 681-599	-0.06	1.02	19.86	19.25	0.97	10.09
LYR 3 P= 774-681	-0.05	1.05	26.17	23.50	0.90	10.72
LYR 2 P= 880-774	-0.04	1.32	32.40	28.42	0.88	10.13
LYR 1 P=1000-880	0.04	1.95	30.12	27.86	0.93	7.29
TSKIN	0.49	0.93	66.84	71.09	1.07	

STRATOSPHERIC RMS= 1.18 WITH AVG VAR RATIO= 0.99
TROPOSPHERIC RMS= 1.62 WITH AVG VAR RATIO= 0.89

INSTMNT 2 PROCESS 4 DATA SET 3 (+ NOISE)
LAT BELT -30- 28 OCEANS ONLY
48 RETRIEVED SNDGS ARE INCLUDED IN THIS TABLE

LAYER	MN ERROR	RMS	TRU VAR	RET VAR	RATIO	RMS HT ERROR (METERS)
LYR 22 P= 25- 16	-0.87	2.02	81.08	77.62	0.96	43.98
LYR 21 P= 40- 25	-0.08	1.54	79.81	78.27	0.99	37.00
LYR 20 P= 63- 40	0.44	1.58	71.35	62.08	0.88	33.77
LYR 19 P= 100- 63	0.55	1.93	60.24	45.11	0.75	33.46
LYR 18 P= 114-100	-0.12	1.85	46.49	35.90	0.78	39.11
LYR 17 P= 129-114	-0.39	1.48	38.43	34.36	0.90	40.62
LYR 16 P= 147-129	-0.80	1.69	32.07	33.86	1.06	41.01
LYR 15 P= 167-147	-1.05	2.35	30.82	32.67	1.07	39.27
LYR 14 P= 190-167	-0.81	2.93	40.19	32.47	0.81	35.98
LYR 13 P= 215-190	-0.26	3.21	45.90	31.90	0.70	31.27
LYR 12 P= 245-215	0.82	3.17	35.81	27.04	0.76	27.49
LYR 11 P= 278-245	1.04	2.53	20.84	23.18	1.12	26.73
LYR 10 P= 316-278	0.59	1.81	15.78	18.33	1.17	26.80
LYR 9 P= 359-316	0.17	1.41	19.41	18.70	0.97	27.43
LYR 8 P= 408-359	0.01	1.81	29.66	22.40	0.76	25.63
LYR 7 P= 464-408	-0.36	1.88	36.72	27.53	0.75	21.43
LYR 6 P= 527-464	-0.53	1.63	39.18	31.99	0.82	16.74
LYR 5 P= 599-527	-0.36	1.70	43.13	33.03	0.77	13.23
LYR 4 P= 681-599	-0.05	1.58	40.39	32.88	0.82	10.85
LYR 3 P= 774-681	0.33	1.37	36.24	31.91	0.89	10.45
LYR 2 P= 880-774	0.22	1.29	29.40	29.51	1.01	9.34
LYR 1 P=1000-880	-0.01	1.66	22.28	24.68	1.11	6.20
TSKIN	0.40	0.87	30.41	30.55	1.01	
STRATOSPHERIC RMS=	1.77 WITH AVG VAR RATIO=				0.90	
TROPOSPHERIC RMS=	2.05 WITH AVG VAR RATIO=				0.91	

INSTMNT 2 PROCESS 4 DATA SET 3 (+ NOISE)
LAT BELT -30- 28 CONTINENTS ONLY
48 RETRIEVED SNDGS ARE INCLUDED IN THIS TABLE

LAYER	MN ERROR	RMS	TRU VAR	RET VAR	RATIO	RMS HT ERROR (METERS)
LYR 22 P= 25- 16	-0.65	3.15	86.74	64.56	0.75	45.85
LYR 21 P= 40- 25	0.42	1.77	67.92	55.65	0.82	57.83
LYR 20 P= 63- 40	0.74	2.05	54.40	48.21	0.89	60.16
LYR 19 P= 100- 63	0.50	2.57	46.50	41.90	0.91	48.38
LYR 18 P= 114-100	-0.42	1.87	39.25	38.24	0.98	40.34
LYR 17 P= 129-114	-0.73	1.48	36.82	39.11	1.07	40.36
LYR 16 P= 147-129	-1.08	1.76	35.66	39.45	1.11	40.79
LYR 15 P= 167-147	-1.23	2.24	39.85	38.04	0.96	40.20
LYR 14 P= 190-167	-0.94	2.66	42.82	35.57	0.84	39.18
LYR 13 P= 215-190	-0.78	3.10	42.25	32.07	0.76	37.33
LYR 12 P= 245-215	0.01	2.69	33.21	23.26	0.71	35.48
LYR 11 P= 278-245	0.67	2.78	28.05	20.74	0.74	32.97
LYR 10 P= 316-278	0.80	2.56	29.03	21.41	0.74	29.19
LYR 9 P= 359-316	0.84	2.42	34.40	26.33	0.77	25.13
LYR 8 P= 408-359	0.82	2.17	42.80	33.21	0.78	20.35
LYR 7 P= 464-408	0.66	1.91	48.40	39.36	0.82	15.67
LYR 6 P= 527-464	0.40	1.51	47.38	44.02	0.93	13.00
LYR 5 P= 599-527	0.35	1.19	45.98	45.30	0.99	12.63
LYR 4 P= 681-599	-0.05	1.21	46.69	45.68	0.98	12.62
LYR 3 P= 774-681	-0.48	1.32	50.12	47.26	0.95	12.03
LYR 2 P= 880-774	-0.14	1.56	49.91	52.92	1.07	11.56
LYR 1 P=1000-880	-0.38	2.26	63.03	69.07	1.10	8.46
TSKIN	1.19	1.54	129.75	115.45	0.89	
STRATOSPHERIC RMS=	2.44 WITH AVG VAR RATIO=				0.85	
TROPOSPHERIC RMS=	2.11 WITH AVG VAR RATIO=				0.91	

INSTMNT 2 PROCESS 4 DATA SET 3 (+ NOISE)
LAT BELT -30- 28 BOTH CONTINENT AND OCEAN
96 RETRIEVED SNDGS ARE INCLUDED IN THIS TABLE

LAYER	MN ERROR	RMS	TRU VAR	RET VAR	RATIO	RMS HT ERROR (METERS)
LYR 22 P= 25- 16	-0.76	2.64	84.60	71.60	0.85	44.93
LYR 21 P= 40- 25	0.17	1.66	75.82	68.29	0.91	48.55
LYR 20 P= 63- 40	0.59	1.83	65.33	57.15	0.88	48.78
LYR 19 P= 100- 63	0.53	2.27	55.24	45.45	0.83	41.60
LYR 18 P= 114-100	-0.27	1.86	44.09	38.65	0.88	39.73
LYR 17 P= 129-114	-0.56	1.48	38.78	38.30	0.99	40.49
LYR 16 P= 147-129	-0.94	1.73	34.92	38.03	1.09	40.90
LYR 15 P= 167-147	-1.14	2.30	36.21	36.42	1.01	39.74
LYR 14 P= 190-167	-0.88	2.80	42.01	34.63	0.83	37.61
LYR 13 P= 215-190	-0.52	3.16	44.13	32.23	0.74	34.43
LYR 12 P= 245-215	0.41	2.93	34.62	25.14	0.73	31.74
LYR 11 P= 278-245	0.86	2.66	24.69	22.05	0.90	30.01
LYR 10 P= 316-278	0.69	2.22	22.54	20.10	0.90	28.02
LYR 9 P= 359-316	0.51	1.98	26.96	22.83	0.85	26.31
LYR 8 P= 408-359	0.41	2.00	36.26	28.14	0.78	23.15
LYR 7 P= 464-408	0.15	1.89	42.56	33.74	0.80	18.77
LYR 6 P= 527-464	-0.06	1.57	43.28	38.22	0.89	14.99
LYR 5 P= 599-527	-0.01	1.47	44.56	39.31	0.89	12.93
LYR 4 P= 681-599	-0.05	1.40	43.59	39.33	0.91	11.77
LYR 3 P= 774-681	-0.07	1.35	43.30	39.59	0.92	11.27
LYR 2 P= 880-774	0.04	1.43	39.88	41.64	1.05	10.51
LYR 1 P=1000-880	-0.20	1.99	46.09	51.02	1.11	7.42
TSKIN	0.79	1.25	96.99	86.84	0.90	
STRATOSPHERIC RMS=	2.13 WITH AVG VAR RATIO=				0.87	
TROPOSPHERIC RMS=	2.08 WITH AVG VAR RATIO=				0.91	

INSTMNT 2 PROCESS 5 DATA SET 3
LAT BELT -30- 28 OCEANS ONLY
48 RETRIEVED SNDGS ARE INCLUDED IN THIS TABLE

LAYER	MN ERROR	RMS	TRU VAR	RET VAR	RATIO	RMS HT ERROR (METERS)
LYR 22 P= 25- 16	0.83	1.83	187.08	165.57	0.89	40.17
LYR 21 P= 40- 25	0.63	1.70	136.50	131.24	0.97	29.66
LYR 20 P= 63- 40	0.51	1.26	63.87	62.94	0.99	19.84
LYR 19 P= 100- 63	-0.23	1.37	38.63	32.49	0.85	18.21
LYR 18 P= 114-100	-0.57	1.53	30.88	28.41	0.93	18.52
LYR 17 P= 129-114	-0.04	1.40	22.58	19.40	0.86	19.28
LYR 16 P= 14/-129	0.18	1.50	16.26	12.92	0.80	19.26
LYR 15 P= 167-147	0.04	1.59	10.11	7.81	0.78	19.00
LYR 14 P= 190-167	-0.10	1.33	5.84	6.18	1.06	19.01
LYR 13 P= 215-190	-0.13	1.45	5.93	6.61	1.12	17.78
LYR 12 P= 245-215	0.04	1.17	8.56	6.59	0.77	16.10
LYR 11 P= 278-245	0.21	1.10	9.39	7.20	0.77	13.62
LYR 10 P= 316-278	0.39	1.05	10.25	8.13	0.80	10.83
LYR 9 P= 359-316	0.21	0.80	10.26	8.98	0.88	8.15
LYR 8 P= 408-359	0.01	0.78	10.43	9.58	0.92	6.46
LYR 7 P= 464-408	-0.07	0.78	10.23	8.87	0.87	5.32
LYR 6 P= 527-464	-0.23	0.87	9.69	8.36	0.87	3.92
LYR 5 P= 599-527	-0.14	0.82	8.82	7.91	0.90	3.76
LYR 4 P= 681-599	0.20	0.76	8.42	8.26	0.99	4.70
LYR 3 P= 774-681	-0.11	0.87	11.21	9.01	0.81	5.21
LYR 2 P= 880-774	0.03	1.14	14.22	11.39	0.81	5.33
LYR 1 P=1000-880	0.37	1.03	14.08	13.69	0.98	3.82
TSKIN	-0.14	0.28	16.37	16.53	1.01	
STRATOSPHERIC RMS=	1.56 WITH AVG VAR RATIO=				0.93	
TROPOSPHERIC RMS=	1.14 WITH AVG VAR RATIO=				0.89	

INSTMNT 2 PROCESS 5 DATA SET 3
LAT BELT -30- 28 CONTINENTS ONLY
48 RETRIEVED SNDGS ARE INCLUDED IN THIS TABLE

LAYER	MN ERROR	RMS	TRU VAR	RET VAR	RATIO	RMS HT ERROR (METERS)
LYR 22 P= 25- 16	2.18	3.08	184.63	142.12	0.77	38.98
LYR 21 P= 40- 25	-0.18	1.80	141.32	151.60	1.08	24.61
LYR 20 P= 63- 40	-0.17	1.47	64.78	70.96	1.10	20.91
LYR 19 P= 100- 63	-0.07	1.69	25.55	18.49	0.73	22.32
LYR 18 P= 114-100	0.07	1.88	15.78	14.16	0.90	18.05
LYR 17 P= 129-114	0.12	1.26	9.83	9.12	0.93	19.51
LYR 16 P= 147-129	0.04	1.54	8.09	5.92	0.74	19.52
LYR 15 P= 167-147	0.17	1.71	5.91	4.11	0.70	17.94
LYR 14 P= 190-167	0.14	1.36	4.83	3.69	0.77	17.07
LYR 13 P= 215-190	0.13	1.16	6.95	5.20	0.75	16.28
LYR 12 P= 245-215	-0.04	1.04	9.68	6.83	0.71	14.46
LYR 11 P= 278-245	-0.29	1.06	11.69	8.79	0.76	11.86
LYR 10 P= 316-278	-0.43	1.19	12.21	10.70	0.88	9.29
LYR 9 P= 359-316	-0.23	1.02	11.75	12.04	1.03	7.45
LYR 8 P= 408-359	0.14	0.87	12.32	12.97	1.06	7.16
LYR 7 P= 464-408	0.08	0.95	13.12	12.93	0.99	6.46
LYR 6 P= 527-464	-0.15	1.10	12.39	12.21	0.99	5.16
LYR 5 P= 599-527	-0.23	0.87	12.76	10.41	0.82	4.20
LYR 4 P= 681-599	-0.12	1.03	13.55	10.29	0.76	4.77
LYR 3 P= 774-681	0.29	0.90	15.32	13.88	0.91	5.19
LYR 2 P= 880-774	0.39	1.24	25.99	26.77	1.03	6.19
LYR 1 P=1000-880	-0.02	1.14	43.30	39.03	0.91	4.24
TSKIN	-0.07	0.23	85.42	86.60	1.02	
STRATOSPHERIC RMS=	2.10 WITH AVG VAR RATIO=				0.93	
TROPOSPHERIC RMS=	1.21 WITH AVG VAR RATIO=				0.87	

INSTMNT 2 PROCESS 5 DATA SET 3
LAT BELT -30- 28 BOTH CONTINENT AND OCEAN
96 RETRIEVED SNDGS ARE INCLUDED IN THIS TABLE

LAYER	MN ERROR	RMS	TRU VAR	RET VAR	RATIO	RMS HT ERROR (METERS)
LYR 22 P= 25- 16	1.50	2.53	188.06	154.50	0.83	39.58
LYR 21 P= 40- 25	0.22	1.75	140.40	144.07	1.03	27.25
LYR 20 P= 63- 40	0.17	1.37	64.39	67.28	1.05	20.38
LYR 19 P= 100- 63	-0.15	1.54	32.52	26.05	0.81	20.37
LYR 18 P= 114-100	-0.25	1.71	23.65	22.04	0.94	18.28
LYR 17 P= 129-114	0.04	1.34	16.61	14.77	0.89	19.39
LYR 16 P= 147-129	0.11	1.52	12.59	9.75	0.78	19.39
LYR 15 P= 167-147	0.11	1.65	8.22	6.24	0.76	18.48
LYR 14 P= 190-167	0.02	1.34	5.47	5.19	0.95	18.07
LYR 13 P= 215-190	0.00	1.31	6.54	6.10	0.94	17.05
LYR 12 P= 245-215	0.00	1.11	9.29	6.85	0.74	15.30
LYR 11 P= 278-245	-0.04	1.08	10.92	8.13	0.75	12.77
LYR 10 P= 316-278	-0.02	1.12	11.90	9.58	0.81	10.09
LYR 9 P= 359-316	-0.01	0.92	11.46	10.71	0.94	7.80
LYR 8 P= 408-359	0.07	0.83	11.52	11.47	1.00	6.82
LYR 7 P= 464-408	0.00	0.87	11.76	11.03	0.94	5.92
LYR 6 P= 527-464	-0.19	0.99	11.09	10.35	0.94	4.58
LYR 5 P= 599-527	-0.19	0.84	10.81	9.16	0.85	3.99
LYR 4 P= 681-599	0.04	0.90	11.03	9.27	0.85	4.74
LYR 3 P= 774-681	0.09	0.88	13.39	11.76	0.88	5.20
LYR 2 P= 880-774	0.21	1.19	21.18	20.57	0.98	5.78
LYR 1 P=1000-880	0.17	1.08	30.32	27.52	0.91	4.03
TSKIN	-0.11	0.25	52.30	53.05	1.02	
STRATOSPHERIC RMS=	1.85 WITH AVG VAR RATIO=				0.93	
TROPOSPHERIC RMS=	1.18 WITH AVG VAR RATIO=				0.89	

INSTMNT 2 PROCESS 5 DATA SET 3
LAT BELT 30- 58 OCEANS ONLY
48 RETRIEVED SNDGS ARE INCLUDED IN THIS TABLE

LAYER	MN ERROR	RMS	TRU VAR	RET VAR	RATIO	RMS HT ERROR (METERS)
LYR 22 P= 25- 16	-0.34	2.19	81.08	74.40	0.92	41.47
LYR 21 P= 40- 25	-0.53	1.85	79.81	84.52	1.06	27.37
LYR 20 P= 63- 40	0.22	1.31	71.35	71.95	1.01	24.77
LYR 19 P= 100- 63	0.66	1.67	60.24	50.13	0.84	24.29
LYR 18 P= 114-100	0.34	1.61	46.49	39.18	0.85	24.04
LYR 17 P= 129-114	-0.11	1.05	38.43	37.27	0.97	25.69
LYR 16 P= 147-129	-0.49	1.36	32.07	36.19	1.13	26.44
LYR 15 P= 167-147	-0.88	2.06	30.82	36.14	1.18	26.33
LYR 14 P= 190-167	-0.83	2.29	40.19	35.52	0.89	26.67
LYR 13 P= 215-190	-0.47	2.33	45.90	33.51	0.74	27.62
LYR 12 P= 245-215	0.32	2.19	35.81	28.05	0.79	29.16
LYR 11 P= 278-245	0.86	2.50	20.84	20.83	1.00	28.21
LYR 10 P= 316-278	0.68	2.14	15.78	18.16	1.16	23.62
LYR 9 P= 359-316	0.51	1.72	19.41	21.68	1.12	20.04
LYR 8 P= 408-359	0.44	1.73	29.66	26.68	0.90	16.58
LYR 7 P= 464-408	-0.04	1.55	36.72	33.38	0.91	12.56
LYR 6 P= 527-464	-0.21	1.47	39.18	38.77	0.99	8.53
LYR 5 P= 599-527	-0.05	0.97	43.13	40.80	0.95	6.10
LYR 4 P= 681-599	0.28	1.17	40.39	39.21	0.98	6.30
LYR 3 P= 774-681	0.43	1.23	36.24	34.67	0.96	5.28
LYR 2 P= 880-774	-0.11	0.90	29.40	27.97	0.96	5.20
LYR 1 P=1000-880	-0.11	1.12	22.28	23.64	1.07	4.17
TSKIN	-0.18	0.34	30.41	29.46	0.97	
STRATOSPHERIC RMS=	1.78 WITH AVG VAR RATIO=				0.96	
TROPOSPHERIC RMS=	1.70 WITH AVG VAR RATIO=				0.98	

INSTMNT 2 PROCESS 5 DATA SET 3
LAT BELT 30- 58 CONTINENTS ONLY
48 RETRIEVED SNDGS ARE INCLUDED IN THIS TABLE

LAYER	MN ERROR	RMS	TRU VAR	RET VAR	RATIO	RMS HT ERROR (METERS)
LYR 22 P= 25- 16	-0.60	3.46	86.74	57.71	0.67	43.25
LYR 21 P= 40- 25	0.08	1.61	67.92	60.92	0.90	33.52
LYR 20 P= 63- 40	0.18	1.22	54.40	54.46	1.01	32.58
LYR 19 P= 100- 63	0.29	1.21	46.50	49.01	1.06	28.47
LYR 18 P= 114-100	-0.39	1.44	39.25	39.07	1.00	26.31
LYR 17 P= 129-114	-0.63	1.41	36.82	36.34	0.99	27.74
LYR 16 P= 147-129	-0.76	1.63	35.66	33.79	0.95	29.43
LYR 15 P= 167-147	-0.75	1.94	39.65	32.77	0.83	31.96
LYR 14 P= 190-167	-0.27	2.02	42.82	32.58	0.77	34.92
LYR 13 P= 215-190	0.14	2.11	42.25	30.27	0.72	37.24
LYR 12 P= 245-215	0.63	1.82	33.21	26.18	0.79	38.81
LYR 11 P= 278-245	1.12	2.31	28.05	25.02	0.90	37.32
LYR 10 P= 316-278	0.90	2.23	29.03	27.55	0.95	32.81
LYR 9 P= 359-316	0.78	2.11	34.40	31.29	0.91	27.89
LYR 8 P= 408-359	0.78	2.06	42.80	37.28	0.88	22.07
LYR 7 P= 464-408	0.79	1.99	48.40	43.16	0.90	15.42
LYR 6 P= 527-464	0.64	1.66	47.38	48.26	1.02	8.85
LYR 5 P= 599-527	0.49	1.07	45.98	48.26	1.05	4.25
LYR 4 P= 681-599	-0.08	0.73	46.69	47.48	1.02	3.98
LYR 3 P= 774-681	-0.37	0.91	50.12	47.92	0.96	4.61
LYR 2 P= 880-774	0.09	1.37	49.91	50.26	1.01	6.01
LYR 1 P=1000-880	0.12	1.56	63.03	62.88	1.00	5.84
TSKIN	-0.12	0.30	129.75	127.00	0.98	
STRATOSPHERIC RMS=	2.09 WITH AVG VAR RATIO=				0.91	
TROPOSPHERIC RMS=	1.74 WITH AVG VAR RATIO=				0.93	

INSTMNT 2 PROCESS 5 DATA SET 3
LAT BELT 30- 58 BOTH CONTINENT AND OCEAN
96 RETRIEVED SNDGS ARE INCLUDED IN THIS TABLE

LAYER	MN ERROR	RMS	TRU VAR	RET VAR	RATIO	RMS HT ERROR (METERS)
LYR 22 P= 25- 16	-0.47	2.90	84.60	66.98	0.80	42.37
LYR 21 P= 40- 25	-0.23	1.73	75.82	73.94	0.98	30.60
LYR 20 P= 63- 40	0.20	1.27	65.33	65.72	1.01	28.94
LYR 19 P= 100- 63	0.47	1.46	55.24	51.99	0.95	26.46
LYR 18 P= 114-100	-0.03	1.53	44.09	41.30	0.94	25.20
LYR 17 P= 129-114	-0.37	1.24	38.78	38.59	1.00	26.73
LYR 16 P= 147-129	-0.63	1.50	34.92	36.35	1.05	27.97
LYR 15 P= 167-147	-0.81	2.00	36.21	35.22	0.98	29.28
LYR 14 P= 190-167	-0.55	2.16	42.01	34.23	0.82	31.07
LYR 13 P= 215-190	-0.17	2.22	44.13	31.88	0.73	32.79
LYR 12 P= 245-215	0.47	2.02	34.62	27.35	0.80	34.33
LYR 11 P= 278-245	0.99	2.41	24.69	23.32	0.95	33.08
LYR 10 P= 316-278	0.79	2.19	22.54	23.08	1.03	28.59
LYR 9 P= 359-316	0.65	1.93	26.96	26.62	0.99	24.28
LYR 8 P= 408-359	0.61	1.90	36.26	32.10	0.89	19.52
LYR 7 P= 464-408	0.37	1.78	42.56	38.47	0.91	14.06
LYR 6 P= 527-464	0.22	1.57	43.28	43.70	1.01	8.69
LYR 5 P= 599-527	0.22	1.02	44.56	44.62	1.01	5.26
LYR 4 P= 681-599	0.10	0.98	43.59	43.35	1.00	5.27
LYR 3 P= 774-681	0.03	1.08	43.30	41.30	0.96	4.95
LYR 2 P= 880-774	-0.01	1.16	39.88	39.26	0.99	5.62
LYR 1 P=1000-880	0.00	1.36	46.09	46.29	1.01	5.07
TSKIN	-0.15	0.32	96.99	94.92	0.98	
STRATOSPHERIC RMS=	1.94 WITH AVG VAR RATIO=				0.94	
TROPOSPHERIC RMS=	1.72 WITH AVG VAR RATIO=				0.95	

INSTMNT 2 PROCESS 5 DATA SET 4
LAT BELT -30- 28 OCEANS ONLY
56 RETRIEVED SNDGS ARE INCLUDED IN THIS TABLE

LAYER	MN ERROR	RMS	TRU VAR	RET VAR	RATIO	RMS HT ERROR (METERS)
LYR 22 P= 25- 16	-0.22	1.71	8.86	4.60	0.52	23.65
LYR 21 P= 40- 25	0.25	0.75	4.28	3.57	0.84	18.90
LYR 20 P= 63- 40	-0.06	1.32	7.57	5.28	0.70	19.17
LYR 19 P= 100- 63	-0.09	1.86	12.19	11.49	0.95	14.96
LYR 18 P= 114-100	0.15	1.78	24.77	17.88	0.73	16.89
LYR 17 P= 129-114	-0.00	1.41	17.79	13.24	0.75	17.53
LYR 16 P= 14/-129	0.05	1.45	10.39	8.13	0.79	17.27
LYR 15 P= 167-147	-0.05	1.82	6.53	4.11	0.63	15.58
LYR 14 P= 190-167	-0.06	1.49	4.32	2.77	0.65	13.96
LYR 13 P= 215-190	0.05	1.17	5.50	4.42	0.81	13.63
LYR 12 P= 245-215	0.04	0.87	8.44	7.19	0.86	12.99
LYR 11 P= 278-245	0.05	0.97	12.89	10.04	0.78	11.71
LYR 10 P= 316-278	0.09	1.01	16.48	12.34	0.75	9.92
LYR 9 P= 359-316	0.13	0.88	16.99	13.25	0.79	7.97
LYR 8 P= 408-359	0.10	0.80	15.37	13.02	0.85	5.79
LYR 7 P= 464-408	0.09	0.65	13.40	11.93	0.89	4.12
LYR 6 P= 527-464	-0.06	0.77	11.33	10.82	0.96	3.08
LYR 5 P= 599-527	-0.05	0.68	10.90	9.42	0.87	3.54
LYR 4 P= 681-599	0.07	0.61	11.17	9.44	0.85	4.68
LYR 3 P= 774-681	0.11	0.95	12.77	9.84	0.78	5.00
LYR 2 P= 880-774	0.13	1.02	13.75	12.41	0.91	4.83
LYR 1 P=1000-880	-0.02	0.95	15.06	17.17	1.14	3.54
TSKIN	-0.09	0.23	26.18	25.79	0.99	

STRATOSPHERIC RMS= 1.26 WITH AVG VAR RATIO= 0.76
TROPOSPHERIC RMS= 1.13 WITH AVG VAR RATIO= 0.83

INSTMNT 2 PROCESS 5 DATA SET 4
LAT BELT -30- 28 CONTINENTS ONLY
40 RETRIEVED SNDGS ARE INCLUDED IN THIS TABLE

LAYER	MN ERROR	RMS	TRU VAR	RET VAR	RATIO	RMS HT ERROR (METERS)
LYR 22 P= 25- 16	-0.73	2.07	12.01	5.81	0.49	29.62
LYR 21 P= 40- 25	0.21	1.17	8.69	5.68	0.66	16.92
LYR 20 P= 63- 40	-0.07	1.42	13.69	10.11	0.74	17.56
LYR 19 P= 100- 63	0.10	1.20	21.66	17.82	0.83	19.49
LYR 18 P= 114-100	0.10	1.86	22.86	15.67	0.69	21.23
LYR 17 P= 129-114	-0.17	2.04	14.62	9.85	0.68	18.10
LYR 16 P= 147-129	-0.43	1.58	9.49	6.83	0.72	15.90
LYR 15 P= 167-147	-0.35	1.32	7.43	5.90	0.80	16.12
LYR 14 P= 190-167	-0.00	1.09	10.25	8.72	0.86	16.63
LYR 13 P= 215-190	0.10	1.21	15.49	13.25	0.86	14.62
LYR 12 P= 245-215	0.04	1.11	19.90	18.39	0.93	12.21
LYR 11 P= 278-245	0.07	1.13	24.94	23.05	0.93	9.85
LYR 10 P= 316-278	0.04	0.81	28.03	25.95	0.93	8.21
LYR 9 P= 359-316	-0.07	0.73	26.26	24.37	0.93	7.02
LYR 8 P= 408-359	-0.04	0.79	23.50	22.43	0.96	5.88
LYR 7 P= 464-408	-0.02	0.73	19.79	19.41	0.99	4.76
LYR 6 P= 527-464	0.10	0.98	15.71	14.07	0.90	4.39
LYR 5 P= 599-527	0.05	0.79	11.05	10.58	0.96	4.18
LYR 4 P= 681-599	0.36	1.11	13.21	9.84	0.75	4.82
LYR 3 P= 774-681	0.18	1.24	21.78	19.20	0.89	5.71
LYR 2 P= 880-774	-0.23	0.98	29.62	28.84	0.98	7.03
LYR 1 P=1000-880	-0.20	1.40	44.55	40.61	0.92	5.24
TSKIN	0.02	0.23	89.12	91.38	1.03	

STRATOSPHERIC RMS= 1.50 WITH AVG VAR RATIO= 0.68
TROPOSPHERIC RMS= 1.21 WITH AVG VAR RATIO= 0.88

INSTMNT 2 PROCESS 5 DATA SET 4
LAT BELT -30- 28 BOTH CONTINENT AND OCEAN
96 RETRIEVED SNDGS ARE INCLUDED IN THIS TABLE

LAYER	MN ERROR	RMS	TRU VAR	RET VAR	RATIO	RMS HT ERROR (METERS)
LYR 22 P= 25- 16	-0.43	1.87	11.17	5.66	0.51	26.30
LYR 21 P= 40- 25	0.23	0.95	6.94	5.23	0.76	18.10
LYR 20 P= 63- 40	-0.07	1.36	10.81	7.98	0.74	18.52
LYR 19 P= 100- 63	-0.01	1.12	16.63	14.77	0.89	17.00
LYR 18 P= 114-100	0.13	1.82	24.90	17.84	0.72	18.82
LYR 17 P= 129-114	-0.07	1.70	17.41	12.61	0.73	17.77
LYR 16 P= 147-129	-0.15	1.50	11.34	8.42	0.75	16.71
LYR 15 P= 167-147	-0.17	1.63	7.83	5.52	0.71	15.80
LYR 14 P= 190-167	-0.04	1.34	7.20	5.70	0.80	15.13
LYR 13 P= 215-190	0.07	1.19	9.90	8.37	0.85	14.05
LYR 12 P= 245-215	0.04	0.98	13.33	11.98	0.90	12.67
LYR 11 P= 278-245	0.06	1.04	17.97	15.52	0.87	10.97
LYR 10 P= 316-278	0.07	0.93	21.34	18.05	0.85	9.25
LYR 9 P= 359-316	0.05	0.82	20.93	17.92	0.86	7.58
LYR 8 P= 408-359	0.04	0.79	18.82	16.97	0.91	5.83
LYR 7 P= 464-408	0.04	0.68	16.13	15.09	0.94	4.40
LYR 6 P= 527-464	0.01	0.87	13.22	12.28	0.93	3.68
LYR 5 P= 599-527	-0.01	0.73	11.15	10.14	0.91	3.82
LYR 4 P= 681-599	0.19	0.85	12.18	9.90	0.82	4.74
LYR 3 P= 774-681	0.14	1.08	16.64	13.89	0.84	5.31
LYR 2 P= 880-774	-0.02	1.01	20.81	19.49	0.94	5.85
LYR 1 P=1000-880	-0.09	1.16	28.15	27.58	0.98	4.33
TSKIN	-0.05	0.23	53.40	54.22	1.02	

STRATOSPHERIC RMS= 1.36 WITH AVG VAR RATIO= 0.73
TROPOSPHERIC RMS= 1.16 WITH AVG VAR RATIO= 0.86

INSTMNT 2 PROCESS 5 DATA SET 4
LAT BELT 30- 58 OCEANS ONLY
48 RETRIEVED SNDGS ARE INCLUDED IN THIS TABLE

LAYER	MN ERROR	RMS	TRU VAR	RET VAR	RATIO	RMS HT ERROR (METERS)
LYR 22 P= 25- 16	-0.04	1.02	7.07	6.05	0.86	24.55
LYR 21 P= 40- 25	-0.18	0.96	9.73	7.55	0.78	18.68
LYR 20 P= 63- 40	-0.08	0.60	12.54	11.85	0.95	15.73
LYR 19 P= 100- 63	0.29	1.14	20.26	18.53	0.92	14.95
LYR 18 P= 114-100	-0.09	1.29	22.26	19.75	0.89	19.12
LYR 17 P= 129-114	-0.31	1.19	20.35	19.56	0.97	20.73
LYR 16 P= 147-129	-0.48	1.54	20.31	19.75	0.98	21.42
LYR 15 P= 167-147	-0.27	1.88	23.16	19.81	0.86	21.15
LYR 14 P= 190-167	0.43	2.43	28.44	21.01	0.74	20.24
LYR 13 P= 215-190	1.06	2.82	27.05	19.16	0.71	17.83
LYR 12 P= 245-215	0.48	2.01	15.37	11.00	0.72	13.78
LYR 11 P= 278-245	-0.02	1.22	9.48	7.72	0.82	12.97
LYR 10 P= 316-278	-0.17	1.37	10.93	8.67	0.80	12.35
LYR 9 P= 359-316	-0.03	1.21	11.93	10.33	0.87	10.01
LYR 8 P= 408-359	0.04	1.17	12.52	11.86	0.95	7.39
LYR 7 P= 464-408	0.10	0.92	13.48	13.33	0.99	5.88
LYR 6 P= 527-464	0.28	0.91	16.47	14.63	0.89	5.62
LYR 5 P= 599-527	0.25	0.93	17.08	15.94	0.94	4.52
LYR 4 P= 681-599	0.12	0.73	18.74	18.53	0.99	5.00
LYR 3 P= 774-681	-0.00	0.89	26.97	23.43	0.87	5.62
LYR 2 P= 880-774	0.05	1.14	34.07	30.07	0.89	5.70
LYR 1 P=1000-880	0.28	1.28	21.53	22.31	1.04	4.79
TSKIN	-0.20	0.35	19.53	18.95	0.98	
STRATOSPHERIC RMS=	0.95	WITH AVG VAR RATIO=			0.88	
TROPOSPHERIC RMS=	1.48	WITH AVG VAR RATIO=			0.89	

INSTMNT 2 PROCESS 5 DATA SET 4
LAT BELT 30- 58 CONTINENTS ONLY
48 RETRIEVED SNDGS ARE INCLUDED IN THIS TABLE

LAYER	MN ERROR	RMS	TRU VAR	RET VAR	RATIO	RMS HT ERROR (METERS)
LYR 22 P= 25- 16	-0.07	1.00	11.00	8.80	0.80	26.44
LYR 21 P= 40- 25	0.05	1.01	13.40	12.09	0.91	22.67
LYR 20 P= 63- 40	0.09	0.81	21.68	18.98	0.88	21.80
LYR 19 P= 100- 63	0.15	1.18	40.18	35.43	0.89	20.56
LYR 18 P= 114-100	0.11	1.36	48.38	48.68	1.01	19.61
LYR 17 P= 129-114	-0.21	1.35	39.56	43.19	1.10	18.74
LYR 16 P= 147-129	-0.51	1.46	33.94	34.12	1.01	18.72
LYR 15 P= 167-147	-0.65	1.67	28.69	24.84	0.87	19.36
LYR 14 P= 190-167	-0.34	1.96	25.28	17.93	0.71	20.72
LYR 13 P= 215-190	0.17	2.11	23.50	16.27	0.70	21.40
LYR 12 P= 245-215	0.62	1.86	19.93	17.69	0.89	20.83
LYR 11 P= 278-245	0.77	1.87	25.63	22.79	0.89	17.83
LYR 10 P= 316-278	0.60	1.52	30.90	25.35	0.83	14.20
LYR 9 P= 359-316	0.22	1.09	29.66	25.52	0.87	10.69
LYR 8 P= 408-359	0.13	0.97	24.55	25.62	1.05	8.72
LYR 7 P= 464-408	0.35	0.78	21.45	24.69	1.16	6.70
LYR 6 P= 527-464	0.29	0.76	20.55	22.94	1.12	5.08
LYR 5 P= 599-527	0.14	0.68	20.55	20.32	0.99	4.60
LYR 4 P= 681-599	-0.02	0.89	20.97	19.97	0.96	5.07
LYR 3 P= 774-681	0.17	0.86	25.37	23.10	0.92	6.11
LYR 2 P= 880-774	0.13	1.11	29.82	25.46	0.86	6.87
LYR 1 P=1000-880	0.02	1.35	29.22	27.74	0.95	5.04
TSKIN	-0.10	0.27	84.69	84.69	1.01	
STRATOSPHERIC RMS=	1.00	WITH AVG VAR RATIO=			0.87	
TROPOSPHERIC RMS=	1.39	WITH AVG VAR RATIO=			0.94	

INSTMNT 2 PROCESS 5 DATA SET 4
LAT BELT 30- 58 BOTH CONTINENT AND OCEAN
96 RETRIEVED SNDGS ARE INCLUDED IN THIS TABLE

LAYER	MN ERROR	RMS	TRU VAR	RET VAR	RATIO	RMS HT ERROR (METERS)
LYR 22 P= 25- 16	-0.05	1.11	9.44	7.81	0.83	25.51
LYR 21 P= 40- 25	-0.06	0.98	11.99	10.40	0.87	20.77
LYR 20 P= 63- 40	0.00	0.71	17.25	15.64	0.91	19.01
LYR 19 P= 100- 63	0.22	1.06	30.21	26.96	0.90	17.97
LYR 18 P= 114-100	0.01	1.32	35.30	34.21	0.97	19.37
LYR 17 P= 129-114	-0.26	1.27	30.02	31.47	1.05	19.76
LYR 16 P= 147-129	-0.49	1.50	27.46	27.25	1.00	20.11
LYR 15 P= 167-147	-0.46	1.78	27.06	23.09	0.86	20.27
LYR 14 P= 190-167	0.05	2.21	29.56	21.06	0.72	20.48
LYR 13 P= 215-190	0.61	2.49	28.22	19.32	0.69	19.70
LYR 12 P= 245-215	0.55	1.94	18.43	15.26	0.83	17.66
LYR 11 P= 278-245	0.37	1.58	17.65	15.74	0.90	15.59
LYR 10 P= 316-278	0.22	1.45	20.92	17.20	0.83	13.31
LYR 9 P= 359-316	0.10	1.25	20.79	17.95	0.87	10.36
LYR 8 P= 408-359	0.09	1.07	18.54	18.74	1.02	8.09
LYR 7 P= 464-408	0.23	0.85	17.50	19.01	1.09	6.30
LYR 6 P= 527-464	0.29	0.84	18.51	18.78	1.02	5.36
LYR 5 P= 599-527	0.20	0.82	18.82	18.13	0.97	4.56
LYR 4 P= 681-599	0.05	0.82	19.86	19.25	0.97	5.03
LYR 3 P= 774-681	0.08	0.88	26.17	23.27	0.89	5.87
LYR 2 P= 880-774	0.09	1.13	32.40	28.28	0.88	6.31
LYR 1 P=1000-880	0.15	1.32	30.12	29.21	0.97	4.92
TSKIN	-0.15	0.31	66.84	66.94	1.01	
STRATOSPHERIC RMS=	0.98	WITH AVG VAR RATIO=			0.88	
TROPOSPHERIC RMS=	1.43	WITH AVG VAR RATIO=			0.92	

INSTMNT 2 PROCESS 5 DATA SET 3 (+ NOISE)
LAT BELT -30- 28 OCEANS ONLY
48 RETRIEVED SNDGS ARE INCLUDED IN THIS TABLE

LAYER	MN ERROR	RMS	TRU VAR	RET VAR	RATIO	RMS HT ERROR (METERS)
LYR 22 P= 25- 16	-0.37	2.33	81.08	74.41	0.92	53.40
LYR 21 P= 40- 25	-0.55	1.92	79.81	82.76	1.04	35.97
LYR 20 P= 63- 40	0.19	1.63	71.35	70.14	0.99	27.37
LYR 19 P= 100- 63	0.56	1.81	60.24	48.68	0.81	28.68
LYR 18 P= 114-100	-0.00	1.73	46.49	37.51	0.81	36.07
LYR 17 P= 129-114	-0.49	1.37	38.43	35.28	0.92	37.48
LYR 16 P= 147-129	-0.95	1.65	32.07	34.44	1.08	37.51
LYR 15 P= 167-147	-1.32	2.42	30.82	34.44	1.12	36.08
LYR 14 P= 190-167	-1.14	2.84	40.19	33.89	0.85	34.26
LYR 13 P= 215-190	-0.54	2.97	45.90	32.74	0.72	32.33
LYR 12 P= 245-215	0.49	3.01	35.81	29.55	0.83	30.63
LYR 11 P= 278-245	1.10	2.71	20.84	22.52	1.09	27.26
LYR 10 P= 316-278	0.91	2.07	15.78	18.37	1.17	22.77
LYR 9 P= 359-316	0.67	1.52	19.41	20.67	1.07	20.06
LYR 8 P= 408-359	0.54	1.63	29.66	25.56	0.87	17.59
LYR 7 P= 464-408	-0.01	1.61	36.72	32.31	0.88	14.32
LYR 6 P= 527-464	-0.23	1.48	39.18	38.06	0.98	10.77
LYR 5 P= 599-527	-0.11	1.04	43.13	41.00	0.96	8.90
LYR 4 P= 681-599	0.20	1.19	40.39	39.71	0.99	9.33
LYR 3 P= 774-681	0.38	1.29	36.24	35.39	0.98	8.25
LYR 2 P= 880-774	0.02	1.06	29.40	28.31	0.97	6.45
LYR 1 P=1000-880	0.09	1.25	22.28	24.67	1.11	4.68
TSKIN	-0.16	0.33	30.41	29.47	0.97	
STRATOSPHERIC RMS=	1.93	WITH AVG VAR RATIO=			0.95	
TROPOSPHERIC RMS=	1.93	WITH AVG VAR RATIO=			0.97	

INSTMNT 2 PROCESS 5 DATA SET 3 (+ NOISE)
LAT BELT -30- 28 CONTINENTS ONLY
48 RETRIEVED SNDGS ARE INCLUDED IN THIS TABLE

LAYER	MN ERROR	RMS	TRU VAR	RET VAR	RATIO	RMS HT ERROR (METERS)
LYR 22 P= 25- 16	-0.60	3.80	86.74	56.14	0.65	52.87
LYR 21 P= 40- 25	0.32	1.71	67.92	60.66	0.90	42.89
LYR 20 P= 63- 40	0.32	1.40	54.40	53.33	0.99	43.28
LYR 19 P= 100- 63	0.16	1.57	46.50	46.41	1.00	37.76
LYR 18 P= 114-100	-0.74	1.73	39.25	39.91	1.02	35.49
LYR 17 P= 129-114	-0.97	1.60	36.82	38.08	1.04	36.92
LYR 16 P= 147-129	-1.10	1.73	35.66	35.41	1.00	39.04
LYR 15 P= 167-147	-1.06	2.11	39.85	33.96	0.86	41.42
LYR 14 P= 190-167	-0.52	2.35	42.82	34.02	0.80	43.74
LYR 13 P= 215-190	-0.08	2.61	42.25	31.13	0.74	44.78
LYR 12 P= 245-215	0.44	2.18	33.21	27.78	0.84	45.06
LYR 11 P= 278-245	0.99	2.55	28.05	27.36	0.98	42.72
LYR 10 P= 316-278	0.87	2.57	29.03	28.99	1.00	37.36
LYR 9 P= 359-316	0.85	2.48	34.40	30.65	0.90	31.48
LYR 8 P= 408-359	0.87	2.35	42.80	35.18	0.83	24.96
LYR 7 P= 464-408	0.84	2.12	48.40	40.08	0.83	17.67
LYR 6 P= 527-464	0.69	1.73	47.38	43.83	0.93	11.16
LYR 5 P= 599-527	0.55	1.14	45.98	44.87	0.98	7.39
LYR 4 P= 681-599	-0.02	0.81	46.69	45.90	0.99	7.52
LYR 3 P= 774-681	-0.31	0.87	50.12	49.05	0.98	8.58
LYR 2 P= 880-774	0.13	1.61	49.91	55.12	1.11	9.35
LYR 1 P=1000-880	0.14	1.80	63.03	69.86	1.11	6.72
TSKIN	-0.12	0.30	129.75	126.53	0.98	
STRATOSPHERIC RMS=	2.33	WITH AVG VAR RATIO=			0.89	
TROPOSPHERIC RMS=	1.98	WITH AVG VAR RATIO=			0.95	

INSTMNT 2 PROCESS 5 DATA SET 3 (+ NOISE)
LAT BELT -30- 28 BOTH CONTINENT AND OCEAN
96 RETRIEVED SNDGS ARE INCLUDED IN THIS TABLE

LAYER	MN ERROR	RMS	TRU VAR	RET VAR	RATIO	RMS HT ERROR (METERS)
LYR 22 P= 25- 16	-0.49	3.15	84.60	66.17	0.79	53.14
LYR 21 P= 40- 25	-0.12	1.81	75.82	72.64	0.96	39.58
LYR 20 P= 63- 40	0.26	1.52	65.33	63.99	0.98	36.21
LYR 19 P= 100- 63	0.36	1.69	55.24	50.00	0.91	33.53
LYR 18 P= 114-100	-0.37	1.73	44.09	40.89	0.93	35.78
LYR 17 P= 129-114	-0.73	1.49	38.78	38.41	1.00	37.20
LYR 16 P= 147-129	-1.02	1.69	34.92	36.14	1.04	38.28
LYR 15 P= 167-147	-1.19	2.27	36.21	34.85	0.97	38.85
LYR 14 P= 190-167	-0.83	2.61	42.01	34.11	0.82	39.29
LYR 13 P= 215-190	-0.31	2.79	44.13	31.93	0.73	39.06
LYR 12 P= 245-215	0.46	2.63	34.62	28.75	0.84	38.52
LYR 11 P= 278-245	1.05	2.63	24.69	25.14	1.02	35.83
LYR 10 P= 316-278	0.89	2.33	22.54	23.81	1.06	30.94
LYR 9 P= 359-316	0.76	2.06	26.96	25.76	0.96	26.40
LYR 8 P= 408-359	0.70	2.02	36.26	30.48	0.85	21.59
LYR 7 P= 464-408	0.42	1.88	42.56	36.40	0.86	16.08
LYR 6 P= 527-464	0.23	1.61	43.28	41.16	0.96	10.97
LYR 5 P= 599-527	0.22	1.09	44.56	43.06	0.97	8.18
LYR 4 P= 681-599	0.09	1.02	43.59	42.81	0.99	8.47
LYR 3 P= 774-681	0.03	1.10	43.30	42.22	0.98	8.42
LYR 2 P= 880-774	0.08	1.37	39.88	41.89	1.06	8.03
LYR 1 P=1000-880	0.12	1.55	46.09	50.62	1.10	5.79
TSKIN	-0.14	0.31	96.99	94.76	0.98	
STRATOSPHERIC RMS=	2.14	WITH AVG VAR RATIO=			0.92	
TROPOSPHERIC RMS=	1.96	WITH AVG VAR RATIO=			0.96	

INSTMNT 1 PROCESS 4 DATA SET 5

LAT BELT 30-58 BOTH CONTINENT AND OCEAN

36 RETRIEVED SNDGS ARE INCLUDED IN THIS TABLE

LAYER	MN ERROR	RMS	TRU VAR	RET VAR	RATIO	RMS HT ERROR (METERS)
LYR 22 P= 25- 16	-1.65	3.91	73.53	73.61	1.01	77.10
LYR 21 P= 40- 25	0.06	3.07	88.56	74.96	0.85	53.70
LYR 20 P= 63- 40	1.05	2.39	76.25	64.77	0.85	47.82
LYR 19 P= 100- 63	0.87	3.44	58.51	50.51	0.87	47.67
LYR 18 P= 114-100	0.09	2.77	42.47	39.63	0.94	53.74
LYR 17 P= 129-114	0.18	2.59	38.06	38.90	1.03	56.51
LYR 16 P= 147-129	-0.22	2.85	38.12	38.26	1.01	55.44
LYR 15 P= 167-147	-0.48	3.50	42.74	35.89	0.84	51.98
LYR 14 P= 190-167	-0.39	4.28	51.69	32.50	0.63	46.52
LYR 13 P= 215-190	-0.19	4.90	59.31	27.67	0.47	40.10
LYR 12 P= 245-215	0.30	3.97	49.11	17.93	0.37	37.56
LYR 11 P= 278-245	0.84	2.95	25.37	15.84	0.63	39.93
LYR 10 P= 316-278	0.39	2.59	18.51	19.12	1.04	38.50
LYR 9 P= 359-316	-0.01	2.46	21.67	26.09	1.21	34.82
LYR 8 P= 408-359	-0.17	2.34	28.50	33.31	1.17	30.28
LYR 7 P= 464-408	-0.50	2.24	34.11	38.52	1.13	25.71
LYR 6 P= 527-464	-0.84	2.05	35.84	40.23	1.13	21.01
LYR 5 P= 599-527	-0.66	1.59	36.15	38.01	1.06	17.06
LYR 4 P= 681-599	-0.68	1.44	33.30	34.47	1.04	14.48
LYR 3 P= 774-681	-0.72	1.25	30.87	32.25	1.05	12.66
LYR 2 P= 880-774	0.00	1.58	30.67	33.63	1.10	10.94
LYR 1 P=1000-880	-0.64	1.89	37.37	38.58	1.04	7.07
TSKIN	0.35	1.76	62.01	80.91	1.31	

STRATOSPHERIC RMS= 3.24 WITH AVG VAR RATIO= 0.90
TROPOSPHERIC RMS= 2.80 WITH AVG VAR RATIO= 0.94

INSTMNT 1 PROCESS 5 DATA SET 5

LAT BELT 30-58 BOTH CONTINENT AND OCEAN

40 RETRIEVED SNDGS ARE INCLUDED IN THIS TABLE

LAYER	MN ERROR	RMS	TRU VAR	RET VAR	RATIO	RMS HT ERROR (METERS)
LYR 22 P= 25- 16	0.30	3.14	75.62	69.84	0.93	74.43
LYR 21 P= 40- 25	1.17	2.84	85.14	64.08	0.76	68.19
LYR 20 P= 63- 40	1.57	3.01	74.68	56.29	0.76	48.89
LYR 19 P= 100- 63	0.92	3.17	55.17	45.78	0.83	29.14
LYR 18 P= 114-100	-0.30	2.55	38.10	40.60	1.07	33.32
LYR 17 P= 129-114	-0.79	1.84	34.50	39.34	1.15	36.80
LYR 16 P= 147-129	-1.18	2.12	35.48	37.62	1.07	37.80
LYR 15 P= 167-147	-1.66	2.80	41.35	36.94	0.90	36.47
LYR 14 P= 190-167	-1.91	3.58	51.58	36.74	0.72	33.07
LYR 13 P= 215-190	-1.74	4.06	60.30	33.08	0.55	28.45
LYR 12 P= 245-215	-0.98	3.36	49.66	26.12	0.53	26.79
LYR 11 P= 278-245	0.34	2.70	25.99	20.52	0.79	28.55
LYR 10 P= 316-278	0.69	2.37	17.82	18.35	1.03	25.27
LYR 9 P= 359-316	0.94	2.19	20.15	19.99	1.00	21.54
LYR 8 P= 408-359	1.19	2.14	26.38	23.96	0.91	18.21
LYR 7 P= 464-408	1.07	1.78	31.73	28.42	0.90	15.92
LYR 6 P= 527-464	0.77	1.42	33.79	31.40	0.93	15.11
LYR 5 P= 599-527	0.53	1.26	34.81	32.39	0.94	15.29
LYR 4 P= 681-599	0.00	1.10	32.75	32.83	1.01	15.44
LYR 3 P= 774-681	-0.61	1.32	31.01	34.47	1.12	14.29
LYR 2 P= 880-774	-0.66	1.64	33.78	36.20	1.08	11.30
LYR 1 P=1000-880	-0.78	1.87	43.65	45.49	1.05	7.00
TSKIN	-0.66	1.06	71.09	70.27	0.99	

STRATOSPHERIC RMS= 3.03 WITH AVG VAR RATIO= 0.82
TROPOSPHERIC RMS= 2.36 WITH AVG VAR RATIO= 0.94

INSTMNT 2 PROCESS 4 DATA SET 5

LAT BELT 30-58 BOTH CONTINENT AND OCEAN

36 RETRIEVED SNDGS ARE INCLUDED IN THIS TABLE

LAYER	MN ERROR	RMS	TRU VAR	RET VAR	RATIO	RMS HT ERROR (METERS)
LYR 22 P= 25- 16	-1.02	1.57	73.52	67.80	0.93	35.62
LYR 21 P= 40- 25	1.06	1.94	88.58	73.46	0.83	40.45
LYR 20 P= 63- 40	1.14	1.97	76.40	64.48	0.85	31.56
LYR 19 P= 100- 63	1.08	2.29	58.68	47.95	0.82	29.33
LYR 18 P= 114-100	-0.14	2.06	42.22	40.43	0.96	31.46
LYR 17 P= 129-114	-0.46	1.61	37.79	43.80	1.16	33.67
LYR 16 P= 147-129	-0.84	1.99	37.97	44.38	1.18	34.92
LYR 15 P= 167-147	-1.10	2.35	42.88	43.73	1.02	34.27
LYR 14 P= 190-167	-1.06	2.70	52.14	42.51	0.82	32.12
LYR 13 P= 215-190	-0.84	3.04	60.06	40.35	0.68	28.75
LYR 12 P= 245-215	-0.04	2.61	49.20	29.95	0.61	26.25
LYR 11 P= 278-245	0.85	2.54	25.41	23.38	0.93	25.79
LYR 10 P= 316-278	0.66	2.28	18.44	18.40	1.00	21.71
LYR 9 P= 359-316	0.53	1.97	21.62	19.22	0.89	18.64
LYR 8 P= 408-359	0.51	1.78	28.54	23.07	0.81	16.88
LYR 7 P= 464-408	0.27	1.44	34.15	27.28	0.80	15.99
LYR 6 P= 527-464	-0.04	1.26	35.90	30.10	0.84	15.12
LYR 5 P= 599-527	0.00	1.10	36.20	31.05	0.86	13.98
LYR 4 P= 681-599	-0.27	1.08	33.51	31.61	0.95	12.72
LYR 3 P= 774-681	-0.62	1.27	31.17	32.86	1.06	11.25
LYR 2 P= 880-774	-0.10	1.45	30.89	36.82	1.20	8.68
LYR 1 P=1000-880	-0.66	1.56	37.36	42.06	1.13	5.82
TSKIN	0.97	1.82	62.11	81.01	1.31	

STRATOSPHERIC RMS= 1.95 WITH AVG VAR RATIO= 0.86
TROPOSPHERIC RMS= 1.97 WITH AVG VAR RATIO= 0.94

INSTMNT 2 PROCESS 5 DATA SET 5

LAT BELT 30-58 BOTH CONTINENT AND OCEAN

40 RETRIEVED SNDGS ARE INCLUDED IN THIS TABLE

LAYER	MN ERROR	RMS	TRU VAR	RET VAR	RATIO	RMS HT ERROR (METERS)
LYR 22 P= 25- 16	-0.18	2.04	75.73	68.05	0.90	45.39
LYR 21 P= 40- 25	-0.10	2.20	85.12	74.98	0.89	35.30
LYR 20 P= 63- 40	0.37	1.43	74.41	68.51	0.93	25.64
LYR 19 P= 100- 63	0.32	1.50	54.75	52.80	0.97	24.91
LYR 18 P= 114-100	-0.29	1.77	38.20	41.01	1.08	21.27
LYR 17 P= 129-114	-0.57	1.17	34.82	37.67	1.09	23.02
LYR 16 P= 147-129	-0.68	1.59	35.68	35.33	1.00	23.82
LYR 15 P= 167-147	-0.75	2.06	41.22	35.06	0.86	23.67
LYR 14 P= 190-167	-0.62	2.42	51.40	36.33	0.71	24.19
LYR 13 P= 215-190	-0.42	2.62	60.11	37.16	0.62	26.46
LYR 12 P= 245-215	0.02	2.05	49.20	35.65	0.73	30.01
LYR 11 P= 278-245	0.85	2.36	25.95	29.93	1.16	31.43
LYR 10 P= 316-278	0.80	2.18	17.97	24.53	1.37	26.10
LYR 9 P= 359-316	0.78	1.85	20.13	23.20	1.16	20.77
LYR 8 P= 408-359	0.83	1.68	25.86	25.29	0.98	16.26
LYR 7 P= 464-408	0.64	1.42	31.14	29.15	0.94	12.40
LYR 6 P= 527-464	0.37	1.20	33.23	32.20	0.97	9.93
LYR 5 P= 599-527	0.35	0.99	34.13	33.02	0.97	9.22
LYR 4 P= 681-599	0.10	0.82	31.79	33.01	1.04	7.86
LYR 3 P= 774-681	-0.26	1.01	30.46	33.13	1.09	6.38
LYR 2 P= 880-774	0.11	0.95	32.82	34.35	1.05	4.99
LYR 1 P=1000-880	0.01	1.28	42.82	43.54	1.02	4.77
TSKIN	-0.17	0.73	71.21	69.36	0.98	

STRATOSPHERIC RMS= 1.82 WITH AVG VAR RATIO= 0.93
TROPOSPHERIC RMS= 1.72 WITH AVG VAR RATIO= 1.00

☆U.S. Government Printing Office : 1989 - 242-312/04016

(Continued from inside front cover)

NESDIS 16 Temporal and Spatial Analyses of Civil Marine Satellite Requirements. Nancy J. Hooper and John W. Sherman III, February 1985. (PB86 212123/AS)

NESDIS 17 reserved

NESDIS 18 Earth Observations and the Polar Platform. John H. McElroy and Stanley R. Schneider, January 1985. (PB85 177624/AS)

NESDIS 19 The Space Station Polar Platform: Intergrating Research and Operational Missions. John H. McElroy and Stanley R. Schneider, January 1985. (PB85 195279/AS)

NESDIS 20 An Atlas of High Altitude Aircraft Measured Radiance of White Sands, New Mexico, in the 450-1050nm Band. Gilbert R. Smith, Robert H. Levin and John S. Knoll, April 1985. (PB85 204501/AS)

NESDIS 21 High Altitude Measured Radiance of White Sands, New Mexico, in the 400-2000nm Band Using a Filter Wedge Spectrometer. Gilbert R. Smith and Robert H. Levin, April 1985. (PB85 206084/AS)

NESDIS 22 The Space Station Polar Platform: NOAA Systems Considerations and Requirements. John H. McElroy and Stanley R. Schneider, June 1985. (PB86 6109246/AS)

NESDIS 23 The Use of TOMS Data in Evaluating and Improving the Total Ozone from TOVS Measurements. James H. Lienesch and Prabhat K.K. Pandey, July 1985. (PB86 108412/AS)

NESDIS 24 Satellite-Derived Moisture Profiles. Andrew Timchalk, April 1986. (PB86 232923/AS)

NESDIS 25 reserved

NESDIS 26 Monthly and Seasonal Mean Outgoing Longwave Radiation and Anomalies. Arnold Gruber, Marylin Varnadore, Phillip A. Arkin, and Jay S. Winston, October 1987. (PB87160545/AS)

NESDIS 27 Estimation of Broadband Planetary Albedo from Operational Narrowband Satellite Measurements. James Wydick, April 1987. (PB88-107644/AS)

NESDIS 28 The AVHRR/HIRS Operational Method for Satellite Based Sea Surface Temperature Determination. Charles Walton, March 1987. (PB88-107594/AS)

NESDIS 29 The Complementary Roles of Microwave and Infrared Instruments in Atmospheric Sounding. Larry McMillin, February 1987. (PB87 184917/AS)

NESDIS 30 Planning for Future Generational Sensors and Other Priorities. James C. Fischer, June 1987. (PB87 220802/AS)

NESDIS 31 Data Processing Algorithms for Inferring Stratospheric Gas Concentrations from Balloon-Based Solar Occultation Data. I-Lok Chang (American University) and Michael P. Weinreb, April 1987. (PB87 196424)

NESDIS 32 Precipitation Detection with Satellite Microwave Data. Yang Chenggang and Andrew Timchalk, June 1988. (PB88-240239)

NESDIS 33 An Introduction to the GOES I-M Imager and Sounder Instruments and the GVAR Retransmission Format. Raymond J. Komajda (Mitre Corp) and Keith McKenzie, October 1987. (PB88-132709)

NESDIS 34 Balloon-Based Infrared Solar Occultation Measurements of Stratospheric O3, H2O, HNo3, and CF2C12. Michael P. Weinreb and I-Lok Chang (American University), September 1987. (PB88-132725)

NESDIS 35 Passive Microwave Observing From Environmental Satellites, A Status Report Based on NOAA's June 1-4, 1987, Conference in Williamsburg, Virginia. James C. Fischer, November 1987. (PB88-208236)

NESDIS 36 Pre-Launch Calibration of Channels 1 and 2 of the Advanced Very High Resolution Radiometer. C.R. Nagaraja Rao, October 1987. (PB88-157169 A/S)

NESDIS 39 General Determination of Earth Surface Type and Cloud Amount Using Multispectral AVHRR Data. Irwin Ruff and Arnold Gruber, February 1988. (PB88-199195/AS)

NESDIS 40 The GOES I-M System Functional Description. Carolyn Bradley (Mitre Corp), November 1988.

NESDIS 41 Report of the Earth Radiation Budget Requirements Review - 1987 Rosslyn, Virginia, 30 March - 3 April 1987. L.L. Stowe (Editor), June 1988.

NESDIS 42 Simulation Studies of Improved Sounding Systems. H. Yates, D. Wark, H. Aumann, N. Evans, N. Phillips, J. Sussking, L. McMillin, A. Goldman, M. Chahine, and L. Crone, February 1989.

NESDIS 43 Adjustment of Microwave Spectral Radiances of the Earth to a Fixed Angle of Progagation. D. Q. Wark, December 1988.

NOAA SCIENTIFIC AND TECHNICAL PUBLICATIONS

The National Oceanic and Atmospheric Administration was established as part of the Department of Commerce on October 3, 1970. The mission responsibilities of NOAA are to assess the socioeconomic impact of natural and technological changes in the environment and to monitor and predict the state of the solid Earth, the oceans and their living resources, the atmosphere, and the space environment of the Earth.

The major components of NOAA regularly produce various types of scientific and technical information in the following kinds of publications:

PROFESSIONAL PAPERS—Important definitive research results, major techniques, and special investigations.

CONTRACT AND GRANT REPORTS—Reports prepared by contractors or grantees under NOAA sponsorship.

ATLAS—Presentation of analyzed data generally in the form of maps showing distribution of rainfall, chemical and physical conditions of oceans and atmosphere, distribution of fishes and marine mammals, ionospheric conditions, etc.

TECHNICAL SERVICE PUBLICATIONS—Reports containing data, observations, instructions, etc. A partial listing includes data serials; prediction and outlook periodicals; technical manuals, training papers, planning reports, and information serials; and miscellaneous technical publications.

TECHNICAL REPORTS—Journal quality with extensive details, mathematical developments, or data listings.

TECHNICAL MEMORANDUMS—Reports of preliminary, partial, or negative research or technology results, interim instructions, and the like.

U.S. DEPARTMENT OF COMMERCE
NATIONAL OCEANIC AND ATMOSPHERIC ADMINISTRATION
NATIONAL ENVIRONMENTAL SATELLITE, DATA, AND INFORMATION SERVICE
Washington, D.C. 20233